Low Complexity Optimal Hard Decision Fusion under Neyman-Pearson Criterion

Mohammad Fayazur Rahaman

A Dissertation Submitted to
Indian Institute of Technology Hyderabad
In Partial Fulfillment of the Requirements for
The Degree of *Doctor of Philosophy*

Department of Electrical Engineering
Indian Institute of Technology Hyderabad

September 2018

Declaration

I declare that this written submission represents my ideas in my own words, and where ideas or words of others have been included, I have adequately cited and referenced the original sources. I also declare that I have adhered to all principles of academic honesty and integrity and have not misrepresented or fabricated or falsified any idea/data/fact/source in my submission. I understand that any violation of the above will be a cause for disciplinary action by the Institute and can also evoke penal action from the sources that have thus not been properly cited, or from whom proper permission has not been taken when needed.

Signature: M. Fayazur Rahaman

Mohammad Fayazur Rahaman
EE12P1003

Approval Sheet

This Dissertation entitled **Low Complexity Optimal Hard Decision Fusion under Neyman-Pearson Criterion** by *Mohammad Fayazur Rahaman* is approved for the degree of *Doctor of Philosophy* from Indian Institute of Technology Hyderabad.

Signature: Adrish Banerjee

Prof. Adrish Banerjee

Dept. of Electrical Engineering, Indian Institute of Technology Kanpur

Examiner 1

Signature:

Prof. Mrityunjoy Chakraborty

Dept. of Electronics and Electrical Communication Engg, Indian Institute of Technology Kharagpur

Examiner 2

Signature: G.V.V. Sarma

Dr. G.V.V. Sharma

Dept. of Electrical Engineering, Indian Institute of Technology Hyderabad

Internal Examiner

Signature: Zafar

Prof. Mohammed Zafar Ali Khan

Dept. of Electrical Engineering, Indian Institute of Technology Hyderabad

Supervisor

Signature: B L Reddy

Dr. Bheemarjuna Reddy Tamma

Dept. of Computer Science and Engg, Indian Institute of Technology Hyderabad

Chairman

Acknowledgements

I am grateful to my institute, *Indian Institute of Technology Hyderabad* and my department of *Electrical Engineering* for showing confidence in me and giving me this oppurtunity to carry-out this work. I am especially in-debt to my guide *Prof. Mohammed Zafar Ali Khan* for giving me the freedom and time to gradually grow this work. He was there to show me the opportunities when things appeared blocked. He helped me think creative and believe in the saying '*nothing is impossible*'. On the personal front he taught me what hardwork is and always raised the bar when I thought I had reached the destination, enabling me to realize and unlock my potential.

I am thankful to my friends and colleagues at IITH who were always there to help me, those useful discussions, team treats and the de-stressing humour to mention a few, that energized me from time to time. The IITH Doctoral committee, the thesis defense committe, IEEE associate editors, IEEE anonymous reviewers and collaborators who contributed in improvising this work. My sponsors who provided me financial support; the MHRD, the Visvesvarya YFRF and the Miety.

I am thankful to my family members who always encouraged me, patiently sat through my practice lectures (though they did not understand much) to help me clear my concepts and shared my joy whenever a paper was accepted. Especially my youngest 5 years old child pateintly waited all these years for her father to complete his PhD to accompany her to the zoo (though she has visited it multiple times with others). A special thanks to my younger brother Imtiaz for the productive discussions we have had. And all those who directly or indirectly helped me complete this work.

Finally, the power of my parent's prayers and prayers of all others without which I could not have traversed this far.

Dedication

To my parents and my family.

Abstract

Decision fusion is a fundamental operation in many signal processing systems where multiple sensors collaborate to improve the accuracy and robustness of the decision being made. The decision of each individual binary decision maker (or sensor) is often error-prone due to various environment challenges. These challenges are mitigated to certain extent using the spatial diversity obtained by deploying the sensors over a geographically distributed area. Subsequently, the decisions from the individual sensors are collected and fused at a fusion center to obtain a global decision.

One such recent application of decision fusion is cooperative spectrum sensing in cognitive radio networks (CRN). The secondary users (SUs) of the CRN are tasked to garner the much needed unutilized spectrum allocated to the primary users (PUs). It is important for the SUs to precisely detect the spectrum usage opportunities inorder to improve the spectral efficiency and also to restrict the interference caused to PUs in this process. However, these are two conflicting objectives. Tuning the system to low levels of interference to the primary network will result in higher missed spectrum utilization oppurtunities. Similarly, increasing the detection of spectral usage opportunities will lead to increased interference to the primary users.

The fusion centers require optimal fusion rules that improve the spectral efficiency of the CRN and minimize the interference caused to the primary network. The spectrum sensing in this case is generally modeled as a binary hypothesis problem: 'PU signal present' and 'PU signal absent'. The fusion rules are broadly classified into two categories, namely (i) non-randomized (ii) randomized. In a 'non-randomized' rule, the global decision generated is deterministic for all the combinations of the local observations received. And in a 'randomized' rule the global decision generated is random (0 or 1) with a certain probability distribution for some local observations. The design of the optimal randomized decision fusion is generally simple, however introduce randomness in the decision equations and are difficult to implement. Whereas

the design of the optimal non-randomized hard decision fusion rule is difficult, and under the Neyman-Pearson (NP) criterion is known to be exponential in complexity.

In this thesis, we develop low-complexity (i) optimal and (ii) near-optimal algorithms for two variants of non-randomized hard decision fusion problems under NP crierion (i) clairvoyant[1] decision fusion and (ii) novel (semi-)blind decision fusion. In all the sub-categories considered therein, we present low-complexity algorithms and obtain receiver operating characteristics (ROCs) for different number of participating sensors (N) which was intractable with the existing approaches.

We formulate a more generalized version of this problem called "Generalized Decision Fusion Problem (GDFP)" and relate it to the classical $0-1$ Knapsack problem. Consequently we show that the GDFP has a worst case pseudo-polynomial time solution using dynamic programming approach. Additionaly, we show that the decision fusion problem exhibits semi-monotonic property in most practical cases. We propose to exploit this property to reduce the dimension of the feasible solution space. Subsequently, we apply dynamic programming to efficiently solve the problem with further reduction in complexity.

Further, we show that though the non-randomized single-threshold likelihood ratio based test (*non-rand-st* LRT) is sub-optimal, its performance approaches the upper bound obtained by randomized LRT (*rand* LRT) with increase in N. This alleviates the need for employing the exponentially complex non-randomized optimal solution for N larger than a specific value.

As a variant of GDFP, we propose novel (semi-)blind hard decision fusion rules that use the mean of the secondary user characteristics instead of their actual values. We show that these rules with slight (or no) additional system knowledge achieve better ROC than existing (semi-)blind alternatives.

Finally, we present a branch and bound algorithm with novel termination to obtain

[1]A rule that has complete knowledge of the system

a near-optimal solution as the proposed dynamic programming approach exhibits limitations for the GDFP that require high-precision computations. We validate the performance of the proposed branch and bound algorithm for a wide range of {high, low} precision and {monotonic, semi, non-monotonic} GDFPs.

All the algorithms have been rigorously verified by simulations in Matlab.

Contents

List of Plots

List of Tables

List of Symbols and Notations

H_0	Event (PU signal) absent hypothesis
H_1	Event (PU signal) present hypothesis
P_{d_i}	Probability of detection of the i^{th} SU (or sensor)
P_{f_i}	Probability of false alarm of the i^{th} SU (or sensor)
P_{e_i}	Probability of error of the reporting channel between the i^{th} SU (or sensor) and the FC
$P_{d_i}^e$	Effective Probability of detection of the i^{th} SU as observed by the FC
$P_{f_i}^e$	Effective Probability of false alarm of the i^{th} SU as observed by the FC
$\mathbb{P}_d$	Distribution family of probability of detection ($\triangleq \{P_{d_i}\}_{i=0}^{N-1}$)
$\mathbb{P}_f$	Distribution family of probability of false alarm ($\triangleq \{P_{f_i}\}_{i=0}^{N-1}$)
P_D	System probability of detection obtained at FC
P_F	System probability of false alarm obtained at FC
P_D^*	System probability of detection obtained at the FC for the optimal fusion rule
P_F^*	System probability of false alarm obtained at the FC for the optimal fusion rule
α	Limit specified on the system probability of false alarm under NP criterion

N	Number of SUs in the network
v_i	Local binary decision of the i^{th} SU
u_i	Local binary decision received by the FC from the i^{th} SU over the reporting channel
u_{fc}	Global binary decision generated by the FC
$\mathbf{u}$	N-dimensional binary decision vector received by the FC ($\triangleq [u_{N-1} \cdots u_0]^T$)
$\mathbf{u}_m$	m^{th} realization of the vector $\mathbf{u}$
$u_{i,m}$	Binary decision of the i^{th} SU in the m^{th} realization of the vector $\mathbf{u}$
$\mathcal{U}$	Discrete observation space ($\triangleq \{\mathbf{u}_m\}_{m=0}^{M-1}$)
M	Cardinality of the observation space ($\triangleq |\mathcal{U}|$) and $= 2^N$
$\mathfrak{R}_0$	Decision region in the N-dimensional real space corresponding to H_0
$\mathfrak{R}_1$	Decision region in the N-dimensional real space corresponding to H_1
$p(\mathbf{u}|H_0)$	Conditional probability of $\mathbf{u}$ given H_0
$p(\mathbf{u}|H_1)$	Conditional probability of $\mathbf{u}$ given H_1
$\Lambda(\mathbb{P}_d, \mathbb{P}_f, \mathbf{u})$	Likelihood ratio function of $\mathbf{u}$ for a realization of $\{\mathbb{P}_d, \mathbb{P}_f\}$
$\Omega(\mathbb{P}_d, \mathbb{P}_f, \mathbf{u})$	Simplified likelihood ratio function of $\mathbf{u}$ for a realization of $\{\mathbb{P}_d, \mathbb{P}_f\}$
λ	Threshold(s) to be computed for the LR decision equation
ω	Threshold(s) to be computed for the simplified LR decision equation
$\mathbf{x}$	M-dimensional binary vector representing a fusion rule ($\triangleq [x_{M-1} \cdots x_0]^T$)
x_m	Binary variable where $\{x_m = 1 \implies \mathbf{u}_m \in \mathfrak{R}_1\}$ and $\{x_m = 0 \implies \mathbf{u}_m \in \mathfrak{R}_0\}$
$T(\mathbf{u})$	Arbitrary function ($T : \mathbb{B}^N \mapsto \mathbb{R}$)

k	Number of decisions in $\mathbf{u}$ declaring H_1 ($\triangleq \sum_{i=0}^{N-1} u_i$), $N \leq k \leq 0$
$\mathcal{U}_k$	Sub-space ($\triangleq \{\mathbf{u}_m : \sum_{i=0}^{N-1} u_{m,i} = k, \forall m\}$) of the discrete observation space $\mathcal{U}$
$\mathbf{y}$	$(N+1)$-dimensional binary vector representing a combination of multiple K-out-of-N fusion rules ($\triangleq [y_N \cdots y_0]^T$)
y_k	Binary variable where $\{y_k = 1 \implies \mathcal{U}_k \in \mathfrak{R}_1\}$ and $\{y_k = 0 \implies \mathcal{U}_k \in \mathfrak{R}_0\}$
$\mathbf{G}(a, b)$	Parameterized GDFP where $\{a \in \mathbb{N} : 0 \leq a < M\}$ and $\{b \in \mathbb{R} : 0 \leq b \leq \alpha\}$
$\mathbf{x_a}$	Binary vector representing a partial fusion rule ($\triangleq [x_a \cdots x_0]^T$)
$\mathbf{x^a}$	Binary vector representing a partial fusion rule ($\triangleq [x_{M-1} \cdots x_a]^T$)
$I(\cdot)$	Mapping function $\mathbb{R}_{\geq 0} \mapsto \mathbb{N}_{\geq 0}$, (where $I(r) \triangleq \lfloor C \cdot r + \frac{1}{2} \rfloor$)
$\lfloor r \rfloor$	Function to generate greatest integer $\leq r$
C	Scaling factor (typically, $\leq 10^6$)
I_α	Mapping of α onto an integer ($\triangleq I(\alpha)$)
I_b	Integer equivalent of variable b where $\{I_b \in \mathbb{N} : 0 \leq I_b \leq I_\alpha\}$
$\mathbf{G}[\cdot, \cdot]$	Two dimensional array of size $M \times I_\alpha$ to hold real-value solutions of the GDFP sub-problems
$\mathbf{G}[a, I_b]$	Cell in a two dimensional array holding real-value solution corresponding to GDFP sub-problem $G(a, b)$
$\mathcal{U}'$	Reduced observation space with ($M' \triangleq \lvert\mathcal{U}'\rvert) < M$
$\mathcal{S}(\mathbf{u}_{m'})$	Set comprising indices of the SUs that have reported local decision as '1' (i.e., hypothesis H_1) in the observation vector $\mathbf{u}_{m'}$
$\mathbb{S}(\mathbf{u}_{m'})$	Set comprising of indices of other observation vectors that have one or more SUs reporting '1' in addition to those in $\mathbf{u}_{m'}$

s	Index of observation vectors named split-index used for obtaining solution of non-radomized GDFP
$P_{D_{nr}}$	System probability of detection obtained by non-randomized signle-threshold LRT
$P_{F_{nr}}$	System probability of false alarm obtained by non-randomized signle-threshold LRT
P_{D_r}	System probability of detection obtained by randomized signle-threshold LRT
P_{F_r}	System probability of false alarm obtained by randomized signle-threshold LRT
$\epsilon(\alpha)$	Gain in system probability of detection due to randomized LRT over non-randomized LRT ($\triangleq (P_{D_r} - P_{D_{nr}})$)
ϵ_{ub}	Upper-bound of performance gain $\epsilon(\alpha)$
ϵ_{μ}	Expectation of performance gain ($\triangleq \mathbb{E}_{\alpha}\{\epsilon\}$)
μ_f	Mean probability of false alarm of the i^{th} SU ($\triangleq \mathbb{E}\{P_{f_i}\}$)
μ_d	Mean of difference between probability of detection and probability of false alarm of the i^{th} SU ($\triangleq \mathbb{E}\{P_{d_i} - P_{f_i}\}$)
μ_e	Mean probability of error of the i^{th} reporting channel ($\triangleq \mathbb{E}\{P_{e_i}\}$)
$\widehat{P_{d_i}}$	Estimate of the unknown probability of detection of the i^{th} SU
$\widehat{P_{f_i}}$	Estimate of the unknown probability of false alarm of the i^{th} SU
$\widehat{P_{e_i}}$	Estimate of the unknown probability of error of the i^{th} reporting channel
$\mathbf{U}(s_1, s_2)$	Uniform probability distribution with supports s_1 and s_2

Chapter 1

Introduction

The focus of this dissertation is on developing low complexity algorithms for solving 'non-randomized Hard Decision Fusion' problems. Decision fusion is a fundamental operation in many signal processing systems like Communications, Radar, Sonar, Image processing, Speech, Biomedicine, Weather prediction, Control, Internet of Things etc. One of the recent application of decision fusion is in cooperative spectrum sensing in cognitive radio networks.

1.1 Motivation and Scope of the Thesis

The demand for wireless mobile data consumption has grown at a phenomenal rate in the past decade. The rapid deployement of more and more wireless systems and services to cater to the demand has led to a serious problem of lack of availability of radio spectrum for wireless communications. Cognitive radio technologies promise to alleviate this problem by garnering and flexibly using the unutilized licensed spectrum. The secondary users (SUs) are allowed to use the spectrum while it is unutilized by the primary users (PUs).

This requires a robust and accurate mechanism to identify the spectrum white space slot availability to share it among the SUs while strictly controlling the interference caused to the PUs. To acheive this, cooperative spectrum sensing is widely researched to obtain diversity gains in demanding propagation environments such as fading, shadowing and the hidden node problem. All the SUs share a common aim of being able to decide when the PU is not transmitting and the existence of the spectrum usage opportunity for the secondary network. Typically, due to the limitations on (reporting channels) the amount of communication allowed, the SUs make hard (binary) decisions and transmit these results to the fusion center (FC) for decision combining. The distributed sensing problem is generally modeled as a binary hypothesis test. The incorrect decisions: *(i) missed detection* leads to collision in transmission with the PU; *(ii) false alarm* leads to missed oppurtunity for the SUs to utilize the spectrum. The chosen decision-making strategy like Neyman-Pearson, Bayesian etc., specify the criterion to control the interference while maximizing the spectral efficiency.

The computational complexity to obtain a decision fusion rule varies greatly with the nature of the problem and the chosen strategy. Non-randomized hard decision fusion under Neyman-Pearson is known to be exponential in complexity on M (the cardinality of the observation data space), that is double-exponential on N (the number of participating SUs). This problem gets intractable with increase in N.

The scope of this thesis is to develop low-complexity *(i) optimal and (ii) near-optimal algorithms* for two variants of non-randomized hard decision fusion problems *(i) clairvoyant decision fusion and (ii) novel (semi-)blind decision fusion.* In all the sub-categories considered therein, we present low-complexity algorithms and obtain receiver operating characteristics (ROCs) for different values of N which was intractable with the existing approaches. All the algorithms have been rigorously verified by simulations in Matlab.

1.2 Organization of the Thesis

The content of this thesis can be categorized into the following main topics:

(A) formulation of the generalized decision fusion problem (GDFP) and establishing that it is a well-known $0-1$ Knapsack problem;

(B) defining variants of the GDFP:

  (i) the clairvoyant fusion problem and

  (ii) the (semi-) blind decision fusion problem;

(C) categorization of the GDFP based on the properties exhibited:

  (i) monotonic (case-A and case-B),

  (ii) semi-monotonic and

  (iii) non-monotonic;

(D) presentation of different types of low-complexity solutions:

  (i) dynamic programing based optimal solution for low-precision non-monotonic problems,

  (ii) solution space variable reduction method for semi-monotonic problems,

  (iii) near-optimal non-randomized single-threshold likelihood ratio test (*non-rand-st* LRT) for problems with larger number of participating SUs,

  (iv) near-optimal novel termination branch and bound based solution for all types of problems.

Figure 1.1 summarizes the contributions of this thesis in the form of a flowchart.

Chapter 2 We introduce the hard decision fusion problem and categorize the same based on the properties exhibited by its likelihood ratio (LR) based decision equation. We

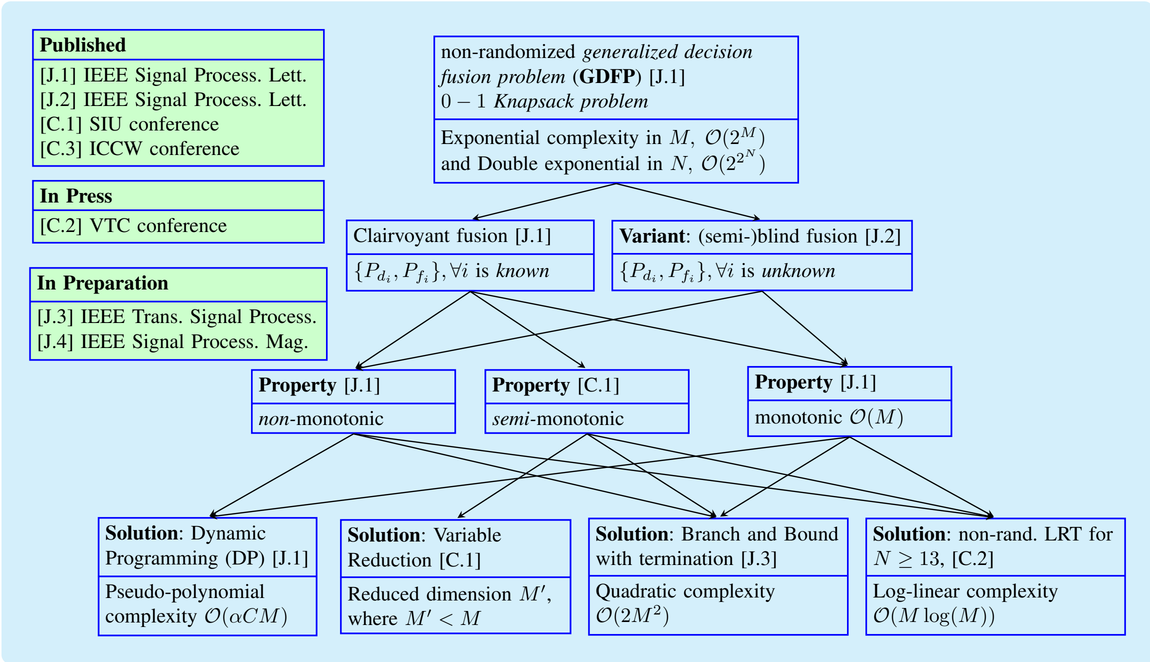

Figure 1.1: Depiction of the contributions in a flowchart.

establish that the optimal fusion rule requires the decision equation to be compared with multi-thresholds for the most general case. Subsequently, we formulate the problem into GDFP and show that it is a $0-1$ Knapsack problem. We present a low-complexity optimal solution that is pseudo-polynomial ($\mathcal{O}(\alpha CM)$) in computation complexity whereas computating the multi-thresholds is exponential ($\mathcal{O}(2^M)$, i.e., $\mathcal{O}(2^{2^N})$) in complexity.

Accordingly, Chapter 2 has seven sections dealing with the GDFP, its properties, categorization, the $0-1$ Knapsack equivalence and the dynamic programming based solution.

Chapter 3 We define a new desirable property of the GDFP namely, semi-monotonic. We show that the feasible solution space of the problems with this property is reduced. Subsequently, the DP based solution for such problems is reduced to $\mathcal{O}(\alpha CM')$ where $M' < M$.

Accordingly, Chapter 3 has six sections dealing with the semi-monotonic property, the feasible solution space reduction of the GDFP and the numerical results.

Chapter 4 We show analytically that the performance of the widely used *non-rand-st* LRT approaches the upper-bound obtained by the randomized likelihood ratio test (*rand* LRT) for asymptotic number of participating SUs. Further, we show numerically that performance difference is insignificant for number of SUs $N \geq 13$, thereby allowing the use of log-linear ($\mathcal{O}(M \log(M))$ complexity solution for such cases.

Accordingly Chapter 4 has five sections dealing with defining the performance difference metrices and numerical computation of the parameters for various network scenarios.

Chapter 5 We introduce novel variants of the GDFP, called (semi-)blind hard decision fusion rules. These use the mean of the SU characteristics instead of their actual values. The semi-blind rules, namely MSB assume that the characteristics under the hypothesis H_1 are unknown and the blind rules, namely MCB assume that the characteristics under both the H_0 and H_1 are unknown. These rules with slight (or no) additional system knowledge achieve better receiver operating characteristics than existing (semi-)blind alternatives.

Accordingly Chapter 5 has six sections dealing with definition of the rules, their monotonic properties, proposed solutions and the numerical results.

Chapter 6 Finally, we present *branch and bound* algorithm with novel termination to obtain the near-optimal solution as the dynamic programming approach proposed in chapter 2 exhibits limitations for the GDFP that require high-precision computations. We validate the performance of the proposed branch and bound algorithm for a wide range of {high, low} precision and {monotonic, semi, non-monotonic} GDFPs.

Accordingly Chapter 6 has five sections dealing with branch and bound algorithm, the proposed termination mechanism and the numerical results.

Chapter 7 We conclude the thesis by summarizing the main results obtained and enumerate future avenues of research.

Chapter B In Appendix, we provide one numerical example each for the different GDFP properties discussed in the thesis.

1.3 Research Contributions

The main contribution of this thesis is developing low-complexity solutions to obtain the optimal and near-optimal fusion rules for non-randomized decision fusion problems under Neyman-Pearson criterion. Details of the research contributions in each chapter are as follows:

Chapter 2 The main result in this chapter is to show that the non-randomized hard decision fusion problem requires multi-threshold decision equation to obtain optimum performance and later mapping it to the well-known $0-1$ Knapsack problem. Thereby this allows us to use dynamic programming to obtain optimal fusion rules. The results of this chapter have been published in one journal paper:

[J.1] **M. F. Rahaman** and M. Z. A. Khan, "Low-Complexity Optimal Hard Decision Fusion Under the Neyman-Pearson Criterion," IEEE Signal Process. Lett., vol. 25, no. 3, pp. 353-357, Mar. 2018.

Chapter 3 The main result in this chapter is definition of a new property, namely semi-monotonic that is exhibited by the GDFP in most practical cases. This property reduces the dimension of the feasible solution space thereby further reducing the solution complexity of proposed algorithms. The results of this chapter have been published in one conference paper:

[C.1] D. Nikhil, **M. F. Rahaman** and M. Z. A. Khan, "Reduced Complexity Optimal Hard Decision Fusion under Neyman-Pearson Criterion," 26^{th} IEEE SIU 2018 conference, pp. 1-4, May 2018, Turkey.

Chapter 4 The main result in this chapter is definition of two metrics to quantify the performance difference between *non-rand-st* LRT and *rand* LRT. This allows us to show analytically that the performance difference approaches zero for asymptotic number of SUs. The results of this chapter have been published in one conference paper:

[C.2] **M. F. Rahaman** and M. Z. A. Khan, "On non-Randomized Hard Decision Fusion under Neyman Pearson Criterion using LRT," 88^{th} IEEE Vehicular Technology Conference, Chicago, *(In Press, June 2018)*.

Chapter 5 The main result in this chapter is the definition of variants of the GDFP. Groups of semi-blind namely MSB and completely-blind fusion rules namely MCB are defined and their monotonic property is established. Numerical results are obtained by the solutions proposed in the previous chapters. The results of this chapter have been published in one journal paper:

[J.2] **M. F. Rahaman**, D. Ciuonzo and M. Z. A. Khan, "Mean-based Hard Decision Fusion Rules," IEEE Signal Process. Lett., vol. 25, no. 5, pp. 630-634, May 2018.

Chapter 6 The main result in this chapter is applying the branch and bound algorithm for the GDFP with a novel termination mechanism to handle the exception scenarios. As a result this mechanism is conjectured to provide the near-optimal solution in quadratic time complexity for a wide range of GDFPs. The results of this chapter are under preparation for a journal paper:

[J.3] **M. F. Rahaman** and M. Z. A. Khan, "Fast Computation of Optimal

Hard Decision Fusion under Neyman-Pearson Criterion," (In preparation for *IEEE Signal Process. Lett.*,).

Chapter 2

Generalized Decision Fusion Problem

2.1 Introduction

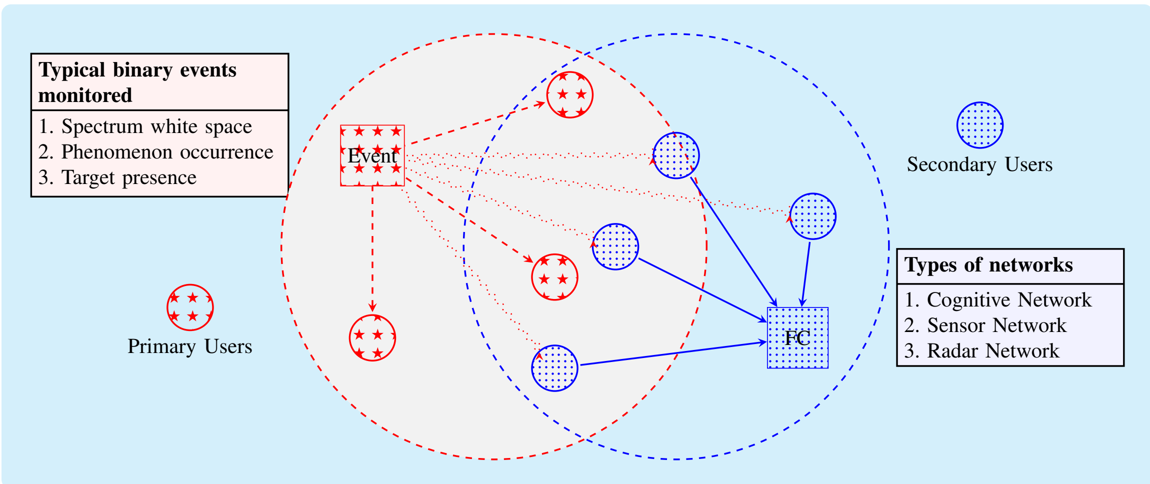

Figure 2.1: Illustration of a Distributed Detection network.

Distributed detection (as illustrated in Figure 2.1) is widely researched in sensor networks [1,2], military surveillance, environment monitoring, internet of things (IoT) and has also found vast application for cooperative spectrum sensing (CSS) in cognitive radio networks (CRN) [3,4]. Typically a distributed sensor network comprises of geographically distributed sensors deployed to monitor the occurrence of an event of interest. The local decisions are collected by a fusion center (FC indicated by *blue dotted* box) to generate a global decision. The fusion rule at the FC makes use of the spatial diversity of the local decisions to increase the accuracy of the global decision.

In a CSS scheme of a CRN [5–9], multiple secondary users (SUs indicated by *blue dotted* circles) (or sensors in some cases) collaborate to increase the reliability of the binary hypothesis test to detect a specturm hole (an event indicated by *red starred* box). The likelihood ratio (LR) function of the SU decisions is used as the fundamental measure to design the optimal fusion rule of the fusion center (FC) [10, 11]. It is desirable that a sufficient statistic[1] function for the LR exist, and that it is monotonic[2], as it simplifies the computation of the threshold for the LR-based decision equation under NP criterion [10, 12]. However, many practical problems are non-monotonic wherein the optimal decision regions in the observation space are not simply connected. In such cases, the optimal fusion rule requires multi-threshold decision equation and the problem often requires computationally intensive exhaustive search methods.

Different factors that influence the complexity[3] of the decision fusion problem can be categorized as follows:

(i) the property of the LR function {*monotonic, non-monotonic*};

(ii) the performance criterion {*Bayesian, Neyman-Pearson*};

(iii) the decision threshold equations used {*single (st), multi (mt)*};

(iv) the test used {*randomized (rand), non-randomized (non-rand)*};

(v) the nature of the observation space {*discrete (D-OS), continuous (C-OS)*};

[1] A compressed statistic that provides complete knowledge of the observation data.

[2] A decision fusion problem is called monotonic if the sufficient statistics function exists and the LR function is monotonic on it [12].

[3] Complexity is defined as the number of addition/multiplication floating-point operations (flops) required by an algorithm to compute a solution.

Table 2.1: Categorization of Decision fusion problems with references

	LR Fn.	*monotonic*	*non-monotonic*	
	Thres. Eq.	*single*	*single*	*multi*
Bayesian $\rightarrow$		[13–16], [*]	[17, 18], [*]	x
NP $\rightarrow$	**non-rand.**	[19, 20], [*]	[22–26]	[*]
	rand.	[21]	[26–28]	x

[*] Represents all the special cases of the proposed GDFP.
x These categories do not exist.

(vi) the SU decisions $\{$*dependent, independent*$\}$ etc.

Table 2.1 lists some of the categories and the corresponding references in the literature where these problems have been considered.

Under Bayesian criterion it is straight forward to compute the single-threshold for the LR test when the apriori probabilities of the hypothesis and the Bayes costs are known. Using the threshold, the probability of error P_E can be computed in logarithmic time for monotonic problems [13–16] and in linear time for non-monotonic problems [17, 18].

In general, the constrained optimization of the NP criterion increases the problem complexity. For problems with monotonic property, low complexity methods like bisection, gradient descent etc., can be used to compute the optimal threshold in some cases [19–21]. The non-monotonic property of the LR complicates the optimal decision equation, which is generally intractable in C-OS [12]. To circumvent this difficulty, *sub-optimal* single-threshold weighted decision equation is used in [22–26]. In D-OS, the exhaustive search method can be employed, however it is exponential in complexity [1, 2]. Alternatively, the randomized test as in [26–28] reduces the complexity at the cost of introducing randomness in the decision equation. Additional background information related to the existing work is provided in the Appendix A.

In this thesis, we focus on the non-randomized optimal hard decision fusion in the discrete observation space. The main contributions in this chapter are:

(i) We formulate a generalized decision fusion problem (GDFP) wherein both monotonic / non-monotonic problems under both Bayesian and NP criterion are special cases (categories marked with [*] in Table 2.1).

(ii) We subsequently present an approach that reduces the exponentially complex non-monotonic hard decision fusion NP criterion special case into pseudo-polynomial[4] time by showing that the proposed GDFP is related to the classical $0-1$ Knapsack problem (KP).

(iii) The proposed approach is valid for system with dependent SU decisions as well.

(iv) The solution complexity can be further reduced for monotonic relevant cases of the GDFP. A special case of monotonic GDFP is identified where the complexity reduces to linear time in the worst case.

(v) Boolean switching equation is introduced as a convinient way of implementing the multi-threshold decision equation.

The outline of this chapter is as follows: In Section 2.2 we explain the system model, formulate the GDFP and show that the problem is non-monotonic in general. We relate the GDFP to 0-1 KP and present dynamic programming (DP) based solution in Section 2.3. Section 2.6 contains the numerical results, followed by conclusions in Section 2.7.

2.2 System Model

We consider a parallel network of N distributed SUs and a FC as depicted in the Figure 2.2. The SUs (indicated by the *blue dotted* circles) sense the spectrum for PU transmissions and generate individual local binary decisions u_i, where $u_i = 0$ implies hypothesis H_0 : *PU signal absent* and $u_i = 1$ implies hypothesis H_1 : *PU*

[4] Computation time is polynomial in the numeric value of an input parameter

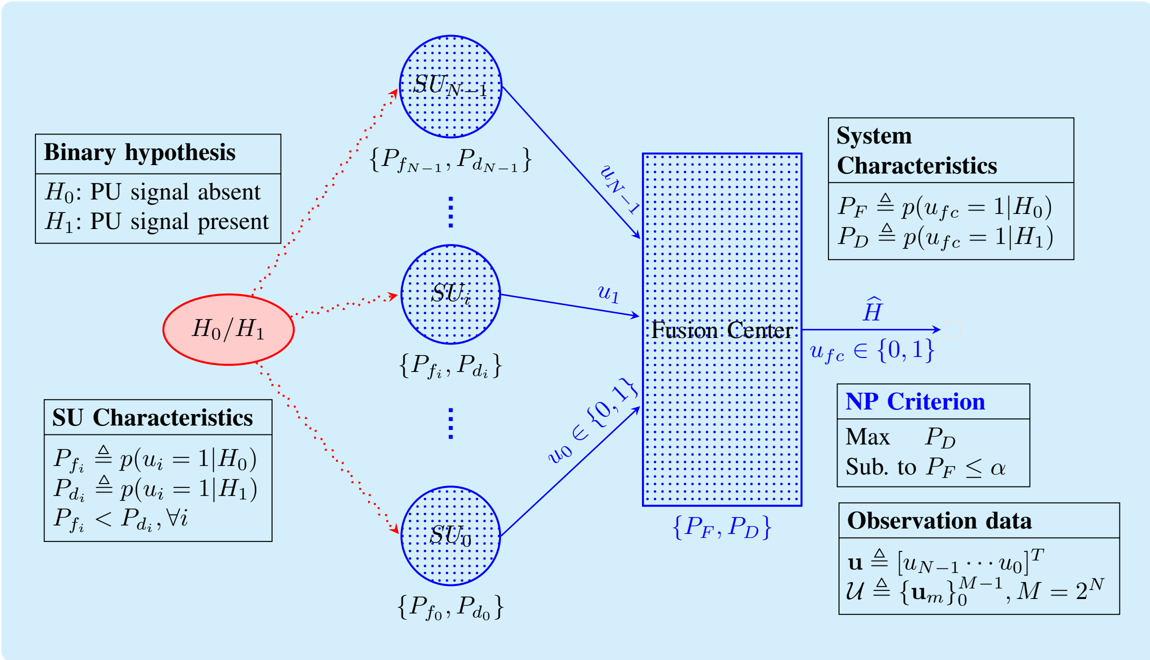

Figure 2.2: Depiction of System Model.

signal present respectively. These local decisions are received by the FC (indicated by *blue dotted* rectangle) over *non-erroneous* reporting channels as a N-dimensional observation vector $\mathbf{u}$, where $\mathbf{u} \triangleq [u_{N-1} \cdots u_0]^T$. As a result, the observation space $\mathcal{U}$, is discrete $(= \mathbb{B}^N$ where $\mathbb{B} \in \{0,1\})$ with cardinality $M = 2^N$. The m^{th} vector in the observation space is represented as $\mathbf{u}_m$, $m \in \{0, \cdots, M-1\}$. Figure 2.3 represents all the observation vectors possible for an example using $N = 2$.

$M = 2^N (= 2^2)$

	$\mathbf{u}_3$	$\mathbf{u}_2$	$\mathbf{u}_1$	$\mathbf{u}_0$
u_1	1	1	0	0
u_0	1	0	1	0

$N(= 2)$

Figure 2.3: Observation vectors for $N = 2$.

Each SU is characterized by its average probability of detection $P_{d_i} \triangleq p(u_i = 1 \mid H_1)$ and probability of false alarm $P_{f_i} \triangleq p(u_i = 1 \mid H_0)$, $\forall i$. Based on the received observation vector $\mathbf{u}$, the fusion rule $\Gamma(\cdot)$, of the FC generates the global decision

$u_{fc} = \Gamma(\mathbf{u})$, where $u_{fc} = 0$ implies hypothesis H_0 and $u_{fc} = 1$ implies hypothesis H_1 respectively. The performance of the fusion rule is characterized by the system probability of detection P_D ($\triangleq p(u_{fc} = 1|H_1)$) and probability of false alarm P_F ($\triangleq p(u_{fc} = 1|H_0)$), that are obtained as [10],

$$P_D = \sum_{\mathbf{u} \in \mathfrak{R}_1} p(\mathbf{u}|H_1), \qquad P_F = \sum_{\mathbf{u} \in \mathfrak{R}_1} p(\mathbf{u}|H_0), \tag{2.1}$$

where $\mathfrak{R}_0, \mathfrak{R}_1$ are two decision regions in the N-dimensional continuous real space $\mathbb{R}^N$, such that $\mathcal{U} \subset \{\mathfrak{R}_0 \cup \mathfrak{R}_1\}$, $\{\mathfrak{R}_0 \cap \mathfrak{R}_1\} = \varnothing$ (empty set), $\mathbf{u}_m \in \mathfrak{R}_0$ implies $\Gamma(\mathbf{u}_m) = 0$ and $\mathbf{u}_m \in \mathfrak{R}_1$ implies $\Gamma(\mathbf{u}_m) = 1, \forall m$. This indicates that an optimal definition of decision regions results in an optimal fusion rule. Figure 2.4 depicts two types of decision regions possible for the example with $N = 2$.

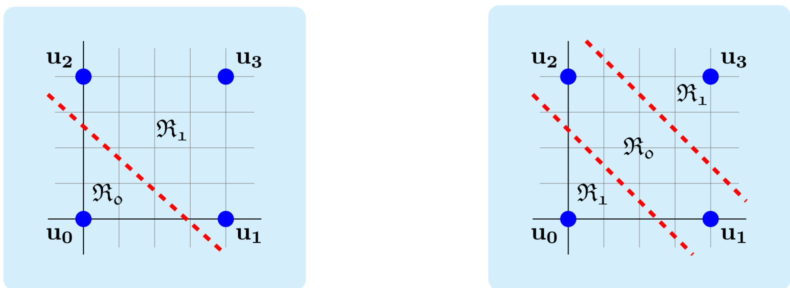

(a) Connected regions (b) Disconnected regions

Figure 2.4: Depiction of sample decision regions for $N = 2$.

We now formulate the generalized decision fusion problem (GDFP) as,

$$\underset{\mathfrak{R}_1}{\text{Maximize}} \quad C_D\, P_D - C_F\, P_F, \quad \text{Sub to: } P_F \leq \alpha, \tag{2.2}$$

where C_D, C_F are coefficients in the objective function and α is the constraint value on the system P_F.

By substituting $\alpha = 1$, $C_D = \pi_1\,(C_{01} - C_{11})$, $C_F = \pi_0\,(C_{10} - C_{00})$ in (2.2), where C_{jl} is the cost of deciding H_j when H_l is true, and π_l is the apriori probability of hypothesis H_l, for $j, l \in \{0, 1\}$, we get

$$\underset{\mathfrak{R}_1}{\text{Maximize}} \quad \pi_1 \left(C_{01} - C_{11}\right) \; P_D - \pi_0 \left(C_{10} - C_{00}\right) \; P_F, \tag{2.3}$$

which by definition [11] is an unconstrained fusion problem under Bayesian criterion. This special case of the GDFP with independent SU decisions is the Chair-Varshney problem [17] for which a linear complexity solution to compute the P_E exists. Similarly, substituting $C_D = 1, C_F = 0$ in (2.2) we get,

$$\underset{\mathfrak{R}_1}{\text{Maximize}} \quad P_D, \quad \text{Sub to:} \quad P_F \leq \alpha, \tag{2.4}$$

which by definition [11] is a constrained optimization problem under NP criterion for which the solution is exponential in complexity [1].

We now focus on reducing the complexity of obtaining the optimum decision region $\mathfrak{R}_1$, for the GDFP. The Lagrangian function that needs to be maximized is,

$$F = C_D \; P_D - C_F \; P_F + \lambda'(P_F - \alpha), \tag{2.5}$$

where λ' is the Lagrange multiplier [10]. Using (2.1), we have

$$F = -\lambda' \alpha + \sum_{\mathbf{u} \in \mathfrak{R}_1} \left[C_D \, p(\mathbf{u}|H_1) + (\lambda' - C_F) \, p(\mathbf{u}|H_0)\right], \tag{2.6}$$

which indicates that, the optimal decision region $\mathfrak{R}_1$ for the GDFP can also be obtained by LR test given by,

$$\left(\Lambda(\mathbb{P}_d, \mathbb{P}_f, \mathbf{u}) \triangleq \frac{p(\mathbf{u}|H_1)}{p(\mathbf{u}|H_0)} \right) \quad \underset{u_{fc}=0}{\overset{u_{fc}=1}{\gtrless}} \quad \lambda, \tag{2.7}$$

where $\mathbb{P}_d \triangleq \{P_{d_i}\}_{i=0}^{N-1}$, $\mathbb{P}_f \triangleq \{P_{f_i}\}_{i=0}^{N-1}$ and λ $(= \frac{C_F - \lambda'}{C_D})$ is the threshold to be computed. When the SU decisions are independent (assuming the SUs are spatially segregated and experience different listening channel characteristics), we have

$$\begin{aligned} p(\mathbf{u}|H_1) &= \prod_{i=0}^{N-1} (P_{d_i})^{u_i} (\bar{P}_{d_i})^{1-u_i}, \\ p(\mathbf{u}|H_0) &= \prod_{i=0}^{N-1} (P_{f_i})^{u_i} (\bar{P}_{f_i})^{1-u_i}, \end{aligned} \tag{2.8}$$

where $\bar{P} \triangleq (1 - P)$. As an example, Table 2.2 lists the conditional probabilities of the observation vectors for $N = 2$.

Table 2.2: Conditional probability of the observation vectors for $N = 2$.

$\mathbf{u}$	$p(\mathbf{u}\|H_1)$	$p(\mathbf{u}\|H_0)$
$\mathbf{u}_3 = [1\ 1]^T$	$P_{d_1} P_{d_0}$	$P_{f_1} P_{f_0}$
$\mathbf{u}_2 = [1\ 0]^T$	$P_{d_1} \bar{P}_{d_0}$	$P_{f_1} \bar{P}_{f_0}$
$\mathbf{u}_1 = [0\ 1]^T$	$\bar{P}_{d_1} P_{d_0}$	$\bar{P}_{f_1} P_{f_0}$
$\mathbf{u}_0 = [0\ 0]^T$	$\bar{P}_{d_1} \bar{P}_{d_0}$	$\bar{P}_{f_1} \bar{P}_{f_0}$

Equation (2.7) can further be simplified as [1],

$$\left(\Omega(\mathbb{P}_d, \mathbb{P}_f, \mathbf{u}) \triangleq \sum_{i=0}^{N-1} g(P_{d_i}, P_{f_i})\, u_i \right) \quad \underset{u_{fc}=0}{\overset{u_{fc}=1}{\gtrless}} \quad \omega, \tag{2.9}$$

where $g(P_{d_i}, P_{f_i}) \triangleq \log(\frac{P_{d_i}\, \bar{P}_{f_i}}{\bar{P}_{d_i}\, P_{f_i}})$ and $\omega = \log(\lambda \prod_{i=0}^{N-1} \frac{\bar{P}_{f_i}}{\bar{P}_{d_i}})$. For this case, the threshold ω of (2.9) is to be computed that optimizes the GDFP.

Next we describe the $\{$*monotonic, non-monotonic*$\}$ properties of the GDFP which influence the type of $\{$*single-threshold, multi*-threshold$\}$ decision equations required to obtain the optimal solution.

2.2.1 GDFP properties

Monotonic property:

The GDFP is said to be monotonic when there exist an arbitrary function $T(\mathbf{u})$ [10,12] ($T : \mathbb{B}^N \mapsto \mathbb{R}$) such that

(i) it is a *sufficient statistic* [5] and $\Omega(\cdot)$ is monotonic on it, or

(ii) $\Lambda(\mathbb{P}_d, \mathbb{P}_f, \mathbf{u})$, $p(\mathbf{u}|H_1)$ and $p(\mathbf{u}|H_0)$ are all monotonic on it.

Further there are two scenarios (case-A and case-B) in a monotonic problem which lead to a *single-threshold* and *multi-threshold* decision equation respectively.

<u>**case-A:**</u>

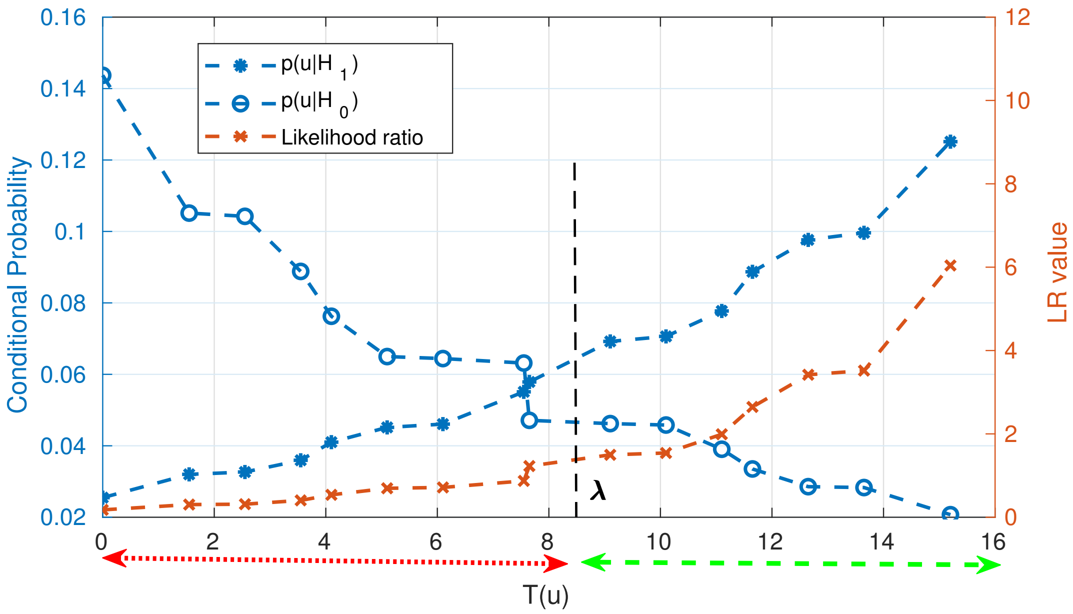

Figure 2.5: Illustration of the decision regions of a GDFP in $\mathbb{R}$ with monotonic case-A property.

In Figure 2.5, we plot the conditional probabilities of an example GDFP for $N = 4$ whose numerical values are provided in Appendix B.1. A $T(\mathbf{u})$ function is chosen

[5] A statistic $T(\mathbf{u})$ is a sufficient statistic for $\{\mathbb{P}_d, \mathbb{P}_f\}$ if the conditional distribution of the sample $\mathbf{u}$ given the value of $T(\mathbf{u})$ does not depend on $\{\mathbb{P}_d, \mathbb{P}_f\}$ [29].

(given by (B.1)) such that the LR function $\Lambda(\cdot)$ is monotonic on it. Further note from the figure that $p(\mathbf{u}|H_1)$ and $p(\mathbf{u}|H_0)$ are also monotonic on the chosen $T(\mathbf{u})$,

(i) $p(\mathbf{u}|H_1)$ is *non-decreasing* and $p(\mathbf{u}|H_0)$ is *non-increasing* with $T(\mathbf{u})$, as a result

(ii) the optimal decision regions $\{\mathfrak{R}_0, \mathfrak{R}_1\}$ (represented by *red dotted* marker and *green dashed* marker respectively under the real-line) are connected under NP criterion (Lemma 2.2.1) and a *single-threshold* suffices for the decision equations (2.7) and (2.9), thereby simplifying the computations for obtaining the optimum solution.

Lemma 2.2.1. *The optimal decision regions $\{\mathfrak{R}_0, \mathfrak{R}_1\}$ are connected under NP criterion for a monotonic case-A problem.*

Proof: (By contradiction) Without loss of generality, consider

$$\cdots < T(\mathbf{u}_{m-1}) < T(\mathbf{u}_m) < T(\mathbf{u}_{m+1}) < \cdots$$

then,

$$\begin{aligned} \cdots < p(\mathbf{u}_{m-1}|H_1) < p(\mathbf{u}_m|H_1) < p(\mathbf{u}_{m+1}|H_1) < \cdots \quad &\text{and} \\ \cdots > p(\mathbf{u}_{m-1}|H_0) > p(\mathbf{u}_m|H_0) > p(\mathbf{u}_{m+1}|H_)) > \cdots \quad &. \end{aligned} \tag{2.10}$$

Assume an optimal decision region that is not simply connected exists. i.e., $\{\mathbf{u}_m\} \in \mathfrak{R}_0$ and $\{\mathbf{u}_{m-1}, \mathbf{u}_{m+1}\} \in \mathfrak{R}_1$. Then from (2.1) we have,

$$P_D^* = \sum_{\mathbf{u}\in\mathfrak{R}_1} p(\mathbf{u}|H_1), \tag{2.11}$$

$$\left(P_F^* = \sum_{\mathbf{u}\in\mathfrak{R}_1} p(\mathbf{u}|H_0)\right) \leq \alpha. \tag{2.12}$$

However from (2.10) we have,

$$\left(P_D \triangleq P_D^* - p(\mathbf{u}_{m-1}|H_1) + p(\mathbf{u}_m|H_1)\right) > P_D^* \quad \textit{and}$$
$$\left(P_F \triangleq P_F^* - p(\mathbf{u}_{m-1}|H_0) + p(\mathbf{u}_m|H_0)\right) < \alpha \quad , \tag{2.13}$$

contradicting the assumption about the existence of a disconnected optimal decision region. ■

case-B:

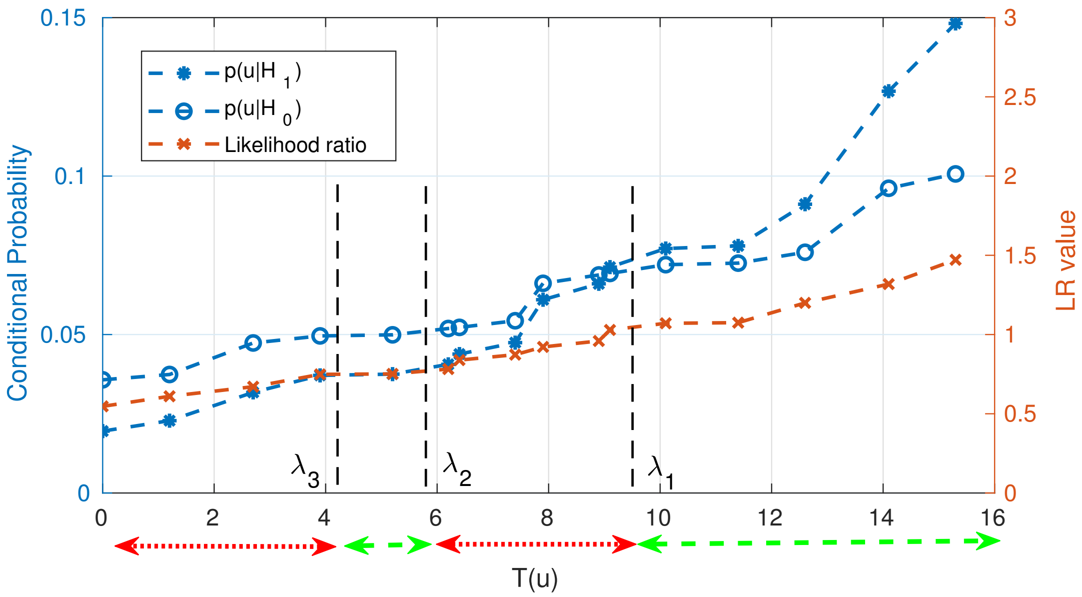

Figure 2.6: Illustration of the decision regions of a GDFP in $\mathbb{R}$ with monotonic case-B property.

In Figure 2.6, we plot the conditional probabilities of an example GDFP for $N = 4$ whose numerical values are provided in Appendix B.2. A $T(\mathbf{u})$ function is chosen (given by (B.2)) such that the LR function $\Lambda(\cdot)$ is monotonic on it. Further note from the figure that $p(\mathbf{u}|H_1)$ and $p(\mathbf{u}|H_0)$ are also monotonic on the chosen $T(\mathbf{u})$. However,

(i) $p(\mathbf{u}|H_1)$ and $p(\mathbf{u}|H_0)$ are both *non-decreasing* with $T(\mathbf{u})$, as a result

(ii) the optimal decision regions $\{\mathfrak{R}_0, \mathfrak{R}_1\}$ (represented by *red dotted* marker and *green dashed* marker respectively under the real-line) are generally not connected under NP criterion [10] and *multi-thresholds* are required for (2.7) and (2.9), there by complicating the computations for obtaining the optimum solution.

non-Monotonic property:

The GDFP is said to be non-monotonic when

(i) no *sufficient statistic* function exist or

(ii) no function $T(\mathbf{u})$ exist on which $\Lambda(\cdot)$, $p(\mathbf{u}|H_1)$ and $p(\mathbf{u}|H_0)$ are all monotonic.

In Figure 2.7, we plot the conditional probabilities of an example GDFP for $N = 4$ whose numerical values are provided in Appendix B.3. As seen from the figure, in this non-monotonic case both $p(\mathbf{u}|H_1)$ and $p(\mathbf{u}|H_0)$ are non-monotonic on the $T(\mathbf{u})$ of (B.3), where as $\Lambda(\cdot)$ is monotonic (as shown in Table B.6).

Note that in this case

(i) $p(\mathbf{u}|H_1)$ and $p(\mathbf{u}|H_0)$ are non-monotonic on $T(\mathbf{u})$, where as $\Lambda(\cdot)$ is monotonic. In this case, no function $T(\mathbf{u})$ exists on which all the three functions are monotonic.

(ii) the optimal decision regions $\{\mathfrak{R}_0, \mathfrak{R}_1\}$ are not simply connected [10] and the decision equations (2.7) and (2.9) require multi-thresholds, there by complicating the computations for obtaining the optimum solution in this case.

Table 2.3 summarizes the different properties considered in this subsection and their corresponding optimal decision equations.

The property of a particular GDFP is based on its realization of the $\{\mathbb{P}_d, \mathbb{P}_f\}$ distribution family. We now focus on analytical classification of the GDFP instances based on their properties.

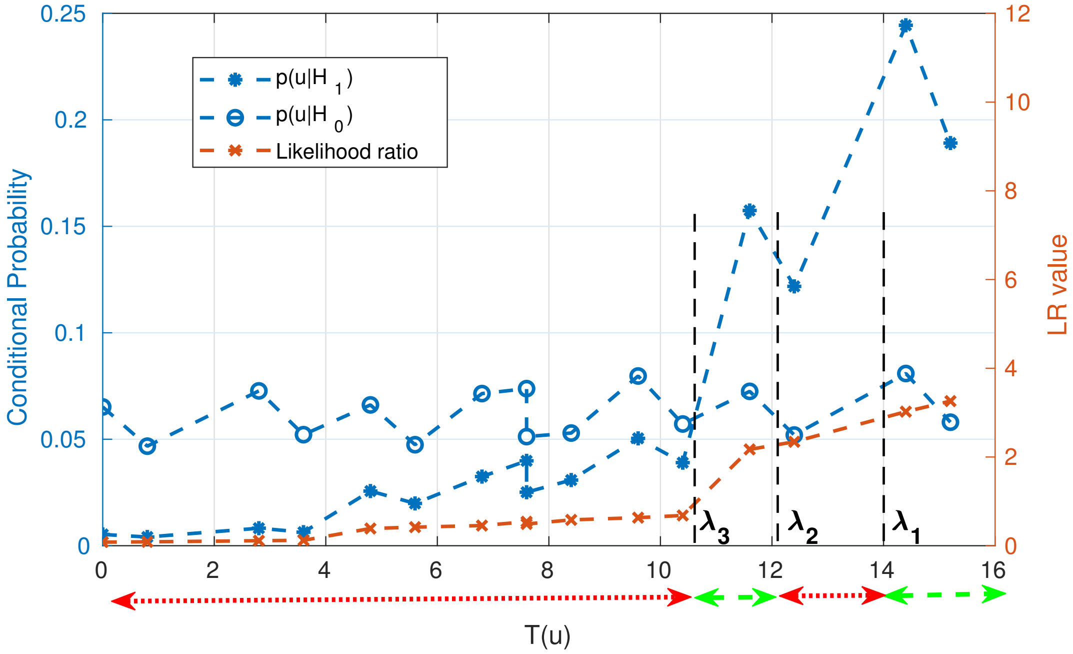

Figure 2.7: Illustration of the decision regions of a GDFP in $\mathbb{R}$ with non-monotonic property.

Table 2.3: Summary of GDFP properties and decision equations under NP Criterion

GDFP property	**Optimal Decision Equation**
monotonic case-A	single-threshold
monotonic case-B	multi-threshold
non-monotonic	multi-threshold

2.2.2 GDFP Classification

Remark 2.2.2.1 (**Independent Homogeneous**). Consider a system with identical (Homogeneous) and independent SUs, i.e., $P_{d_i} = P_d$, $P_{f_i} = P_f$, $\forall i$ and $P_d > P_f$, as in [15, 16]. Then $\Omega(\cdot)$ of (2.9) can be factored as

$$\Omega(\mathbb{P}_d, \mathbb{P}_f, \mathbf{u}) \;=\; g(P_d, P_f)\, T(\mathbf{u}), \tag{2.14}$$

where $T(\mathbf{u}) = \sum_{i=0}^{N-1} u_i$.

(i) From the definition of *factorization criterion* in [12], the factor $T(\mathbf{u})$ is the sufficient statistic of $\Omega(\cdot)$ as it is independent of the parameter family $\{\mathbb{P}_d, \mathbb{P}_f\}$ in this case.

(ii) As the factor $g(P_d, P_f)$ is always positive for all $P_d > P_f$, $\Omega(\cdot)$ is increasing on $T(\mathbf{u})$, thereby implying the GDFP is monotonic for this case.

As a result, (2.9) can be replaced with the *sufficient statistic test* as [16],

$$k \underset{u_{fc}=0}{\overset{u_{fc}=1}{\gtrless}} \omega_k, \quad \text{where } k \triangleq \sum_{i=0}^{N-1} u_i. \tag{2.15}$$

However, with the given system knowledge of the GDFP, this case cannot be classified into the desirable monotonic case-A, there by requiring a multi-threshold decision equation under NP criterion in the general case.

Remark 2.2.2.2 (**Independent Homogeneous with** $P_d > 0.5 > P_f$). With an additional assumption that $P_d > 0.5 > P_f$ for the *Remark* 2.2.2.1 class, the conditional probability $p(\mathbf{u}|H_1)$ becomes non-decreasing with k and $p(\mathbf{u}|H_0)$ becomes non-increasing. As a result, this case can be classified as monotonic case-A.

Remark 2.2.2.3 (**Independent Heterogenous case**). For the general values of $P_{d_i}, P_{f_i}, \forall i$, the function $\Omega(\cdot)$ of (2.9) is non-separable as required by the *factorization criterion* [12], thereby implying that a *sufficient statistic* does not exist and the GDFP is non-monotonic for the most general case.

Remark 2.2.2.4 (**Dependent General case**). Similar to Remark 2.2.2.3, the GDFP for a system with dependent SU decisions for which joint conditional pmfs, $p(\mathbf{u}|H_0)$ and $p(\mathbf{u}|H_1)$ are obtainable as in [18] can be shown to be non-monotonic in the most general case as $\Lambda(\cdot)$ of (2.7) is non-separable.

Table 2.4 lists the GDFP instances and their class covered in this subsection. The complete classification of the special cases of the GDFP into monotonic/non-monotonic problems is not covered in this chapter. It needs to be addressed separately.

Table 2.4: Summary of GDFP Instances and their class

GDFP Instance	**Class**
Independent Homogeneous ($P_{d_i} = P_d,\ P_{f_i} = P_f,\ \forall i$)	monotonic case-B
Independent Homogeneous with $P_f < 0.5 < P_d$	monotonic case-A
Independent Heterogenous	non-monotonic
Dependent General	non-monotonic

However, for the most general case (with both independent/dependent SU decisions), the optimal decision regions $\{\mathfrak{R}_0, \mathfrak{R}_1\}$ are not simply connected and the decision equation (2.7), (2.9) requires multi-thresholds thereby complicating the computations. To alleviate this difficulty, we now reformulate the GDFP and then related it to the $0-1$ Knapsack problem.

2.3 Decision Region-based Fusion Rule

Define a binary-valued vector $\mathbf{x} \triangleq [x_{M-1} \cdots x_0]^T$, each element of which corresponds to an observation vector in the observation space $\mathcal{U}$, and where $x_m = 0$ implies $\mathbf{u}_m \in \mathfrak{R}_0$ and $x_m = 1$ implies $\mathbf{u}_m \in \mathfrak{R}_1$ respectively. Using this notation, (2.1) can be rewritten as,

$$P_D(\mathbf{x}) = \sum_{m=0}^{M-1} x_m\ p(\mathbf{u}_m|H_1), \qquad P_F(\mathbf{x}) = \sum_{m=0}^{M-1} x_m\ p(\mathbf{u}_m|H_0). \tag{2.16}$$

Using (2.16), the GDFP of (2.2) can now be written as,

$$\underset{\mathbf{x}}{\text{Max}}\ C_D\ P_D(\mathbf{x}) - C_F\ P_F(\mathbf{x}), \quad \text{Sub to: } P_F(\mathbf{x})\ \leq \alpha. \tag{2.17}$$

Note that, x_m is the truth table value corresponding to the binary-valued observation vector $\mathbf{u}_m, \forall m$. As a result the optimal fusion rule $\Gamma(.)$, can now be implemented as a boolean switching equation using binary variables $u_i, \forall i$ and the optimal vector

$\mathbf{x}^*$. This *boolean equation generalizes* (i) the single-threshold (*non-rand-st* LRT); (ii) the multi-threshold (*non-rand-mt* LRT) decision equation (2.7), (2.9) of the general cases; and (iii) the K-out-of-N equation (2.15) of the monotonic case [30].

As an example, Figure 2.8 lists few fusion vectors out of the 2^4 values of vector $\mathbf{x}$ for $N = 2$. Note that the widely used rules like 'OR', 'AND', 'MAJORITY' etc., are special cases of the fusion rules that $\mathbf{x}$ can represent.

$M = 2^N (= 2^2)$

	$\mathbf{u}_3$	$\mathbf{u}_2$	$\mathbf{u}_1$	$\mathbf{u}_0$	
u_1	1	1	0	0	$N(= 2)$
u_0	1	0	1	0	
$\mathbf{x} \triangleq$	$[x_3$	x_2	x_1	$x_0]$	
	1	1	1	1	
OR $\rightarrow$	1	1	1	0	
	$\vdots$				
AND $\rightarrow$	1	0	0	0	$2^M = 2^{2^N}$
	0	1	1	1	
	$\vdots$				
	0	0	0	0	

Figure 2.8: Example fusion vectors for $N = 2$.

A total of $2^M (= 2^{2^N})$ distinct fusion vectors ($\mathbf{x}$) are possible, thereby implying that an exhaustive search for the optimum $\mathbf{x}^*$ has an *exponential complexity* in M and *double exponential complexity* in N. As an example, note that for $N = 10$ a total of $2^{2^{10}} (= 2^{1024})$ fusion vectors are possible there by making the exhaustive search mechanism intractable even for small value of N.

However, the GDFP as defined in (2.17) is in the form of the $0 - 1$ Knapsack problem (KP) [31,32], implying that existing efficient solutions can be re-used for the GDFP.

2.4 $0-1$ Knapsack Problem

Definition 2.4.1 ($0-1$ Knapsack problem (KP) [31])**.** Given a set of M items, each with a value and weight $\{V_m, W_m\}$ respectively for $0 \leq m \leq M-1$, choose a subset $\mathbf{s}$, of items such that

$$\underset{\mathbf{s}}{\text{Max}} \sum_{m=0}^{M-1} s_m V_m, \quad \text{Sub to:} \sum_{m=0}^{M-1} s_m W_m \leq W_{lim}, \tag{2.18}$$

where $\mathbf{s} \triangleq [s_{M-1} \cdots s_0]$, $s_m = 0$ implies the item m is *left-out*, $s_m = 1$ implies it is *chosen* and W_{lim} is the total weight limit allowed.

For a better appreciation of the $0-1$ Knapsack problem, we present two simple numerical examples one each with monotonic case-A and non-monotonic property.

2.4.1 Example of a monotonic $0-1$ KP:

Select items from the list 0 to 3 (*blue dotted* cuboids) depicted in the Figure 2.9 and place them in the red box (Knapsack) such that the total value of the items selected is maximized and the weight limit of the box (i.e., 10 kg in this case) is not violated.

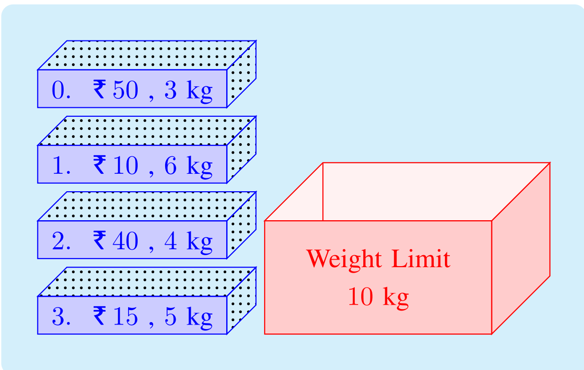

Figure 2.9: Example monotonic problem with $M = 4$.

Table 2.5 lists the items in descending order of their value-weight ratio $(\frac{V_m}{W_m})$ i.e., $\{0, 2, 3, 1\}$. Note that in this case, this sequence results in the values to be in descending order and the weights to be in the ascending order implying that the problem is monotonic. The optimum solution $\mathbf{s}$ is then obtained by sequentially selecting the items with highest ratio until the weight limit of the box is not violated. As a result the maximum value of ₹ 90 and weight 7 kg is obtained when items $\{0, 2\}$ are placed in the box.

Table 2.5: Items sorted based on value-weight ratio

Item (m)	Value (V_m)	Weight (W_m)	Ratio ($\frac{V_m}{W_m}$)	Selection †(s_m)
0	50	3	16.7	1
2	40	4	10.0	1
3	15	5	3.0	0
1	10	6	1.7	0

† Optimum Selection

Also note that the optimum solution can be obtained by a single-threshold decision equation by using an appropriate threshold value λ. The decision equation analogous to the LR-based Test (*non-rand-st* LRT) is given as

$$\frac{V_m}{W_m} \underset{s_m=0}{\overset{s_m=1}{\gtrless}} \lambda, \tag{2.19}$$

with the threshold λ chosen as $3.0 < \lambda < 10.0$ for this example.

However for a non-monotonic problem, a single-threshold decision equation does not suffice to obtain an optimal solution. This is apparent from the below non-monotonic numerical example with slightly different item characteristic values.

2.4.2 Example of a non-monotonic $0 - 1$ KP:

Table 2.6 lists the items in descending order of their value-weight ratio ($\frac{V_m}{W_m}$) i.e., $\{0, 2, 3, 1\}$. Note that both the values and the weights are not in any particular order in this case, there by implying that the problem is non-monotonic. The optimum solution can be obtained only with the exhaustive search of all the combinations (i.e.,

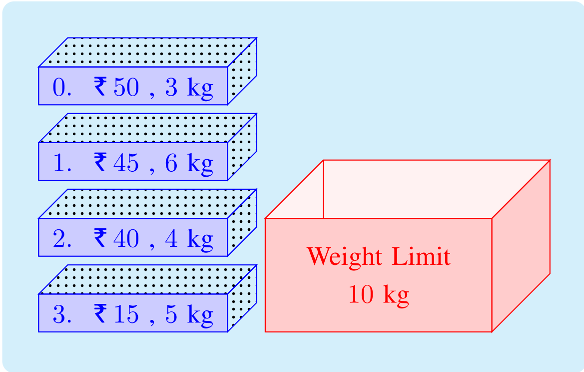

Figure 2.10: Example non-monotonic problem with $M = 4$.

2^4 searches in this case). A maximum value of ₹ 95 and weight 9 kg is obtained when items $\{0, 1\}$ are placed in the box. However note that this choice is not from among the items with the highest value-weight ratio. Thereby implying that a decision equation (2.19) with multi-thresholds (*non-rand-mt* LRT) is required in this case to obtain the optimal result.

Table 2.6: Items sorted based on value-weight ratio

Item (m)	Value (V_m)	Weight (W_m)	Ratio ($\frac{V_m}{W_m}$)	Selection $^\dagger(s_m)$
0	50	3	16.7	1
2	40	4	10.0	0
1	45	6	7.5	1
3	15	5	3.0	0

† Optimum Selection

Also note that applying the low-complexity *non-rand-st* LRT for this case results in a slightly sub-optimal result of ₹ 90 and weight 7 kg.

2.5 GDFP and $0-1$ Knapsack Problem

To the best of our knowledge, the non-randomized hard decision fusion problem is being mapped to the $0-1$ Knapsack problem for the first time.

Theorem 2.5.1. *The GDFP defined in (2.17) is a* $0-1$ *KP (2.18).*

Proof: Define individual objective and constrained parameter corresponding to a observation vector $\mathbf{u}_m$ *as:*

$$\begin{aligned} R_M(m) &\triangleq C_D\, p(\mathbf{u}_m|H_1) - C_F\, p(\mathbf{u}_m|H_0), \\ P_{F_M}(m) &\triangleq p(\mathbf{u}_m|H_0). \end{aligned} \tag{2.20}$$

Then, using (2.16), (2.20), the GDFP of (2.17) can be written as,

$$\underset{\mathbf{x}}{Max} \sum_{m=0}^{M-1} x_m R_M(m), \quad \textit{Sub to:} \sum_{m=0}^{M-1} x_m P_{F_M}(m) \ \le \alpha, \tag{2.21}$$

which by Definition 2.4.1, is a $0-1$ *KP where* $V_m = R_M(m)$*,* $W_m = P_{F_M}(m)$*,* $W_{lim} = \alpha$ *and* $\mathbf{s} = \mathbf{x}$. ■

Now, using the *sufficient statistic* k of the *Remark* 2.2.2.1 monotonic case, define a set of observation vectors with same k value as $\mathcal{U}_k \triangleq \{\mathbf{u}_m : T(\mathbf{u}_m) = k, \forall m\}, \forall k$, and a corresponding vector $\mathbf{y} \triangleq [y_N \cdots y_0]^T$, where $y_k = 0$ implies $\mathcal{U}_k \in \mathfrak{R}_0$ and $y_k = 1$ implies $\mathcal{U}_k \in \mathfrak{R}_1$ respectively. Then the GDFP of (2.17) for this case can be written as,

$$\underset{\mathbf{y}}{\text{Max}} \sum_{k=0}^{N} y_k R_K(k), \quad \text{Sub to:} \sum_{k=0}^{N} y_k P_{F_K}(k) \ \le \alpha, \tag{2.22}$$

where

$$\begin{aligned} R_K(k) &\triangleq C_D\, p(\mathcal{U}_k|H_1) - C_F\, p(\mathcal{U}_k|H_0), \\ P_{F_K}(k) &\triangleq p(\mathcal{U}_k|H_0) \end{aligned} \tag{2.23}$$

and where

$$\begin{aligned} p(\mathcal{U}_k|H_1) &= \binom{N}{k} (P_d)^k (\bar{P}_d)^{N-k}, \\ p(\mathcal{U}_k|H_0) &= \binom{N}{k} (P_f)^k (\bar{P}_f)^{N-k}. \end{aligned} \tag{2.24}$$

2.5.1 GDFP Solution using Dynamic Programming

It is well known that the $0-1$ KP can be solved using *dynamic programming* (DP) [33, 34]. We now present a recursive equation and an algorithm that searches the solution space for the optimum vector $\mathbf{x}^*$ for the GDFP of (2.21) in pseudo-polynomial time in the worst case. Define a parameterized GDFP $\mathbf{G}(a, b)$, as:

$$\mathbf{G}(a,b) \triangleq \begin{cases} \underset{\mathbf{x_a}}{\text{Max}} & \sum_{m=0}^{a} x_m R_M(m), \\ \text{Sub to:} & \sum_{m=0}^{a} x_m P_{F_M}(m) \leq b, \end{cases} \tag{2.25}$$

where $\mathbf{x_a}$ is the later part of vector $\mathbf{x}$ such that $\mathbf{x_a} = [x_a \cdots x_0]$, $\{a \in \mathbb{N} : 0 \leq a < M\}$ and b is a constraint variable, $\{b \in \mathbb{R} : 0 \leq b \leq \alpha\}$. Equation (2.25) can be rewritten in the form of a recursive equation as,

$$\mathbf{G}(a,b) = \max\Big\{R_M(a) + \mathbf{G}(a-1, b - P_{F_M}(a)), \quad \mathbf{G}(a-1,b)\Big\}, \tag{2.26}$$

with initial conditions as,

$$\begin{aligned} \mathbf{G}(0,b) =& \begin{cases} 0 & \text{for } 0 \leq b < P_{F_M}(0), \\ \max\{0, R_M(0)\} & \text{for } P_{F_M}(0) \leq b \leq \alpha, \end{cases} \\ \mathbf{G}(a,0) =&\ 0 \qquad\qquad\qquad \text{for } 0 \leq a \leq M-1. \end{aligned} \tag{2.27}$$

Note that in (2.26) the GDFP of (2.21) is recursively split into sub-GDFP problems. To implement (2.26) as an algorithm, DP requires the constrained parameter $P_{F_M}(\cdot), \forall m$ be mapped one-to-one to the integer scale. To facilitate this, we define a scaling function $I(r) \triangleq \lfloor C \cdot r + \frac{1}{2} \rfloor$, $(\mathbb{R}_{\geq 0} \mapsto \mathbb{N}_{\geq 0})$ where r is a real-valued non-negative input argument, C is a positive scaling factor and $\lfloor \cdot \rfloor$ is the integer floor function. We map the required parameters of (2.26) and (2.27) one-to-one to the integer scale as $P_{F_M}[m] \triangleq I(P_{F_M}(m)), \forall m$; $I_\alpha \triangleq I(\alpha)$ and $\{I_b \in \mathbb{N}_{\geq 0} : I_b \leq I_\alpha\}$. Note that the scaling factor C needs to be sufficiently large such that $P_{F_M}[m] > 0, \forall m$.

The complete algorithm for (2.26) is presented in *Algorithm* 1, which uses a two dimensional array $\mathbf{G}[\cdot,\cdot]_{M\times I_\alpha}$ (depicted in Figure 2.11) to hold the results of the sub-problems $\mathbf{G}(\cdot,\cdot)$ of (2.26).

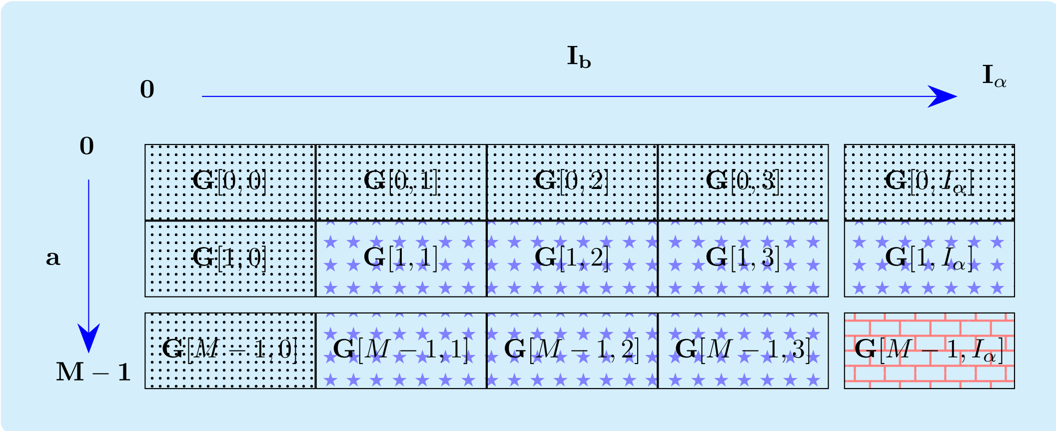

Figure 2.11: Illustration of two dimensional array to hold the results of the sub-problems.

Algorithm 1 DP Solution for GDFP

1: Initialize $\mathbf{G}[\cdot,\cdot]$ with (2.27)
2: **for** $a \leftarrow 1$ to $(M-1)$ **do**
3:     **for** $I_b \leftarrow 1$ to I_α **do**
4:         **if** $P_{F_M}[a] \leq I_b$ **then**
5:             $\mathbf{G}[a, I_b] = \max\Big\{R_M(a) + \mathbf{G}[a-1, I_b - P_{F_M}[a]],\ \mathbf{G}[a-1, I_b]\Big\}$
6:         **else**
7:             $\mathbf{G}[a, I_b] = \mathbf{G}[a-1, I_b]$
8:         **end if**
9:     **end for**
10: **end for**
11: $\mathbf{x}^* \leftarrow \text{getTrace}(\mathbf{G})$

Using the initial values given in (2.27) (represented by the *dotted* cells in Figure 2.11) the *Algorithm* 1 incrementally solves sub-problems (represented by the *star* pattern in Figure 2.11) by looping through variable a (line 2) and I_b (line 3). This results in the maximized objective value of the GDFP (2.21) to be populated into the cell $\mathbf{G}[M-1, I_\alpha]$ (represented by the *brick* pattern in Figure 2.11). The array is then scanned backwards to trace and mark the contributing indices a, to form the optimum vector $\mathbf{x}^*$.

2.5.2 Example application of the algorithm

In this subsection, we apply the dynamic programming algorithm to the example non-monotonic KP problem presented in subsection 2.4.2 given by the Table 2.7.

Table 2.7: Items and their values

Item id (m)	Value (V_m)	Weight (W_m)
0	50	3
1	45	6
2	40	4
3	15	5

In this case the variable a represents the item id and is $a \in \{0, 1, 2, 3\}$. The variable b represents the weights and $\alpha = 10$ Kgs. Note that in this example as the weights are integers, no further scaling is required. Further, in the specified example, the parameterized GDFP $\mathbf{G}(3, 10)$ represents the main problem to be solved.

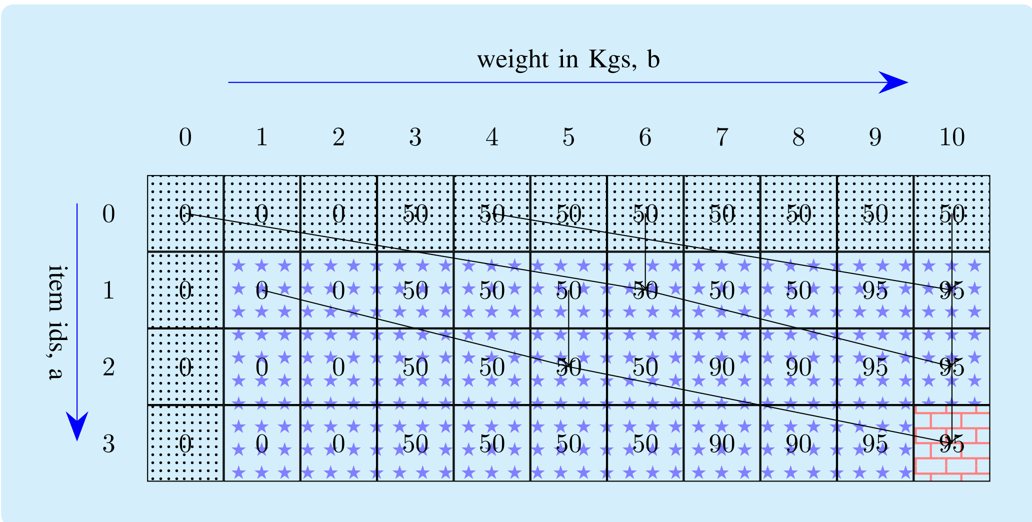

Figure 2.12: Two dimensional array with the results of the sub-problems.

Figure 2.12 represents the two dimensional array populated with the results of the sub-problems $\mathbf{G}(a, b)$ represented by each cell. Each result is obtained using the equivalent of (2.26) given as,

$$\mathbf{G}(a, b) = \max\Big\{V_a + \mathbf{G}(a-1, b-W_a), \quad \mathbf{G}(a-1, b)\Big\}. \tag{2.28}$$

Using (2.28), the main result of the example (cell with *brick* pattern) is obtained as

$$\mathbf{G}(3, 10) = \max\Big\{15 + \mathbf{G}(2, 5), \quad \mathbf{G}(2, 10)\Big\}. \tag{2.29}$$

Similarly, the results for $\mathbf{G}(2, 5)$ and $\mathbf{G}(2, 10)$ are further recursively obtained by lower sub-problems (connected by the arrows in the figure).

2.5.3 Computation complexities

For the general case under the NP criterion, *Algorithm* 1 takes a maximum of three flops to solve each sub-problem (line 4 to 8), and the *getTrace()* method (line 11) requires M flops in the worst case. As a result, a total of $3\, I_\alpha\, (M-1) + M$ flops are required to compute the optimum vector $\mathbf{x}^*$ for the GDFP (2.21) in the worst case.

For the monotonic case-B under the NP criterion, while the GDFP of (2.21) provides the optimal fusion rule, the GDFP of (2.22) reduces computation complexity to $3\, I_\alpha N + (N+1)$ flops at the cost of sub-optimal fusion rule for certain values of α, i.e., when $P_{F_K}(\mathbf{y}^*) < P_{F_M}(\mathbf{x}^*) \leq \alpha$.

For the monotonic case-A in Remark 2.2.2.2 the GDFP of (2.21) reduces in complexity under NP criterion. For this case, consider the observation vectors $\mathbf{u}_m$ are sequenced in non-decreasing order of their k value, i.e., $T(\mathbf{u}_m) \leq T(\mathbf{u}_{m+1})$, $0 \leq m < (M-1)$. Then the conditional probabilities $p(\mathbf{u}_m|H_1)$ and $p(\mathbf{u}_m|H_0)$ become non-decreasing and non-increasing on m respectively. Index a^* can now be identified in linear time in the worst case, such that $\sum_{m=a^*-1}^{M-1} P_{F_M}(m) > \alpha \geq \sum_{m=a^*}^{M-1} P_{F_M}(m)$. The fusion vector $\mathbf{x}^*$ is then set as $x_m = 0, \forall m < a^*$ and $x_m = 1, \forall m \geq a^*$.

Note that under the Bayesian criterion, the constraining loop on I_b in the *Algorithm* 1 is redundant and each sub-problem on a, $\mathbf{G}[a] = \max\{R_M(a)+\mathbf{G}[a-1], \mathbf{G}[a-1]\}$ requires only 1 flop. Consequently the worst case computational complexity is M for the GDFP of (2.21) and $N+1$ for (2.22) respectively, as in [15–18]. Table 2.8 summarizes the algorithmic complexities discussed in this section.

Table 2.8: Worst-case algorithmic complexities in FLOPS

Special cases of GDFP	**Bayesian**	**Neyman-Pearson**
General (Remark 2.2.2.3, 2.2.2.4): $P_{f_i} < P_{d_i}, \forall i$	M	$3\, I_\alpha\, (M-1) + M$
Monotonic case-B (Remark 2.2.2.1): $(P_{f_i} = P_f) < (P_{d_i} = P_d), \forall i$	(N+1)	$3\, I_\alpha\, N + (N+1)$
Monotonic case-A (Remark 2.2.2.2): $(P_{f_i} = P_f) < 0.5 < (P_{d_i} = P_d), \forall i$	(N+1)	M

Computational complexity to compute the fusion rule, the optimum P_D, P_F (under NP criterion) and P_E (under Bayesian).

2.6 Numerical results and Discussions

To validate the effectiveness of the proposed algorithm, as an example we consider each SU to be using energy detector with different local thresholds ϵ_i, common time-bandwidth product L, and experiencing different received signal-to-noise ratios γ_i, over additive white Gaussian noise. The expressions for P_{f_i} and P_{d_i} are given as [35]

$$\begin{aligned} P_{f_i} &= \frac{\Gamma(L, \frac{\epsilon_i}{2})}{\Gamma(L)} \\ P_{d_i} &= \mathcal{Q}_L(\sqrt{2L\gamma_i}, \sqrt{\epsilon_i}), \end{aligned} \tag{2.30}$$

where $\Gamma(\cdot,\cdot)$ is incomplete Gamma function and $\mathcal{Q}_L(\cdot,\cdot)$ is generalized Marcum Q-function. We consider $\gamma_i = -15 + \frac{15\,i}{N-1}$ dB, $\epsilon_i = 21 + \frac{2\,i}{N-1}$, $\forall i \in \{0, \cdots, N-1\}$ and $L = 10$. As a result we obtain $(P_{f_i}, P_{d_i}) \in \{(0.40, 0.44), \cdots, (0.29, 0.96)\}$.

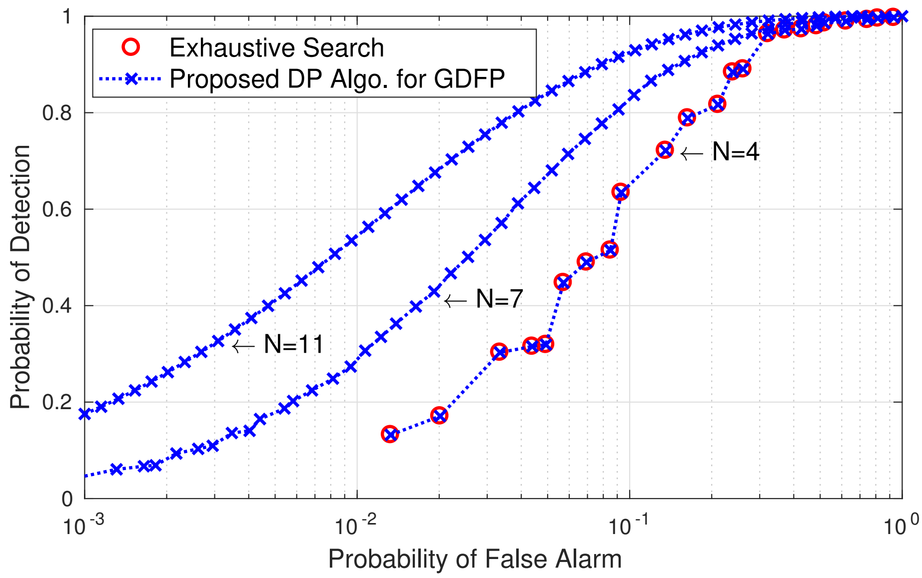

Figure 2.13: Optimum P_D vs P_F plot for the General GDFP under NP Criterion for $N = 4, 7$ and 11.

Figure 2.13 plots the performance points P_D^* Vs P_F^* obtained by the fusion rules for the GDFP under NP criterion using exhaustive search and the proposed *Algorithm* 1 (labelled *"Exhaustive Search"* and *"Proposed DP Algo. for GDFP"*) by varying α in uniform steps. For $N = 4$, as few discrete optimum P_D^* and P_F^* value pairs are obtainable, the curve is not uniformly spaced.

Note that the optimum performance points plotted using the proposed GDFP solution exactly match the exhaustive search results for $N = 4$. For larger values of N, the exhaustive search requires prohibitively large resources and it is intractable to obtain the optimum solution using this method. Whereas, the optimum solutions are easily obtained using the proposed DP algorithm for even $N = 11$.

As listed in Table 2.9 the number of flops required for exhaustive search grow double exponentially with N and get impractical even for small values of N. As an example, for $N = 11$ and $\alpha = 0.01$, the exhaustive search requires $\approx 10^{616}$ flops, whereas the proposed algorithm requires only $\approx 61 \times 10^5$ flops when $C = 10^5$ is used.

Focusing on the limitations, note that the GDFP solution based on dynamic

Table 2.9: Numerical values of worst-case solution complexities in FLOPS

N	**Exh. Search**	**GDFP**	monotonic **GDFP**
4	$\approx 10^6$	$\approx 45\times10^3$	16
5	$\approx 10^{10}$	$\approx 93\times10^3$	32
7	$\approx 10^{38}$	$\approx 38\times10^4$	128
11	$\approx 10^{616}$	$\approx 61\times10^5$	2048

$\alpha = 0.01$ and $C = 10^5$ is used.

programming is practically constrained by the dimensionality (M, I_α) of the problem. The dimension I_α is dependent on the scaling factor C, which needs to be sufficiently large such that the scaled values of $P_{F_M}(m)$, i.e., $P_{F_M}[m] > 0, \forall m$. As a result the dimension I_α becomes large and impractical for scenarios when $\min\{P_{F_M}(m), \forall m\} \ll 10^{-5}$.

Alternative solutions based on branch and bound technique etc., [31, 32] maybe applied to such high-precision GDFP and are discussed in subsequent chapters.

2.7 Conclusions

A generalized decision fusion problem (GDFP) is formulated that allows monotonic/non-monotonic, independent/dependent decisions problems under Bayesian and NP criterion as special cases. The proposed GDFP is shown to be in the form of $0-1$ Knapsack problem and a solution in *pseudo*-polynomial time worst case complexity has been presented. Further, this approach has the potential to be applied to broader categories of problems such as the following:

(i) the C-OS problems using softened hard approach in [21, 24, 36];

(ii) unknown SU characteristics as in [37, 38];

(iii) decision / fusion rule joint optimization as in [26, 39–41];

(iv) generalization of conditionally dependent decisions as in [42];

(v) SU censoring as in [43–46];

(vi) non-ideal reporting channels as in [47].

Chapter 3

Reduced Complexity Optimal Hard Decision Fusion under Neyman-Pearson Criterion

3.1 Introduction

It was shown in Chapter 2 that non-randomized hard decision fusion under Neyman-Pearson criterion is a NP-hard $0-1$ knapsack problem with exponential complexity in general. A pseudo-polynomial complexity dynamic programming based solution was proposed for the same.

In this chapter, we show that the decision fusion problem exhibits *semi-monotonic* property in a relevant case. We propose to exploit this property to reduce the dimension of the feasible solution space. Subsequently, we apply dynamic programming to efficiently solve the problem with further reduction in complexity under Neyman-Pearson Criterion. Numerical results are provided to verify the correctness of the proposed solution.

The main contributions are:

(i) To the best of our knowledge, for the first time we show that a non-monotonic decision fusion problem exhibits the desired monotonic property locally (namely *semi-monotonic*) in a relevant case.

(ii) We show that this property reduces the dimension of the optimal solution space (namely *variable reduction*).

(iii) Subsequently, we apply dynamic programming technique to obtain the solution with further reduced complexity under Neyman-Pearson Criterion.

(iv) We provide numerical comparision of the performance (ROC) and the complexity of

   (a) the proposed *variable reduction* technique and

   (b) the solution of *generalized decision fusion problem* (GDFP) presented in chapter 2.

The outline of the chapter is as follows: Section 3.2 contains the system model, the DP-based solution for GDFP and is followed by the definition of the *semi-monotonic* property in Section 3.3. Section 3.4 contains the proposed solution for variable reduced GDFP followed by the numerical results in Section 3.5 and conclusions in Section 3.6.

3.2 System Model

We focus on GDFP under Neyman-Pearson criterion by substituting $C_D = 1$ and $C_F = 0$ in (2.17) and represented as,

$$\begin{aligned} \underset{\mathbf{x}}{\text{Max}} \quad & \sum_{m=0}^{M-1} x_m \; p(\mathbf{u}_m|H_1), \\ \text{Sub. to} \quad & \sum_{m=0}^{M-1} x_m \; p(\mathbf{u}_m|H_0) \leq \alpha, \quad x_m \in \{0,1\}, \end{aligned} \tag{3.1}$$

where α is the constrain on P_F. Under NP criterion this is a constrained optimization problem for which the solution is exponential in complexity i.e., $\mathcal{O}(2^M)$. The optimal fusion vector $\mathbf{x}^*$ is required to be searched from a solution space of $2^M (= 2^{2^N})$ observation vectors (as illustrated in Figure 3.1).

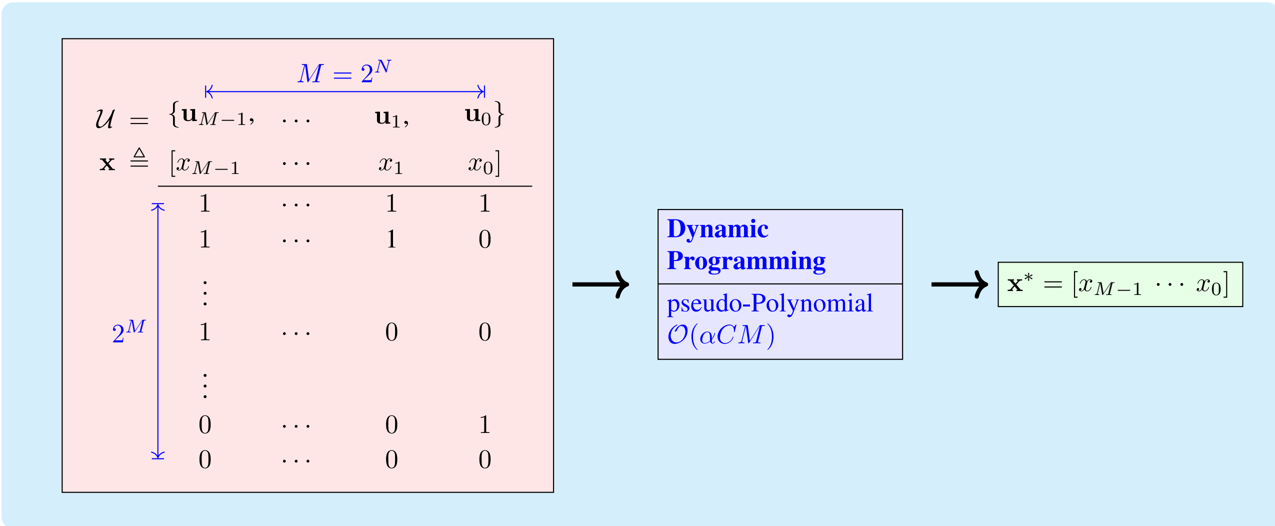

Figure 3.1: An illustration of DP applied to solution space of size 2^M.

In chapter 2 it was shown that in the most general case, the solution can be obtained in pseudo-polynomical time complexity i.e $\mathcal{O}(\alpha CM)$ using the dynamic programming (DP) concepts, where C is the scaling factor used to convert the conditional probability $p(\mathbf{u}|H_0)$ into integers.

However the proposed DP-based solution has the same best-case and worst-case complexity of $\mathcal{O}(\alpha CM)$. We now focus on further *reducing this complexity by showing that the optimum solution $\mathbf{x}^*$ is obtained by using a smaller dimensional observation space $\mathcal{U}'$* in some cases, where $|\mathcal{U}'| = 2^{M'}$ and where $M' < M$ (as illustrated in Figure 3.2).

To facilitate this we define a desirable property namely *semi-monotonic* in the next section.

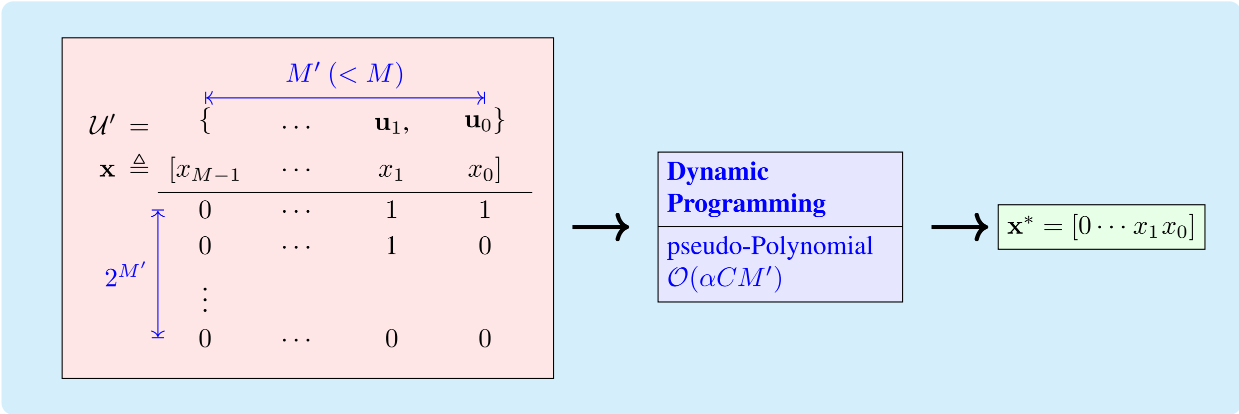

Figure 3.2: An illustration of DP applied to solution space of size $2^{M'}$.

3.3 Semi-Monotonic property

Define a set corresponding to an observation vector $\mathbf{u}_{m'}$ as

$$\mathcal{S}(\mathbf{u}_{m'}) \triangleq \Big\{ i \ : \ u_{i,m'} = 1, \ \forall i \Big\}. \tag{3.2}$$

Note that this set comprises indices of the SUs that have reported their local decision as '1' (i.e., hypothesis H_1) in the observation vector $\mathbf{u}_{m'}$.

Further define another set corresponding to an observation vector $\mathbf{u}_{m'}$ as

$$\mathbb{S}(\mathbf{u}_{m'}) \triangleq \Big\{ m \ : \ \mathcal{S}(\mathbf{u}_{m'}) \subsetneq \mathcal{S}(\mathbf{u}_m), \ \forall m \ \Big\}. \tag{3.3}$$

Note that this set comprises indices of other observation vectors that have one or more SUs reporting '1' in addition to those in $\mathbf{u}_{m'}$.

As an example, the observation vectors and their corresponding set $\mathcal{S}(\cdot)$ and $\mathbb{S}(\cdot)$ values are provided in the Table 3.1 for $N = 3$.

Definition 3.3.1 (semi-monotonic). We name a decision fusion problem as *semi-monotonic* if there exists subsets of the observation vectors on which the LR function and the conditional probabilities are monotonic as in case-A of (2.2.1). A numerical example of semi-monotonic GDFP for $N = 4$ is provided in the Appendix B.4.

Table 3.1: Values of $\mathcal{S}(\cdot)$ and $\mathbb{S}(\cdot)$ for an example with $N = 3$.

m'	$\mathbf{u}_{m'}$	$\mathcal{S}(\mathbf{u}_{m'})$	$\mathbb{S}(\mathbf{u}_{m'})$
0	$[0\,0\,0]^T$	$\{\}$	$\{1,2,3,4,5,6,7\}$
1	$[0\,0\,1]^T$	$\{0\}$	$\{3,5,7\}$
2	$[0\,1\,0]^T$	$\{1\}$	$\{3,6,7\}$
3	$[0\,1\,1]^T$	$\{0,1\}$	$\{7\}$
4	$[1\,0\,0]^T$	$\{2\}$	$\{5,6,7\}$
5	$[1\,0\,1]^T$	$\{0,2\}$	$\{7\}$
6	$[1\,1\,0]^T$	$\{1,2\}$	$\{7\}$
7	$[1\,1\,1]^T$	$\{0,1,2\}$	$\{\}$

Lemma 3.3.1. *GDFP with $P_{f_i} < 0.5 < P_{d_i}, \forall i$ is semi-monotonic.*

Proof: The simplified form of the LRT is given by (2.9)

$$\left[\Omega(\mathbf{u}_m) \triangleq \sum_{i=0}^{N-1} g(P_{d_i}, P_{f_i})\, u_{i,m}\right] \underset{x_m=0}{\overset{x_m=1}{\gtrless}} \omega, \tag{3.4}$$

where $g(P_{d_i}, P_{f_i}) \triangleq \log\left(\frac{P_{d_i}}{1-P_{d_i}} \frac{1-P_{f_i}}{P_{f_i}}\right)$. Note that for this special case, $\frac{P_{d_i}}{1-P_{d_i}} > 1$, $\frac{1-P_{f_i}}{P_{f_i}} > 1$ and thereby $g(\cdot,\cdot)$ is always positive $\forall i$. As a result, using (3.3) we get

$$\Omega(\mathbf{u}_{m'}) < \Omega(\mathbf{u}_m), \quad \forall m \in \mathbb{S}(\mathbf{u}_{m'}). \tag{3.5}$$

Further using (2.8) and (3.3) we get,

$$p(\mathbf{u}_{m'}|H_1) < p(\mathbf{u}_m|H_1), \quad \forall m \in \mathbb{S}(\mathbf{u}_{m'}), \tag{3.6}$$

$$p(\mathbf{u}_{m'}|H_0) > p(\mathbf{u}_m|H_0), \quad \forall m \in \mathbb{S}(\mathbf{u}_{m'}). \tag{3.7}$$

■

Figure 3.3 illustrates the semi-monotonic property exhibited by the observation vectors for $N = 3$. The SU-index set $\mathcal{S}(\mathbf{u}_t)$ of the observation vector at the tail of any

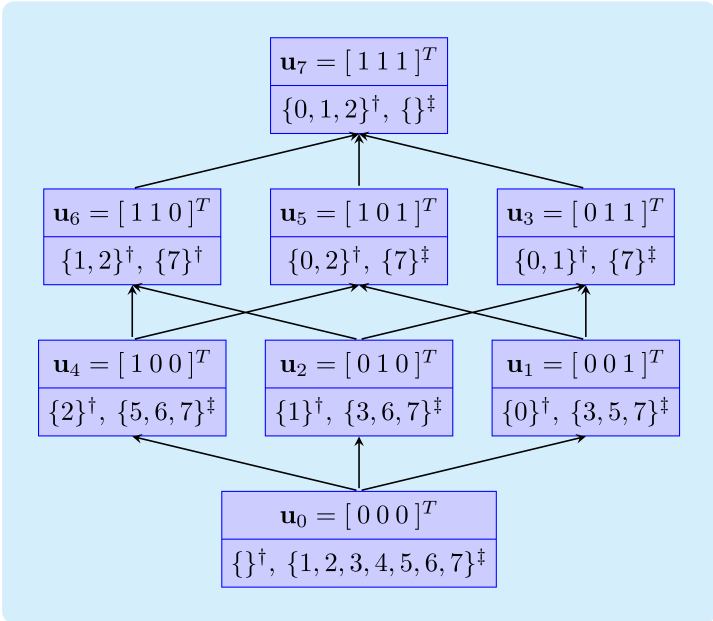

Figure 3.3: An illustration of semi-monotonic property exhibited by the observation vectors for $N = 3$. $\dagger$ represents $\mathcal{S}(\cdot)$ and $\ddagger$ represents $\mathbb{S}(\cdot)$

arbitrary arrow is the subset of the corresponding SU-index set $\mathcal{S}(\mathbf{u}_h)$ of the vector at the head of that arrow, i.e., $\mathcal{S}(\mathbf{u}_t) \subsetneq \mathcal{S}(\mathbf{u}_h)$, where $\{\mathbf{u}_t, \mathbf{u}_h\}$ denote the observation vectors at the tail and head of the arbitrary arrow.

Proposition 3.3.1. *In an optimal fusion rule $\mathbf{x}^*$ of GDFP (3.1), if $x_{m'} = 1$ then*

$$x_m = 1, \quad \forall m \in \mathbb{S}(\mathbf{u}_{m'}), \tag{3.8}$$

in the said fusion rule.

Proof: (by contradiction) Assume $P_F^*(x_{m'} = 1, x_{m_s} = 0)$ and $P_D^*(x_{m'} = 1, x_{m_s} = 0)$ be the system performance corresponding to an optimum fusion rule, where $m_s \in \mathbb{S}(\mathbf{u}_{m'})$.

But from (3.7) and (3.6) we get

$$\begin{aligned} P_D(x_{m'} = 0, x_{m_s} = 1) &> P_D^*(x_{m'} = 1, x_{m_s} = 0), \ \textit{and} \\ P_F(x_{m'} = 0, x_{m_s} = 1) &< \alpha, \end{aligned}$$

thereby contradicting the assumption. ■

Lemma 3.3.2. *If $x_{m'} = 1$ in an optimal fusion rule, then the corresponding system probability of false alarm denoted by $P_F^*(x_{m'} = 1)$ is*

$$P_F^*(x_{m'} = 1) \quad \geq \quad \prod_{i \,\in\, \mathcal{S}(\mathbf{u}_{m'})} p_{f_i} \tag{3.9}$$

Proof: From Proposition 3.3.1, we have

$$P_F^*(x_{m'} = 1) \quad \geq \quad p(\mathbf{u}_{m'}|H_0) + \sum_{m \,\in\, \mathbb{S}(\mathbf{u}_{m'})} p(\mathbf{u}_m|H_0). \tag{3.10}$$

Expanding and simplifying the RHS of (3.10) using (2.8), we get

$$P_F^*(x_{m'} = 1) \quad \geq \quad \prod_{i \,\in\, \mathcal{S}(\mathbf{u}_{m'})} p_{f_i} \tag{3.11}$$

■

We now provide an example for better understanding of the semi-monotonic property and the corresponding Lemmas.

Example 3.3.1. *Using the values provided for a semi-monotonic problem with $N = 3$ in Table 3.1, the Lemma 3.3.2 states that the system P_F^* for an optimum fusion rule $\mathbf{x}^*$ with $x_2 = 1$ as*

$$\begin{aligned} P_F^*(x_2 = 1) \quad &\geq \quad \prod_{i \,\in\, \mathcal{S}(\mathbf{u}_2)} p_{f_i}, \\ &= \quad p_{f_1}. \end{aligned}$$

Explanation:

From the Proposition 3.3.1, given that $x_2 = 1$ in an optimum fusion rule implies

$x_3 = x_6 = x_7 = 1$. *As a result we have*

$$
\begin{aligned}
P_F^*(x_2 = 1) &\geq p(\mathbf{u}_2|H_0) + \sum_{m \in \{3,6,7\}} p(\mathbf{u}_m|H_0), \\
&= \bar{p}_{f_2} p_{f_1} \bar{p}_{f_0} + \bar{p}_{f_2} p_{f_1} p_{f_0} + p_{f_2} p_{f_1} \bar{p}_{f_0} + p_{f_2} p_{f_1} p_{f_0}, \\
&= p_{f_1} \quad .
\end{aligned}
$$

We now focus on using these properties of the semi-monotonic GDFP to obtain a reduced feasible solution space.

3.4 Variable Reduction in GDFP

Using Lemma 3.3.2, we now define a reduced set of observation vector space $\mathcal{U}'$ as

$$
\mathcal{U}' \triangleq \{\mathbf{u}_m : \prod_{i \in \mathcal{S}(\mathbf{u}_m)} p_{f_i} \leq \alpha, \ \forall m\}, \tag{3.12}
$$

and reduced dimension $M' = |\mathcal{U}'|$. Note that the computation of the RHS of (3.11) is $\mathcal{O}(\log(M))$ in complexity. As a result, the complexity to obtain the $\mathcal{U}'$ is $\mathcal{O}(M \ \log(M))$. Further, note that

(i) those observation vectors $\mathbf{u}_m$ that result in the system false alarm $P_F^*(x_m = 1)$ to exceed the specified constraint value α, are not included in the reduced observation space $\mathcal{U}'$,

(ii) the feasible fusion solutions are now confined to the space $\mathcal{U}'$,

(iii) the boolean variables x_m corresponding to the $\mathbf{u}_m$ not in the space $\mathcal{U}'$, can now be fixed to $x_m = 0$ (namely *fixed-variable*),

(iv) to obtain the optimal $\mathbf{x}^*$, we now need to search the optimum value of only the remaining *free-variables*.

Using (3.1) the *reduced variable* GDFP is now defined as

$$\begin{aligned}
\underset{\mathbf{x}}{\text{Max}} \quad & \sum_{m=0}^{M-1} x_m \;\, p(\mathbf{u}_m|H_1), \\
\text{Sub. to} \quad & \sum_{m=0}^{M-1} x_m \;\, p(\mathbf{u}_m|H_0) \leq \alpha, \\
& \quad x_m \in \{0,1\} \quad \forall \mathbf{u}_m \in \mathcal{U}', \\
& \quad x_m = 0 \qquad\quad \forall \mathbf{u}_m \notin \mathcal{U}'.
\end{aligned}$$

The DP-based solution proposed in Section 2.5.1 can now be applied to (3.13) to obtain the optimal value of the *free-variables* in $\mathbf{x}^*$. The computational complexity for GDFP of (3.13) is now reduced to $\mathcal{O}(\alpha\, C\, M')$. In the following section we present the numerical results that *(i)* confirm the correctness of the proposed solution and *(ii)* compute the reduced dimension M' for different N and α.

3.5 Numerical Results and Discussions

We consider a system with $N = \{3, 5, 7, 9\}$, the SU characteristics as $P_{f_i} \sim \mathbf{U}(0.2, 0.4)$ and $P_{d_i} \sim \mathbf{U}(0.6, 0.8), \forall i$ where $\mathbf{U}(s_1, s_2)$ denotes uniform probability distribution with supports as s_1 and s_2. In Figure 3.4 we plot the average system performance (P_D vs α) obtained by applying *(i)* the DP-based solution to the GDFP of (3.1) (labeled "*GDFP*"), *(ii)* the DP-based solution to the reduced GDFP of (3.13) (labeled "*reduced GDFP*") The performance curves are obtained under NP criterion (α is varied from 0.001 to 0.1) using 10^3 realizations of $(\mathbb{P}_f, \mathbb{P}_d)$. Note that as expected the performance curve obtained by the proposed *reduced GDFP* method exactly matches the curve obtained by *GDFP*.

Remark 3.5.0.1. Note that the solution of the reduced GDFP is not confined to the DP-based approach alone. BB-based approach presented in chapter 6 can also be used to obtain the solution.

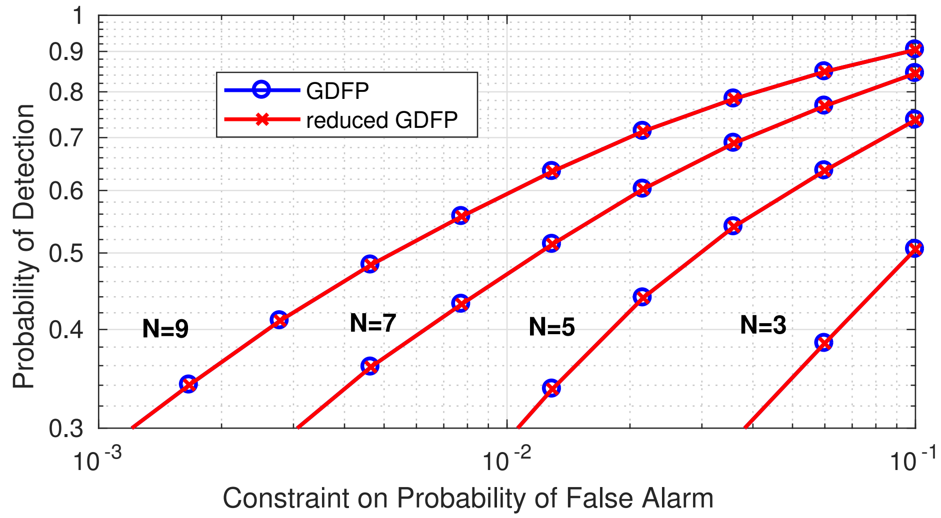

Figure 3.4: P_D vs P_F plot for '*GDFP*' and '*reduced GDFP*' using dynamic programming.

In Figure 3.5 we plot the average reduced dimension we obtain (M' vs α) by varying α for different N values. Note that in this case the solution space dimension

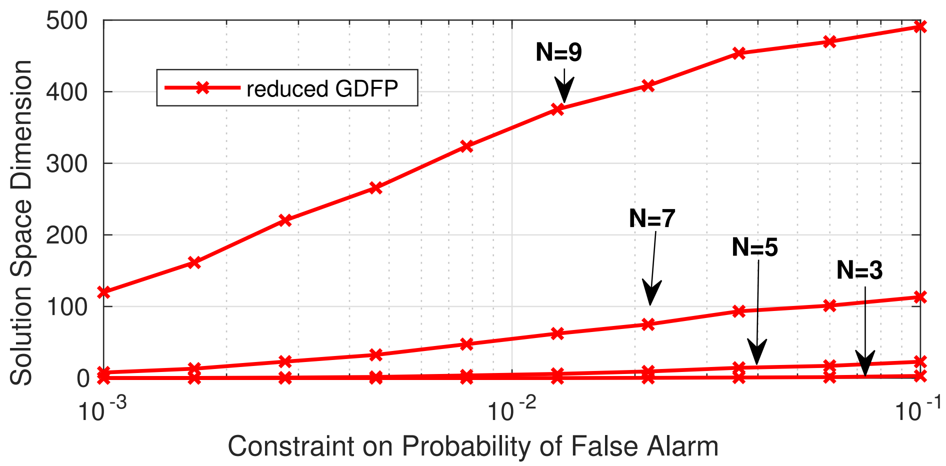

Figure 3.5: M' vs α plot for '*reduced GDFP*' using *variable reduction* method.

M for GDFP is always fixed at $\{8, 32, 128, 512\}$ whereas the reduced dimension M' is significantly low for small α and gradually increases with α.

3.6 Conclusions

We have shown that the decision fusion problem exhibits the *semi-monotonic* in a relevant case. We exploited this property to reduce the dimension of the feasible solution space. Subsequently, we applied dynamic programming to efficiently solve the problem with further reduced complexity. Numerical results are provided to verify the correctness of the proposed solution. Further avenues for research include exploring the properties of the decision fusion problem for other special cases and exploiting them for obtaining effcient solutions.

Chapter 4

On non-Randomized Hard Decision Fusion under Neyman-Pearson Criterion using LRT

4.1 Introduction

The non-randomized optimal hard decision fusion considered in chapters 2 and 3 is known to be an NP-hard classical $0-1$ *Knapsack* Problem with exponential complexity. In this chapter, we show that though the non-randomized single-threshold likelihood ratio based test (*non-rand-st* LRT) is sub-optimal, its performance approaches the upper-bound obtained by randomized LRT (*rand* LRT) with the increase in the number of participating sensors (N). This alleviates the need for employing the exponentially complex non-randomized optimal solution (*non-rand-mt* LRT) for large N. The main contributions in this chapter are

(i) We define metrics to quantify the performance difference between the *non-rand-st* and the *rand* LRT.

(ii) To the best of our knowledge, for the first time we show analytically that the performance of the *non-rand-st* LRT approaches the *rand* LRT with asymptotic number of participating sensors (generally available in the case of IoT).

(iii) Numerical results and the receiver operating characteristics (ROC) are plotted to verify the analytical results.

(iv) Using numerical results we show that the performance difference between the *non-rand-st* and the *rand* LRT becomes insignificant starting with $N \geq 13$.

The outline of this chapter is as follows: In Section 4.2, we present the system model, the GDFP and the (non-rand / rand) LRT decision equations. In Section 4.3 we define the performance metrics for the LRTs and present their asymptotic properties. Section 4.4 contains the ROC plots and numerical results, followed by conclusions in Section 4.5.

4.2 System Model

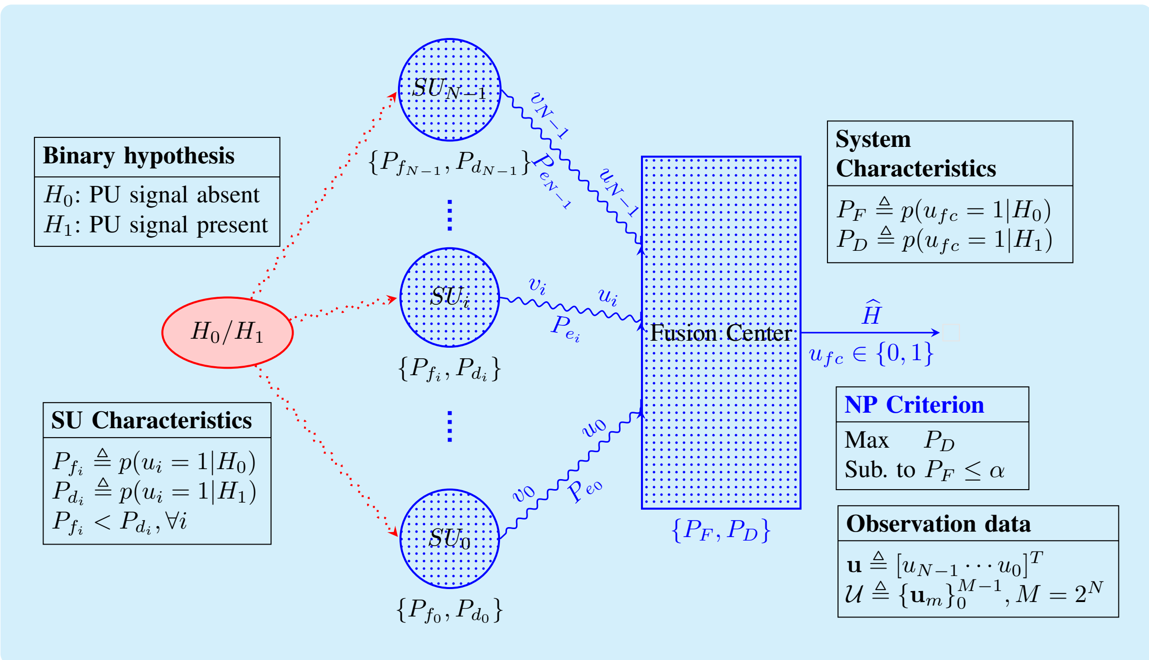

Figure 4.1: Depiction of System Model.

Slightly different from the Chapter 2, in this chapter we considered the reporting channels between the SUs (or sensors) and the FC to be *error-prone* (as depicted in Figure 4.1). The sensors sense the common phenomenon being observed and generate individual local binary decisions v_i, where $v_i = 0$ implies hypothesis H_0 : *event absent* and $v_i = 1$ implies hypothesis H_1 : *event present* respectively. The sensors are assumed to be heterogenous and are characterized by probability of detection $P_{d_i} \triangleq p(v_i = 1 \mid H_1)$ and probability of false alarm $P_{f_i} \triangleq p(v_i = 1 \mid H_0)$ where $P_{d_i} > P_{f_i}, \forall i$. Each local decision is received by the FC (as u_i) over dedicated erroneous reporting channel (modeled as a binary symmetric channel) with bit-error probability (BEP) $P_{e_i}, \forall i$. The FC receives the error infested local decisions as a N-dimensional observation vector $\mathbf{u}$ ($\triangleq [u_{N-1} \cdots u_0]^T$). The observation space $\mathcal{U}$ remains discrete ($= \mathbb{B}^N$ where $\mathbb{B} \in \{0, 1\}$) with cardinality $M = 2^N$. The m^{th} vector in the observation space is represented as $\mathbf{u}_m$, $m \in \{0, \cdots, M-1\}$. Considering the SU decisions to be conditionally independent, we have

$$\begin{aligned}
p(\mathbf{u}|H_1) &= \prod_{i=0}^{N-1} (P^e_{d_i})^{u_i} (\bar{P^e_{d_i}})^{1-u_i} \\
p(\mathbf{u}|H_0) &= \prod_{i=0}^{N-1} (P^e_{f_i})^{u_i} (\bar{P^e_{f_i}})^{1-u_i},
\end{aligned} \tag{4.1}$$

where $\bar{q} \triangleq 1 - q$ and

$$\begin{aligned}
P^e_{d_i} &\triangleq \bar{P}_{e_i} P_{d_i} + P_{e_i} \bar{P}_{d_i} \,, \\
P^e_{f_i} &\triangleq \bar{P}_{e_i} P_{f_i} + P_{e_i} \bar{P}_{f_i} \,.
\end{aligned} \tag{4.2}$$

Based on each observation vector $\mathbf{u}$, the fusion rule $\Gamma(\mathbf{u})$ of the FC generates a global decision $u_{fc} \in \{0, 1\}$ declaring hypothesis H_0 and H_1 respectively. The performance of the fusion rule is characterized by the system probability of detection $P_D \triangleq p(u_{fc} =$

$1|H_1)$ and the false-alarm $P_F \triangleq p(u_{fc} = 1|H_0)$ that are obtained as [10],

$$P_D = \sum_{\mathbf{u} \in \mathfrak{R}_1} p(\mathbf{u}|H_1), \qquad P_F = \sum_{\mathbf{u} \in \mathfrak{R}_1} p(\mathbf{u}|H_0), \tag{4.3}$$

where $\mathfrak{R}_0, \mathfrak{R}_1$ are two decision regions in the N-dimensional continuous real space $\mathbf{R}^N$, such that $\mathcal{U} \subset \{\mathfrak{R}_0 \cup \mathfrak{R}_1\}$, $\{\mathfrak{R}_0 \cap \mathfrak{R}_1\} = \varnothing$ (empty set), $\mathbf{u}_m \in \mathfrak{R}_0$ implies $\Gamma(\mathbf{u}_m) = 0$ and $\mathbf{u}_m \in \mathfrak{R}_1$ implies $\Gamma(\mathbf{u}_m) = 1, \forall m$. This indicates that an optimal definition of decision regions results in an optimal fusion rule. The Generalized Decision Fusion Problem (GDFP) under Neyman-Pearson criterion remains the same as,

$$\underset{\mathfrak{R}_1}{\text{Maximize}} \quad P_D, \quad \text{Sub to: } P_F \leq \alpha, \tag{4.4}$$

where α is the specified constraint value on the system P_F.

4.2.1 non-Randomized decision equation

The optimal decision region $\mathfrak{R}_1$ for the GDFP can be obtained by the *multi-threshold non-rand-mt* LRT given by (2.7),

$$\left(\Lambda(\mathbf{u}) \triangleq \frac{p(\mathbf{u}|H_1)}{p(\mathbf{u}|H_0)} \right) \underset{u_{fc}=0}{\overset{u_{fc}=1}{\gtrless}} \lambda_{nr}, \tag{4.5}$$

where λ_{nr} are the threshold(s) to be computed that is exponential in computational complexity. However in this chapter we confine ourselves to the widely used low-complexity non-randomized *single-threshold* LRT (*non-rand-st* LRT) that is known to be slightly sub-optimal.

4.2.2 Randomized decision equation

The *randomized* decision equation for the GDFP is given by the *rand* LRT as [21]

$$\text{If } \Lambda(\mathbf{u}) \begin{cases} > \lambda_r & u_{fc} = 1, \\ = \lambda_r & u_{fc} = 1 \text{ with probability } \gamma_r, \\ < \lambda_r & u_{fc} = 0, \end{cases} \tag{4.6}$$

where λ_r (a single-threshold) and γ_r (probability) is to be computed. It is well known that the system performance acheived by *rand* LRT is an upper bound to both *non-rand-st* LRT and *non-rand-mt* LRT [48]. We now focus on presenting the solutions for the *non-rand-st* and *rand* LRT of (4.5) and (4.6).

4.3 Solutions for the GDFP

Without loss of generality, assume that the observation vectors are sequenced in descending order of their LR-value $\Lambda(\mathbf{u})$ as

$$\Lambda(\mathbf{u}_0) \geq \cdots \geq \Lambda(\mathbf{u}_{M-1}). \tag{4.7}$$

Note that the sorted sequence of (4.7) can be obtained with a worst-case complexity of $\mathcal{O}(M \log(M))$. Assuming $\alpha < 1$, define a *split*-index s as

$$\left(P_{F_{nr}} \triangleq \sum_{m=0}^{m=s-1} p(\mathbf{u}_m|H_0) \right) \leq \alpha \quad \text{and} \quad P_{F_{nr}} + p(\mathbf{u}_s|H_0) > \alpha \,. \tag{4.8}$$

Further define

$$P_{D_{nr}} \triangleq \sum_{m=0}^{m=s-1} p(\mathbf{u}_m|H_1). \tag{4.9}$$

Note that for a given sensor network with $\{P_{d_i}, P_{f_i}\}, \forall i$, the split-index s is dependent on the specified α and can be computed in linear complexity. Also note that the *single-threshold* λ_{nr} for (4.5) can be obtained by choosing any value in the open interval $\Big(\Lambda(\mathbf{u}_{s-1}), \Lambda(\mathbf{u}_s)\Big)$. Further $P_{F_{nr}}$ and $P_{D_{nr}}$ are the system probabilities obtained by the *non-rand-st* LRT.

The system performance for the *rand* LRT (which is an upper-bound for the *non-rand-st* LRT) in terms of s is given by

$$
\begin{aligned}
P_{F_r} &= \alpha \,, && (4.10)\\
P_{D_r} &= P_{D_{nr}} + \frac{(\alpha - P_{F_{nr}})}{p(\mathbf{u}_s|H_0)}\, p(\mathbf{u}_s|H_1) \,, \\
&= P_{D_{nr}} + \epsilon(\alpha) \,, && (4.11)
\end{aligned}
$$

where the unknown parameters of (4.6) are $\gamma_r = \dfrac{(\alpha - P_{F_{nr}})}{p(\mathbf{u}_s|H_0)}$ and $\lambda_r = \Lambda(\mathbf{u}_s)$. Note that $\epsilon(\alpha)$ is the gain in system performance $(P_{D_r} - P_{D_{nr}})$ obtained by the *rand* LRT over the *non-rand-st* LRT for a specified α. The gain is in the interval $\epsilon(\alpha) \in \Big[0,\ p(\mathbf{u}_s|H_1)\Big)$, where

$$
\begin{aligned}
&\epsilon(\alpha) = 0 && \text{when} \quad (\alpha - P_{F_{nr}}) = 0 \,, \\
&\epsilon(\alpha) \to p(\mathbf{u}_s|H_1) && \text{when} \quad (\alpha - P_{F_{nr}}) \to p(\mathbf{u}_s|H_0). && (4.12)
\end{aligned}
$$

Lemma 4.3.1. *For any specified sensor network, the gain is upper bound by* $\epsilon(\alpha) < \epsilon_{ub}$ *where* $\epsilon_{ub} \leq \prod_{i=0}^{N-1} max\{P_{d_i}, \bar{P_{d_i}}\}, \quad \forall \alpha.$

Proof: From (4.12), we have the upper-bound on gain ϵ_{ub} *for a specified sensor network as*

$$
\epsilon_{ub} = \max_{m} p(\mathbf{u_m}|H_1). \qquad (4.13)
$$

Using (4.1), the upper bound can be simplified as

$$\begin{aligned}\epsilon_{ub} &= \prod_{i=0}^{N-1} max\{P^e_{d_i}, \bar{P}^e_{d_i}\} \\ &\leq \prod_{i=0}^{N-1} max\{P_{d_i}, \bar{P_{d_i}}\} \qquad (4.14)\end{aligned}$$

■

Lemma 4.3.2. *The upper-bound ϵ_{ub} approaches* 0 *for asymptotic number of the participating sensors N.*

Proof: Practically, the sensor characteristic is

$$P_{d_i} < 1, \quad \forall i,$$

except for the ideal sensor. As a result,

$$max\{P_{d_i}, \bar{P_{d_i}}\} < 1, \quad \forall i.$$

There by

$$\prod_{i=0}^{N-1} max\{P_{d_i}, \bar{P_{d_i}}\} \ \rightarrow \ 0 \quad when \quad N \rightarrow \infty,$$

implying,

$$\epsilon_{ub} \ \rightarrow \ 0 \quad when \quad N \rightarrow \infty.$$

■

Proposition 4.3.1. *Lemma 4.3.2 implies that the performance of the non-rand-st LRT approaches the performance of the rand LRT for asymptoic number of participating sensors N.*

Further, we obtain the expectation of the gain ϵ to quantify the performance improvement of *rand* LRT under the non-asymptotic case.

4.3.1 Expectation of the gain

Assuming that α is uniformly distributed with supports $(0, 1)$, the expectation of the gain ($\triangleq \epsilon_\mu$) for a specified sensor network can be obtained as

$$\begin{aligned} \epsilon_\mu &= \mathbb{E}_\alpha\{\epsilon\} \quad , \\ &= \sum_{m=0}^{M-1} p(s=m)\, \frac{p(\mathbf{u_m}|H_1)}{2} \quad , \\ &= \sum_{m=0}^{M-1} p(\mathbf{u_m}|H_0)\, \frac{p(\mathbf{u_m}|H_1)}{2} \quad . \end{aligned} \tag{4.15}$$

We now focus on the numerical results of the *non-rand-st* and *rand* LRT for different scenarios.

4.4 Numerical results and discussion

Firstly, we consider non-errorneous reporting channels i.e., $P_{e_i} = 0, \forall i$. Figure 4.2 plots the numerical average performance gain ϵ obtained against different α logarithmically spaced in $\{10^{-2}, 10^{0}\}$ for 1000 realizations of sensor networks with $P_{f_i} \sim \mathbf{U}(0, 1)$, $P_{d_i} = P_{f_i} + p_i$ and $p_i \sim \mathbf{U}(P_{f_i}, 1), \forall i$, where $\mathbf{U}(s_1, s_2)$ denotes uniform probability distribution with supports as s_1 and s_2. Note that,

(i) theoritically the gain is 0 for $\alpha = \{0, 1\}$ for any N,

(ii) as expected, in Figure 4.2 the gain curve for a given N (visible for $N = \{3, 5\}$), initially increases with α and subsequently decreases.

(iii) the expectation of the gain and the upper-bound are dependent on the value of N.

Table 4.1 presents the average numerical values obtained for 1000 realizations of sensor networks with $\alpha \sim \mathbf{U}(0, 1)$. Note that

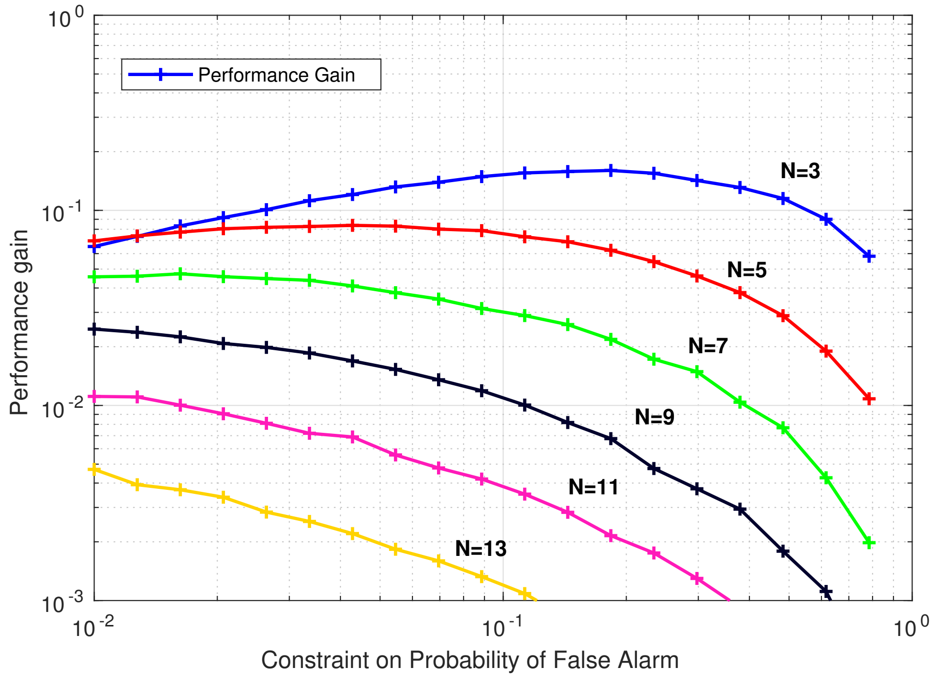

Figure 4.2: ϵ vs α plots under NP criterion for different number of sensors N using non-erroneous reporting channels.

Table 4.1: Average ϵ_μ and ϵ_{ub} obtained for a scenario with non-erroneous reporting channels

$N \rightarrow$	3	5	7	9	11	13
Expected gain, ϵ_μ	0.1	0.032	0.011	0.004	0.001	0.0005
Upper-bound, ϵ_{ub}	0.5	0.32	0.21	0.13	0.08	0.05

(i) The expected gain ϵ_μ and upper-bound ϵ_{ub} decrease with increasing N

(ii) The gain ϵ_μ is insignificant for $N = 13$ indicating that the *non-rand-st* LRT approaches the performance of *rand* LRT for $N \geq 13$.

Figure 4.3 plots the ROC obtained by *non-rand-st* and *rand* LRT for different values of N by varying α between $(0.01, 1)$. Note that while there is significant difference in performance for $N = 3$, the ROCs converge as N increases and nearly overlap for $N = 13$.

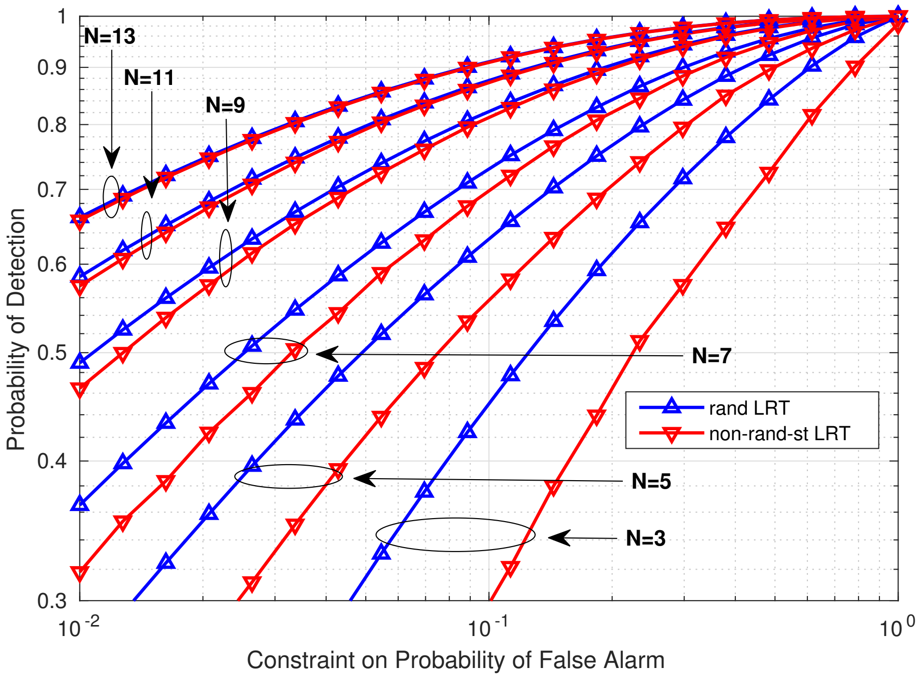

Figure 4.3: P_D vs α plots under NP criterion for different number of sensors N using non-erroneous reporting channels.

4.4.1 With erroneous reporting channels

Secondly, we consider the local decisions $v_i, \forall i$ are transmitted using on-off keying on reporting channels experiencing Rayleigh fading, i.e., $y_i = h_i v_i + w_i$, where $h_i \sim \mathcal{N}_{\mathbb{C}}(0,1)$, $w_i \sim \mathcal{N}_{\mathbb{C}}(0,\sigma_w^2)$ and $y_i \in \mathbb{C}$. The FC employs coherent detection to obtain $u_i, \forall i$ from y_i resulting in $P_{e_i} = \mathcal{Q}(\frac{|h_i|}{2\sigma_w})$. Assuming the a-priori probabilities $\Pr\{H_1\} = \Pr\{H_0\} = \frac{1}{2}$, the individual channel SNR for independent local decisions is defined as $\mathrm{SNR}_i \triangleq \frac{P_{d_i}+P_{f_i}}{2\sigma_{w_i}^2}$.

In Figures 4.4 to 4.6 we plot the average performances of the *non-rand* and *rand* LRT over the erroneous reporting channels under different scenarios with 1000 realizations of the sensor networks.

In Figure 4.4 we plot the P_D versus α curves for $N = 5$ for different reporting channel SNRs. Note that under low SNR ($= 0$ dB), the performance difference between the LRTs is low as they are dominated by the large channel errors. The

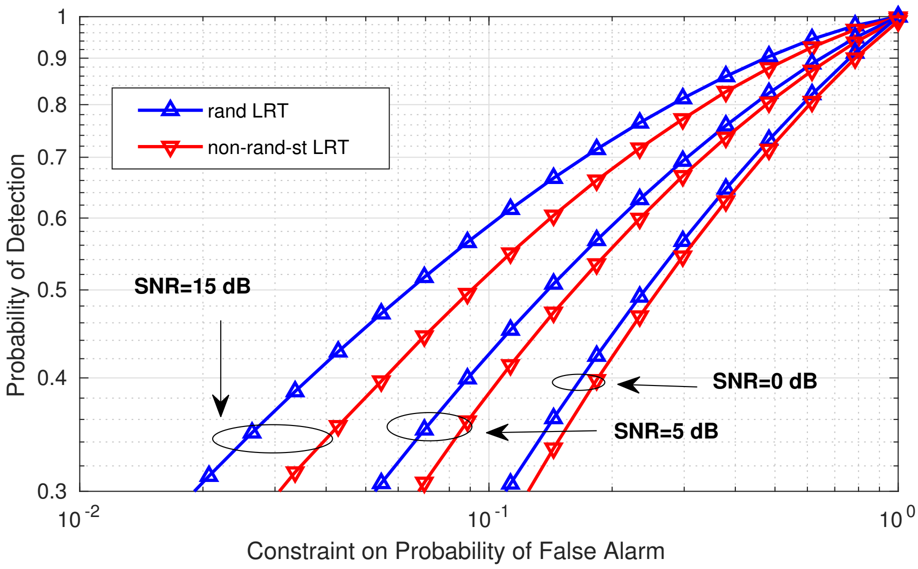

Figure 4.4: P_D vs α plots under NP criterion for N=5 for different reporting channel SNRs.

performance of *rand* LRT gradually improves over *non-rand-st* with increase in SNR.

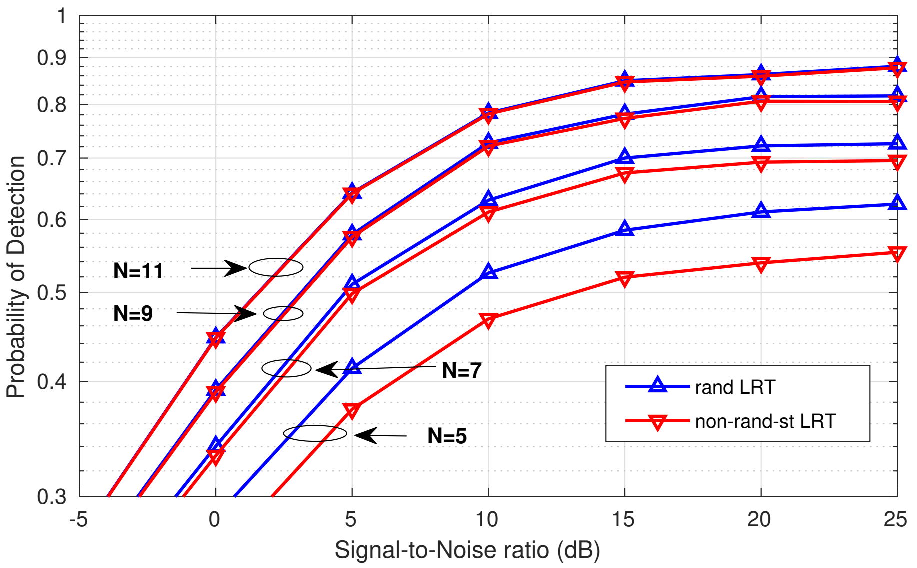

Figure 4.5: P_D vs SNR plots under NP criterion for different number of sensors.

In Figure 4.5 we plot the P_D versus SNR curves for different number of sensors $N \in \{5, 7, 9, 11\}$. Note that for a specific N, the performance of *rand* LRT gradually improves over *non-rand-st* with increase in SNR, however is insignificant for large values of N.

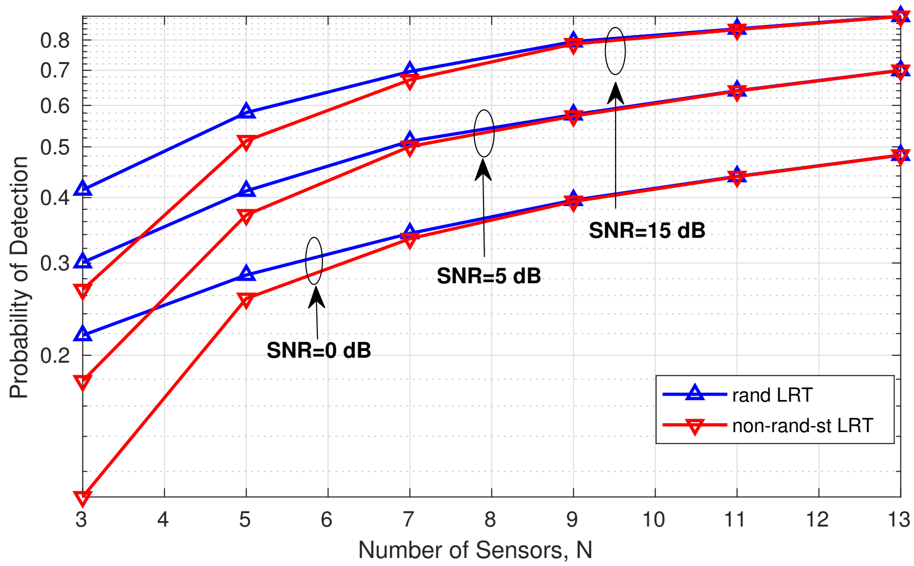

Figure 4.6: P_D vs N plots under NP criterion for different reporting channel SNRs.

In Figure 4.6 we plot the P_D versus N curves for different reporting channel SNRs (SNR $\in \{0, 5, 15\}$ dB). Note that irrespective of the reporting channel SNR, the performance of the *non-rand-st* LRT converges with the *rand* LRT with increase in number of sensors N.

4.5 Conclusion

Two metrics (expected gain and gain upper-bound) are defined to quantify the performance difference between the *non-rand-st* and the *rand* LRT. Using these metrics, it is shown that the performance of the *non-rand-st* LRT approaches the *rand* LRT with asymptotic number of participating sensors, thereby alleviating the need for employing the exponentially complex non-randomized optimal solution for large N. Using numerical results it is further shown that the performance difference between the *non-rand-st* and the *rand* LRT is insignificant even for a low number of sensors $N > 13$.

Chapter 5

Mean-based Blind Hard Decision Fusion Rules

5.1 Introduction

In the previous chapters, it was assumed that the FC (is clairyovant) has the required knowledge of the characteristics of each of the participating SU (probability of detection P_{d_i} and probability of false-alarm P_{f_i}, $\forall i$) and the reporting channel (bit error probability P_{e_i}) to design a decision fusion rule [17, 21]. However, due to the resource constraints of the reporting channels in the CRN, the instantaneous SU characteristics are generally not available at the FC. In such scenarios, the FC is compelled to resort to blind schemes [38, 49] that use the limited system knowledge available to design a fusion rule at the cost of slightly lower system performance, measured in terms of system probability of detection P_D and false-alarm P_F. In [49], it is assumed that the $P_{d_i}, \forall i$ are *not known* and the proposed scheme (namely *Wu* rule) *estimates the unknown* parameters from the received local decisions. A similar semi-blind rule (namely *LOD*) assuming $P_{d_i}, \forall i$ *are unknown* and a completely-blind rule (namely *IS*) assuming both $P_{f_i}, P_{d_i}, \forall i$ *are unknown* is proposed in [38]. Alternatively, in [50] it is assumed that the instantaneous wireless channel coefficients *are unknown*, whereas the SU characteristics *are known*.

In this chapter we propose novel (semi-)blind hard decision fusion rules that are a variant of GDFP presented in previous chapters. These rules use the mean of the secondary user characteristics instead of their (*unknown*) actual values. We show that these rules with slight (or no) additional system knowledge achieve better receiver operating characteristics than existing (semi-)blind alternatives. These rules also have a low-complexity analytical solution under Neyman-Pearson in some relevant cases. Numerical results are reported in a channel-aware scenario to demonstrate their appeal and to confirm the theoretical findings.

More specifically, the main contributions are:

(i) We propose a group of semi-blind rules (MSB) (assuming that the mean value of the $P_{d_i} \forall i$ *is known* instead of the actual instantenous values) and a group of completely-blind rules (MCB) (assuming that the mean value of $\{P_{d_i}, P_{f_i}, \forall i\}$ *is known* instead of the actual instantaneous values) that collectively cover a wide spectrum of system knowledge requirements.

(ii) We formulate the considered fusion rules into *generalized decision fusion problem* (GDFP) [51] equivalent to the classical $0-1$ *knapsack problem* to obtain the nonrandomized and randomized boolean decision equations.

(iii) We compare the receiver operating characteristics (ROCs) of the proposed and the existing rules using both analytical computations and Monte Carlo simulations, showing that the former achieve better ROC than the latter in their respective categories.

Table 5.1 summarizes (other than the proposed rules) the list of existing alternative rules considered for comparison hereinafter, along with corresponding system knowledge required.

Table 5.1: List of Rules and their System Knowledge Requirement

Fusion Rules $\downarrow$	**Parameters Used** under H_0 and H_1	
Semi-blind [*] [2]	P_{f_i}	$\widehat{P_{d_i}} \in \{P_{f_i} + \mu_d, \frac{1+P_{f_i}}{2}, \frac{1}{2}\}$
Completely-blind [*] [3]	$\widehat{P_{f_i}} = \mu_f$	$\widehat{P_{d_i}} \in \{\mu_f + \mu_d, \frac{1+\mu_f}{2}, \frac{1}{2}\}$
cLRT [38, 51] [1]	P_{f_i}	P_{d_i}
LOD [38], *Wu* [49] [2]	P_{f_i}	none
IS and *CR* [38] [3]	$\widehat{P_{f_i}} = 0$, none	$\widehat{P_{d_i}} = 1$, none

[*] New rules proposed in this letter.
[1] Clairvoyant rule (*cLRT*) *with knowledge* of P_{f_i} and $P_{d_i}, \forall i$.
[2] Semi-blind rules with *no knowledge* of $P_{d_i}, \forall i$.
[3] Completely-blind rules with *no knowledge* of P_{f_i} and $P_{d_i}, \forall i$.
The BEP P_{e_i} of reporting channels is assumed to be *known* by all the rules except the *Counting Rule (CR)*.
The *LOD*, *CR* and the proposed new rules implicitly assume $P_{d_i} > P_{f_i}, \forall i$.
The notation $\widehat{a}$ represents the estimate of the parameter where the actual is not known.
The mean values $\mu_f \triangleq \mathbb{E}\{P_{f_i}\}, \forall i$ and $\mu_d \triangleq \mathbb{E}\{P_{d_i} - P_{f_i}\}, \forall i$.

The outline of this chapter is as follows: In Section 5.2, we explain the system model and the GDFP formulation. We propose the blind rules and formulate their likelihood ratio (LR) based decision equations in Section 5.3. Then, in Section 5.4 we provide analytical solutions for the proposed (semi-) blind rules. Section 5.5 contains the numerical results and is followed by conclusions in Section 5.6.

5.2 System Model

Slightly different from the Chapter 4, in this chapter we assume that the local performance $(P_{f_i}, P_{d_i}), \forall i$ are *random variables* with mean values $\mathbb{E}\{P_{f_i}\} = \mu_f$ and $\mathbb{E}\{P_{d_i} - P_{f_i}\} = \mu_d, \forall i$. Following Chapter 4 we have,

(i) the conditional probabilities as

$$p(\mathbf{u}|H_1) = \prod_{i=0}^{N-1}(P_{d_i}^e)^{u_i}(\bar{P_{d_i}^e})^{1-u_i}$$
$$p(\mathbf{u}|H_0) = \prod_{i=0}^{N-1}(P_{f_i}^e)^{u_i}(\bar{P_{f_i}^e})^{1-u_i}, \quad (5.1)$$

where $\bar{q} \triangleq 1-q$, $P_{d_i}^e \triangleq \bar{P_{e_i}}P_{d_i} + P_{e_i}\bar{P_{d_i}}$ and $P_{f_i}^e \triangleq \bar{P_{e_i}}P_{f_i} + P_{e_i}\bar{P_{f_i}}$.

(ii) the system characteristics as

$$P_D(\mathbf{x}) = \sum_{m=0}^{M-1} x_m \; p(\mathbf{u}_m|H_1), \qquad P_F(\mathbf{x}) = \sum_{m=0}^{M-1} x_m \; p(\mathbf{u}_m|H_0). \quad (5.2)$$

(iii) the *non-rand* GDFP formulation under NP criterion as

$$\underset{\mathbf{x}}{\text{Max}} \quad \sum_{m=0}^{M-1} x_m \; p(\mathbf{u}_m|H_1),$$
$$\text{Sub. to} \quad \sum_{m=0}^{M-1} x_m \; p(\mathbf{u}_m|H_0) \leq \alpha, \quad x_m \in \{0,1\}. \quad (5.3)$$

Note that relaxing the constraint on $\mathbf{x}$ to $\{x_m \in \mathbb{R} : 0 \leq x_m \leq 1\}$ results in *rand* GDFP. The optimal fusion vector $\mathbf{x}^*$ for the clairvoyant rule ($cLRT$) i.e., when the complete system knowledge $\{P_{d_i}, P_{f_i}, P_{e_i}\}, \forall i$ *is available*, can be obtained from the *non-rand-mt* LRT given by

$$\left[\Lambda(\mathbf{u}_m) \triangleq \sum_{i=0}^{N-1} u_{i,m} \; \log\left(\frac{\bar{P_{f_i}^e}}{P_{f_i}^e}\,\frac{P_{d_i}^e}{\bar{P_{d_i}^e}}\right)\right] \underset{x_m=0}{\overset{x_m=1}{\gtrless}} \lambda_{clrt}, \quad (5.4)$$

provided the appropriate threshold(s) λ_{clrt} are computed. The *single-threshold non-rand-st* LRT is slightly sub-optimal for *non-rand* GDFP in general (2.2.2.3) and is optimal when the LR function $\Lambda(\mathbf{u})$ is monotonic (case-A, 2.2.2.1). For the *rand* GDFP, the *rand* LRT (4.6) always provides the optimal solution $\mathbf{x}^*$.

We now focus on proposing the (semi-)blind fusion rules and formulating their LR-based decision equations using the *estimate of the unknown* parameters and establish their monotonic property.

5.3 Formulation of the proposed blind rules

5.3.1 Mean-based semi-blind rule (*MSB*)

In this case the false-alarm of the SUs and the link BEPs are assumed to be *known* whereas the detection probabilities are *unknown*. We now propose a group of rules (namely *MSB*) based on the mean value instead of the actual instantaneous values of P_{d_i}. Further, we propose three special cases in the *MSB* with different system knowledge requirements and computational complexities.

MSB-1

In this special case we assume that the mean value μ_d is *known*. We propose to use the estimate of the *unknown* P_{d_i} as

$$\widehat{P_{d_i}} = P_{f_i} + \mu_d, \quad \forall i. \tag{5.5}$$

We then have

$$\widehat{P^e_{d_i}} = P^e_{f_i} + \mu'_{d_i}, \quad \forall i, \tag{5.6}$$

where $\mu'_{d_i} = \mu_d(1-2P_{e_i})$. Substituting the estimate (5.6) in (5.4), the LRT for *MSB-1* can be written as

$$\sum_{i=0}^{N-1} u_{i,m} \log\left(\frac{\bar{P^e_{f_i}}}{P^e_{f_i}} \frac{P^e_{f_i} + \mu'_{d_i}}{\bar{P^e_{f_i}} - \mu'_{d_i}}\right) \underset{x_m=0}{\overset{x_m=1}{\gtrless}} \lambda_{msb1}. \tag{5.7}$$

For the most general values, the LR function in this case is nonseparable as required by the *factorization criterion* [12], thereby implying that *MSB-1* is non-monotonic (2.2.2.3).

MSB-2

In this case we use the information that the support of the probability distribution of the *unknown* P_{d_i} is $(P_{f_i}, 1]$. Adopting the Bayesian inference approach, we propose to use the estimate as

$$\widehat{P_{d_i}} = P_{f_i} + \frac{1 - P_{f_i}}{2}, \quad \forall i, \tag{5.8}$$

i.e., the conditional expectation of P_{d_i} assuming it follows uniform distribution within the support. Differently from the previous case, note that this special case does not require the knowledge of the mean value μ_d.

Using the estimate in (5.8), the LRT is given by

$$\sum_{i=0}^{N-1} u_{i,m} \log \left(\frac{\bar{P}^e_{f_i}}{P^e_{f_i}} \frac{P^e_{f_i} + \bar{P}_{e_i}}{\bar{P}^e_{f_i} + P_{e_i}} \right) \underset{x_m=0}{\overset{x_m=1}{\gtrless}} \lambda_{msb2} \quad . \tag{5.9}$$

For the most general values, the LR function in this case is also nonseparable, thereby implying that *MSB-2* is non-monotonic (2.2.2.3).

MSB-3

We assume a special case of the *MSB* where the mean of the *unknown* P_{d_i}, $\mathbb{E}\{P_{d_i}\} = \frac{1}{2}, \forall i$. We then have

$$\widehat{P^e_{d_i}} \quad = \quad (1 - P_{e_i}) \frac{1}{2} + P_{e_i} \frac{1}{2} \quad = \quad \frac{1}{2}, \quad \forall i, \tag{5.10}$$

and the conditional probability is given by

$$\widehat{p(\mathbf{u}|H_1)} = \frac{1}{2^N}, \tag{5.11}$$

which is constant and independent of $P_{e_i}, \forall i$. As a result the GDFP formulation of the *MSB-3* is simplified to

$$\begin{aligned} \underset{\mathbf{x}}{\text{Max}} \quad & \frac{1}{2^N} \sum_{m=0}^{M-1} x_m, \\ \text{Sub. to} \quad & \sum_{m=0}^{M-1} x_m \; p(\mathbf{u}_m|H_0) \; \leq \alpha. \end{aligned} \tag{5.12}$$

Note that the objective function of (5.12) has simplified to maximizing the count of the observation vectors being declared as H_1 with the system probability of false-alarm P_F constrained by the value α.

To verify the monotonic property of the GDFP of (5.12), we simplify the LR function by applying the monotonically increasing function (i.e., logarithmic operation) as

$$\Lambda(\mathbf{u}) \triangleq \frac{p(\mathbf{u}|H_1)}{p(\mathbf{u}|H_0)} = \frac{1}{2^N}\frac{1}{p(\mathbf{u}|H_0)} \quad , \tag{5.13}$$

$$\begin{aligned} \log\left(\Lambda(\mathbf{u})\right) &= \log\left(\frac{1}{\prod_{i=0}^{N-1}(P_{f_i}^e)^{u_i}(\bar{P_{f_i}^e})^{1-u_i}}\right) + K \quad , \\ &= \sum_{i=0}^{N-1} u_i \log\left(\frac{\bar{P_{f_i}^e}}{P_{f_i}^e}\right) + K' \quad , \\ &= T(\mathbf{u}) + K' \quad , \end{aligned} \tag{5.14}$$

where K, K' are terms independent of $\mathbf{u}$ and $T(\mathbf{u}) = \sum_{i=0}^{N-1} u_i \log\left(\frac{\bar{P_{f_i}^e}}{P_{f_i}^e}\right)$. Further, from (5.13) and (5.14) we infer that

(i) $p(\mathbf{u}|H_0)$ is non-increasing monotonic on $T(\mathbf{u})$,

(ii) $p(\mathbf{u}|H_1)$ is non-decreasing monotonic (as it is constant) on $T(\mathbf{u})$,

(iii) $\Lambda(\mathbf{u})$ is non-decreasing monotonic on $T(\mathbf{u})$.

There by implying that this rule is of type monotonic case-A (2.2.2.1). As a result its *non-rand-st* LRT given by

$$\sum_{i=0}^{N-1} u_{i,m} \log\left(\frac{\bar{P}^e_{f_i}}{P^e_{f_i}}\right) \underset{x_m=0}{\overset{x_m=1}{\gtrless}} \lambda_{msb3} \quad , \tag{5.15}$$

provides the optimal solution for the *non-rand* GDFP under NP criterion.

Table 5.2: List of MSB special cases and the corresponding system knowledge used.

Special Cases	$\widehat{P_{f_i}} =$	$\widehat{P_{d_i}} =$	$\widehat{P_{e_i}} =$	**Required Knowledge**
MSB-1 Rule	$P_{f_i}, \forall i$	$P_{f_i} + \mu_d, \forall i$	$P_{e_i}, \forall i$	$\{P_{f_i}, \mu_d, P_{e_i}\}, \forall i$
MSB-2 Rule	$P_{f_i}, \forall i$	$P_{f_i} + \frac{1-P_{f_i}}{2}, \forall i$	$P_{e_i}, \forall i$	$\{P_{f_i}, \text{none}, P_{e_i}\}, \forall i$
MSB-3 Rule	$P_{f_i}, \forall i$	$\frac{1}{2}, \forall i$	$P_{e_i}, \forall i$	$\{P_{f_i}, \text{none}, P_{e_i}\}, \forall i$

Table 5.2 summarizes the special case of the proposed MSB rules with the system knowledge required under each hypothesis.

5.3.2 Mean-based completely-blind rule (MCB)

In this subsection, we focus on another set of rules assuming that both the instanteneous false-alarm and detection probabilities of the SUs are *unknown*. We now propose a group of rules (namely *MCB*) based on the mean values instead of the actual values of $\{P_{d_i}, P_{f_i}\}$. We propose the following special cases in the *MCB*:

MCB-1

In this special case we assume μ_f and μ_d is *known*. We propose to use the estimates as

$$\begin{aligned}\widehat{P_{f_i}} &= \mu_f, \\ \widehat{P_{d_i}} &= \mu_f + \mu_d, \quad \forall i. \end{aligned} \tag{5.16}$$

Then the LRT is given by

$$\sum_{i=0}^{N-1} u_{i,m} \log \left(\frac{\bar{\mu^e_{f_i}}}{\mu^e_{f_i}} \frac{\mu^e_{f_i} + \mu^e_{d_i}}{\bar{\mu^e_{f_i}} - \mu^e_{d_i}} \right) \underset{x_m=0}{\overset{x_m=1}{\gtrless}} \lambda_{mcb1} \quad , \tag{5.17}$$

where

$$\begin{aligned}\mu^e_{d_i} &\triangleq \bar{P}_{e_i}\mu_d + P_{e_i}\bar{\mu}_d \quad , \\ \mu^e_{f_i} &\triangleq \bar{P}_{e_i}\mu_f + P_{e_i}\bar{\mu}_f \quad . \end{aligned} \tag{5.18}$$

For the most general values, the LR function in this case is nonseparable, thereby implying that *MCB-1* is non-monotonic (2.2.2.3).

MCB-2

In this special case, similar to the *MSB-2* we propose to use the estimates as

$$\begin{aligned}\widehat{P_{f_i}} &= \mu_f \quad , \\ \widehat{P_{d_i}} &= \mu_f + \frac{1-\mu_f}{2} \quad . \end{aligned} \tag{5.19}$$

The conditional probabilities can be obtained as

$$
\begin{aligned}
\widehat{p(\mathbf{u}|H_1)} &= \frac{1}{2^N}\prod_{i=0}^{N-1}(\mu^{e}_{f_i} + \bar{P}_{e_i})^{u_i}(\mu^{\bar{e}}_{f_i} + P_{e_i})^{1-u_i} \quad , \\
\widehat{p(\mathbf{u}|H_0)} &= \prod_{i=0}^{N-1}\left(\mu^{e}_{f_i}\right)^{u_i}\left(\mu^{\bar{e}}_{f_i}\right)^{1-u_i} \quad .
\end{aligned} \tag{5.20}
$$

The LRT is then given by

$$
\sum_{i=0}^{N-1} u_{i,m} \, \log\left(\frac{\mu^{\bar{e}}_{f_i}}{\mu^{e}_{f_i}}\,\frac{\mu^{e}_{f_i} + \bar{P}_{e_i}}{\mu^{\bar{e}}_{f_i} + P_{e_i}}\right) \underset{x_m=0}{\overset{x_m=1}{\gtrless}} \lambda_{mcb2} \quad , \tag{5.21}
$$

and is non-monotonic (2.2.2.3) for the most general values.

MCB-3

Similar to the *MSB-3*, in this special case we propose to use the estimates as

$$
\begin{aligned}
\widehat{P_{f_i}} &= \mu_f \quad , \\
\widehat{P_{d_i}} &= \frac{1}{2} \quad .
\end{aligned} \tag{5.22}
$$

Then the LRT is

$$
\sum_{i=0}^{N-1} u_{i,m} \, \log\left(\frac{\mu^{\bar{e}}_{f_i}}{\mu^{e}_{f_i}}\right) \underset{x_m=0}{\overset{x_m=1}{\gtrless}} \lambda_{mcb3} \quad , \tag{5.23}
$$

and is of type monotonic case-A (2.2.2.1) similar to *MSB-3*.

MCB-4

For this special case we propose to use the estimates as

$$
\begin{aligned}
\widehat{P_{f_i}} &= \mu_f, & \forall i, \\
\widehat{P_{d_i}} &= \mu_f + \mu_d, & \forall i, \\
\widehat{P_{e_i}} &= \mu_e, & \forall i.
\end{aligned} \tag{5.24}
$$

where we assume $\mathbb{E}\{P_{e_i}\} = \mu_e, \forall i$. Then the LRT is given by

$$\sum_{i=0}^{N-1} u_{m,i} \, \log \left(\frac{\bar{\mu}_f^e}{\mu_f^e} \frac{\mu_f^e + \mu_d^e}{\bar{\mu}_f^e - \mu_d^e} \right) \underset{x_m=0}{\overset{x_m=1}{\gtrless}} \lambda_{mcb4} \,, \tag{5.25}$$

where

$$\begin{aligned} \mu_f^e &\triangleq \bar{\mu}_e \mu_f + \mu_e \bar{\mu}_f \quad , \\ \mu_d^e &\triangleq \bar{\mu}_e \mu_d + \mu_e \bar{\mu}_d \quad . \end{aligned} \tag{5.26}$$

This simplifies to the *Counting rule* (CR) [16, 38] (which is monotonic case-B for the most general values),

$$\sum_{i=0}^{N-1} u_{i,m} \underset{x_m=0}{\overset{x_m=1}{\gtrless}} \lambda'_{mcb4} \quad , \tag{5.27}$$

implying that *no system knowledge* is required for the decision equation.

Table 5.3: List of MCB special cases and the corresponding system knowledge used.

Special Cases	$\widehat{P_{f_i}} =$	$\widehat{P_{d_i}} =$	$\widehat{P_{e_i}} =$	**Required Knowledge**
MCB-1 Rule	$\mu_f, \forall i$	$\mu_f + \mu_d, \forall i$	$P_{e_i}, \forall i$	$\{\mu_f, \mu_d, P_{e_i}\}, \forall i$
MCB-2 Rule	$\mu_f, \forall i$	$\mu_f + \frac{1-\mu_f}{2}, \forall i$	$P_{e_i}, \forall i$	$\{\mu_f, \text{none}, P_{e_i}\}, \forall i$
MCB-3 Rule	$\mu_f, \forall i$	$\frac{1}{2}, \forall i$	$P_{e_i}, \forall i$	$\{\mu_f, \text{none}, P_{e_i}\}, \forall i$
MCB-4 Rule	$\mu_f, \forall i$	$\mu_f + \mu_d, \forall i$	$\mu_e, \forall i$	$\{\text{none}, \text{none}, \text{none}\}, \forall i$

Table 5.3 summarizes the special case of the proposed MCB rules with the system knowledge required under each hypothesis.

5.4 Proposed Analytical Solutions

Table 5.4 lists the LR-functions and the monotonic properties established for each special case of the proposed blind rules.

Table 5.4: List of special cases with the simplified LR-function and the problem type.

Special Cases	$\Lambda(\mathbf{u})$	**Problem Type**
MSB-1 Rule	$\sum_{i=0}^{N-1} u_{i,m} \log\left(\frac{P_{f_i}^{\bar{e}}}{P_{f_i}^{e}} \frac{P_{f_i}^{e}+\mu'_{d_i}}{P_{f_i}^{\bar{e}}-\mu'_{d_i}}\right) \overset{x_m=1}{\underset{x_m=0}{\gtrless}} \lambda_{msb1}$	non-monotonic
MSB-2 Rule	$\sum_{i=0}^{N-1} u_{i,m} \log\left(\frac{P_{f_i}^{\bar{e}}}{P_{f_i}^{e}} \frac{P_{f_i}^{e}+P_{e_i}^{\bar{}}}{P_{f_i}^{\bar{e}}+P_{e_i}}\right) \overset{x_m=1}{\underset{x_m=0}{\gtrless}} \lambda_{msb2}$	non-monotonic
MSB-3 Rule	$\sum_{i=0}^{N-1} u_{i,m} \log\left(\frac{P_{f_i}^{\bar{e}}}{P_{f_i}^{e}}\right) \overset{x_m=1}{\underset{x_m=0}{\gtrless}} \lambda_{msb3}$	monotonic case-A
MCB-1 Rule	$\sum_{i=0}^{N-1} u_{i,m} \log\left(\frac{\mu_{f_i}^{\bar{e}}}{\mu_{f_i}^{e}} \frac{\mu_{f_i}^{e}+\mu_{d_i}^{e}}{\mu_{f_i}^{\bar{e}}-\mu_{d_i}^{e}}\right) \overset{x_m=1}{\underset{x_m=0}{\gtrless}} \lambda_{mcb1}$	non-monotonic
MCB-2 Rule	$\sum_{i=0}^{N-1} u_{i,m} \log\left(\frac{\mu_{f_i}^{\bar{e}}}{\mu_{f_i}^{e}} \frac{\mu_{f_i}^{e}+P_{e_i}^{\bar{}}}{\mu_{f_i}^{\bar{e}}+P_{e_i}}\right) \overset{x_m=1}{\underset{x_m=0}{\gtrless}} \lambda_{mcb2}$	non-monotonic
MCB-3 Rule	$\sum_{i=0}^{N-1} u_{i,m} \log\left(\frac{\mu_{f_i}^{\bar{e}}}{\mu_{f_i}^{e}}\right) \overset{x_m=1}{\underset{x_m=0}{\gtrless}} \lambda_{mcb3}$	monotonic case-A
MCB-4 Rule	$\sum_{i=0}^{N-1} u_{i,m} \overset{x_m=1}{\underset{x_m=0}{\gtrless}} \lambda'_{mcb4}$	monotonic

5.4.1 *MSB* rule under NP criterion

In chapter 2, we proposed low complexity dynamic programming (DP) based solution for the non-randomized tests. However the *MSB* rules and the existing rules ($\{LOD, cLRT\}$ used for numerical comparison) require high precision computations for which the DP-based solution is not practical in some cases. Alternatively, algorithms such as *branch and bound* [31] could be used and is discussed in chapter 6. Presently, for performance comparison of the proposed MSB non-monotonic rules, we use the *non-rand-st* and *rand* LRT based solutions proposed in Chapter 4. As a recapulation of the approaches we established in the previous chapters,

(i) Chapter 2 (Table 2.3): The *single-threshold* LRT is optimal for non-randomized tests (*non-rand-st* LRT) for monotonic case-A rules,

(ii) Chapter 4 (Proposition 4.3.1 and Table 4.1): The performance of the *non-rand-st* LRT approaches the upper-bound obtained by *rand* LRT with asymptotic number of sensors. The performance difference is insignificant even for small number of sensors, i.e., $N \geq 13$.

5.4.2 *MCB* rules

As the actual P_{f_i} is *unknown* for this category, the NP criterion cannot be applied. Instead, the performance curve is obtained by sequencing the observation vectors in non-increasing order of their $\Lambda(\mathbf{u})$ values and the fusion vector $\mathbf{x}$ is computed for each $a^* \in \{0, \cdots, M-1\}$.

5.5 Numerical results

Following [38], we consider the local decisions $d_i, \forall i$ are transmitted using on-off keying on reporting channels experiencing Rayleigh fading, i.e., $y_i = h_i d_i + w_i$, where $h_i \sim \mathcal{N}_{\mathbb{C}}(0,1)$, $w_i \sim \mathcal{N}_{\mathbb{C}}(0, \sigma_w^2)$ and $y_i \in \mathbb{C}$. The FC employes coherent detection to obtain $u_i, \forall i$ from y_i resulting in $P_{e_i} = \mathcal{Q}(\frac{|h_i|}{2\sigma_w})$. Assuming the a-priori probabilities $p(H_1) = p(H_0) = \frac{1}{2}$, the individual channel SNR for independent non-identically distributed (i.n.i.d) local decisions is defined as $\text{SNR}_i \triangleq \frac{P_{d_i}+P_{f_i}}{2\sigma_{w_i}^2}$.

In Figure 5.1 we plot the non-randomzied test average system performance (P_D vs P_F) of the rules considered in this letter for i.n.i.d decisions using analytical computations and Monte Carlo simulations. We consider a CRN with $N = 10$, the SU characteristics as $P_{f_i} \sim \mathbf{U}(0, 2\mu_f)$, $P_{d_i} = P_{f_i} + p_i$, $p_i \sim \mathbf{U}(0, 2\mu_d), \forall i$, where $(\mu_f, \mu_d) = (0.05, 0.4)$ and reporting channel $\text{SNR}_i \in \{5, 15\}$ dB $\forall i$. The ROC of the *Wu* and *IS* rule is not plotted as it is found that their performance is lower than the

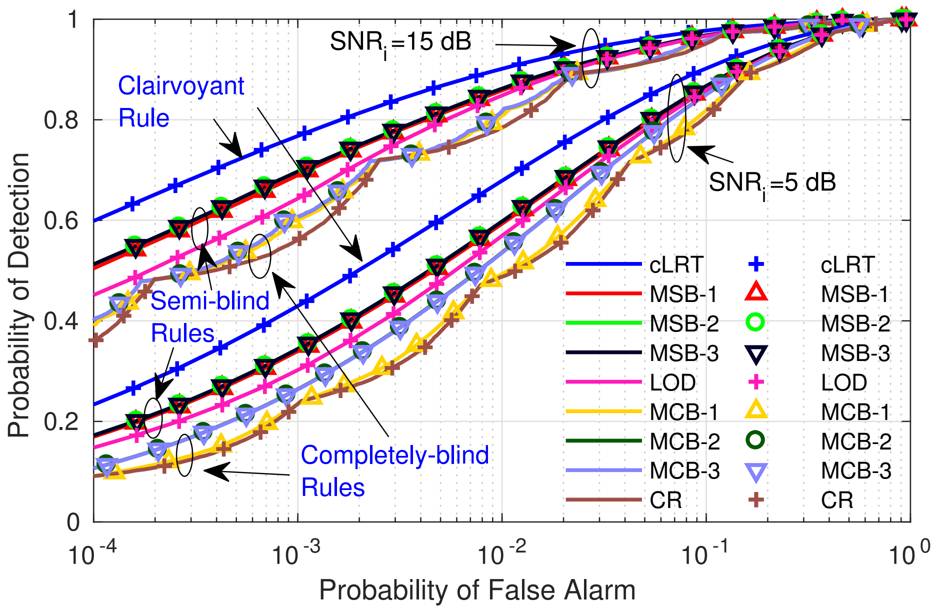

Figure 5.1: Non-randomized test P_D vs P_F plots under NP criterion for $N = 10$, reporting channel $\text{SNR}_i \in \{5, 15\}$ dB, for conditionally i.n.i.d decisions with $(\mu_f, \mu_d) = (0.05, 0.4)$.

MSB and *LOD* rules.

The non-randomized test performance of the clairvoyant and the *MSB* rules are obtained under NP criterion (α is varied from 0 to 1) using 10^2 i.n.i.ds of $(\mathbb{P}_f, \mathbb{P}_d)$, and 10^2 random channel coefficients $h_i, \forall i$ (i.e $P_{e_i}, \forall i$) for each realization of the $(\mathbb{P}_f, \mathbb{P}_d)$. The non-rand fusion vector $\mathbf{x}$ and the system performance $\{P_F, P_D\}$ is obtained analytically (represented by solid lines) using the solutions proposed in Section 5.4. The results are then verified by 10^4 Monte Carlo runs (represented by discrete marks) for each combination of $\{P_{f_i}, P_{d_i}, P_{e_i}, \forall i\}$. Among the semi-blind rules:

(i) as expected, the *MSB-2* rule outperforms all other rules including the existing *LOD* in most of the cases as it uses the optimal estimate of $\widehat{P_{d_i}}$ (using Bayesian inference) from the *known* instantaneous P_{f_i},

(ii) *MSB-2* and *MSB-3* require same system knowledge as the *LOD*.

Among the completely-blind rules:

(i) as expected, the proposed *MCB* rules perform better than the *CR* at the cost of using slightly additional system knowledge,

(ii) the performance of *MCB-1* detoriates for low SNR.

Figure 5.2 and 5.3 report the randomized test P_D vs SNR_i and P_D vs N of the fusion rules generated by Monte Carlo simulations for i.n.i.d decisions and constant $\alpha = 0.01$. The plots confirm that *(i)* among the semi-blind category, the *MSB-2* rule always has the best performance, *(ii)* among the completely-blind category, the *MCB-2* and *MCB-3* perform better than the *CR* with the *MCB-1* detoriating for low SNR.

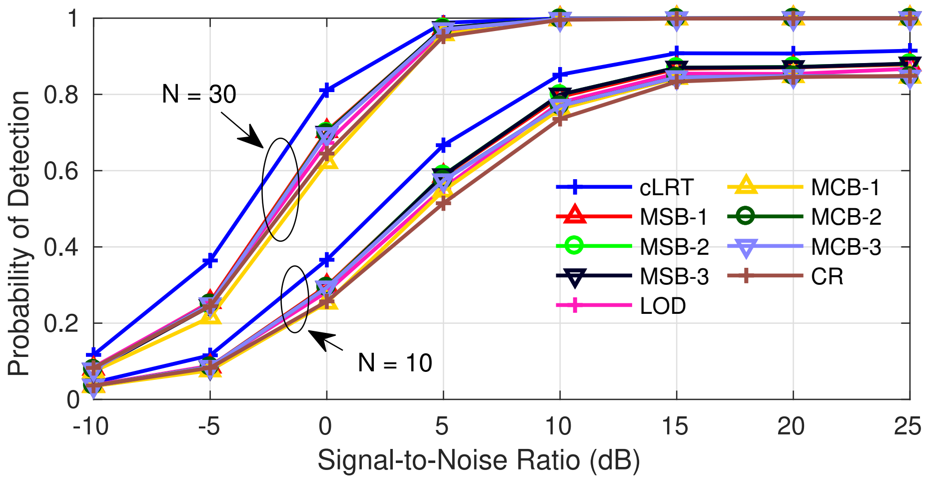

Figure 5.2: Randomized test P_D vs SNR (dB) plots comparison of different rules with $N = \{10, 30\}$ and $\alpha = 0.01$ for conditionally i.n.i.d decisions with $(\mu_f, \mu_d) = (0.05, 0.4)$.

5.6 Conclusions

Novel (semi-)blind fusion rules, using the mean value of the SU characteristics instead of the instantaneous values, have been proposed for the resource-constrained distributed networks. We have shown that these rules with slight (or no) additional system knowledge perform better than the existing rules and have simple decision

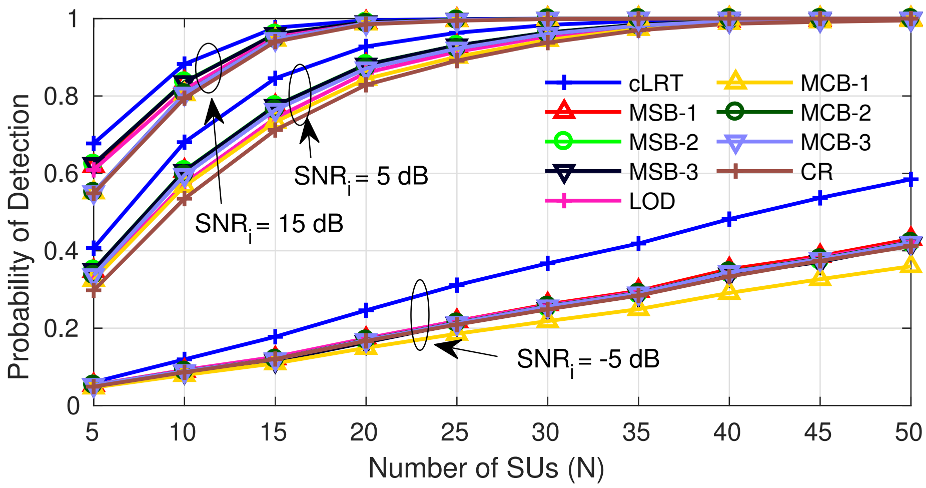

Figure 5.3: Randomized test P_D vs N with SNR $= \{-5, 5, 15\}$ dB and $\alpha = 0.01$, for conditionally i.n.i.d decisions with $(\mu_f, \mu_d) = (0.05, 0.4)$.

equations. The rules $\{$*MSB-2*, *MCB-2*$\}$ of $\{$semi-blind, completely-blind$\}$ categories use Bayesian inference to estimate the *unknown* value and outperform for most of the cases in their respective categories. Further avenues of research include the derivation of blind rules for more advanced cooperative/collaborative spectrum sensing schemes [52].

Chapter 6

Fast Computation of Hard Decision Fusion under Neyman-Pearson Criterion

6.1 Introduction

It is shown in chapter 2 that the optimal solution for the GDFP under the Neyman-Pearson criterion can be computed using low complexity methods like bisection, gradient descent etc., in some cases [19–21] if the LR function is monotonic. However for the non-monotonic problems, the optimal fusion rule requires multi-threshold decision equation and the computations require exponentially complex exhaustive search methods [1, 2, 51].

Secondly, it is shown that the non-randomized hard decision fusion problem is in the form of the classical $0-1$ Knapsack problem (KP) and thereby a low complexity solution using dynamic programming (DP) is proposed. However DP is not an efficient approach for the KP that require high-precision computations, as the space requirement gets impractical for large scaling factor C.

Thirdly, it is shown in Chapter 4 that the performance of the *single-threshold* LRT (*non-rand-st* LRT) approaches the upper-bound obtained by *rand* LRT as the number of sensors N increases. The performance difference gets insignificant even for a low number of sensors, $N > 13$.

In this chapter we focus on using a novel terminiation *branch and bound* algorithm for the non-randomized hard decision fusion under Neyman-Pearson criterion to obtain the near-optimal solution specially for the range $3 \leq N \leq 11$ for wide range of problems with {high, low} precision and {monotonic, semi, non-monotonic} properties. The main contributions are

1. To the best of our knowledge, a novel termination *branch and bound* algorithm (BB) is used for the first time to obtain the solution for non-randomized GDFP in $\mathcal{O}(2M^2)$ *quadratic time* complexity which originally

   (i) required $\mathcal{O}(2^M)$ *exponential time* using exhaustive search,

   (ii) requires $\mathcal{O}(\alpha CM)$ *pseudo-polynomial time* using DP algorithm, that gets impractical for problems with large C.

2. To the best of our knowledge, for the first time we show the performance improvement possible in receiver operating characteristics (ROC) over the conventional *single-threshold* LR-based decision equation (*non-rand-st* LRT) for a wide range of GDFPs.

3. We propose a novel termination mechanism to handle the exception scenarios where the BB gets into repeated unsuccessful searches.

4. We show numerically that the proposed BB obtains the performance ROC that matches with the DP algorithm (i.e., for the low-precision problems where DP can be applied).

The outline of this chapter is as follows. In Section 6.2, we recapitulate the system model and the results from the previous chapters. We present the BB based solution and a novel termination mechanism in 6.3. Section 6.4 contains the ROC plots and numerical results, followed by conclusions in Section 6.5.

6.2 System Model

Using the system model from Chapters 2 and 4 we have,

(i) the conditional probabilities as

$$\begin{aligned} p(\mathbf{u}|H_1) &= \prod_{i=0}^{N-1} (P_{d_i})^{u_i} (\bar{P_{d_i}})^{1-u_i} \\ p(\mathbf{u}|H_0) &= \prod_{i=0}^{N-1} (P_{f_i})^{u_i} (\bar{P_{f_i}})^{1-u_i}. \end{aligned} \tag{6.1}$$

(ii) the system characteristics as

$$P_D(\mathbf{x}) = \sum_{m=0}^{M-1} x_m \; p(\mathbf{u}_m|H_1), \qquad P_F(\mathbf{x}) = \sum_{m=0}^{M-1} x_m \; p(\mathbf{u}_m|H_0). \tag{6.2}$$

(iii) the *non-rand* GDFP formulation under NP criterion as

$$\begin{aligned} \underset{\mathbf{x}}{\text{Max}} \quad & \sum_{m=0}^{M-1} x_m \; p(\mathbf{u}_m|H_1), \\ \text{Sub. to} \quad & \sum_{m=0}^{M-1} x_m \; p(\mathbf{u}_m|H_0) \le \alpha, \quad x_m \in \{0,1\}. \end{aligned} \tag{6.3}$$

(iv) the optimal multi-threshold *non-rand-mt* LRT given by,

$$\left(\Lambda(\mathbf{u}) \triangleq \frac{p(\mathbf{u}|H_1)}{p(\mathbf{u}|H_0)} \right) \underset{u_{fc}=0}{\overset{u_{fc}=1}{\gtrless}} \lambda_{nr}, \tag{6.4}$$

where λ_{nr} are the thresholds to be computed that is exponential in computational complexity. The *non-rand-st* LRT is slightly sub-optimal for *non-rand* GDFP in general (2.2.2.3) and is optimal when the LR function $\Lambda(\mathbf{u})$ is monotonic (case-A, 2.2.2.1).

Assuming the observation vectors are sequenced in descending order of their LR-value $\Lambda(\mathbf{u})$ as

$$\Lambda(\mathbf{u}_0) \geq \cdots \geq \Lambda(\mathbf{u}_{M-1}),$$

the *split*-index s and the system performance corresponding to *non-rand-st* LRT is obtained as (4.3)

$$\left(P_{F_{nr}} \triangleq \sum_{m=0}^{m=s-1} p(\mathbf{u}_m|H_0) \right) \leq \alpha \quad \text{and} \quad P_{Fnr} + p(\mathbf{u}_s|H_0) > \alpha \ ,$$

and

$$P_{Dnr} \triangleq \sum_{m=0}^{m=s-1} p(\mathbf{u}_m|H_1). \tag{6.5}$$

(v) the optimal *rand* LRT (for *rand* GDFP) as

$$\text{If } \Lambda(\mathbf{u}) \begin{cases} > \lambda_r & u_{fc} = 1, \\ = \lambda_r & u_{fc} = 1 \text{ with probability } \gamma_r, \\ < \lambda_r & u_{fc} = 0, \end{cases} \tag{6.6}$$

where λ_r (a single-threshold) and γ_r (probability) is to be computed. The system performance for the *rand* LRT (which is an upper bound for the *non-*

rand LRT) in terms of s is given by

$$\begin{aligned} P_{Fr} &= \alpha\,, \\ P_{Dr} &= P_{Dnr} + \frac{(\alpha - P_{Fnr})}{p(\mathbf{u}_s|H_0)}\, p(\mathbf{u}_s|H_1)\,, \end{aligned} \tag{6.7}$$

where the unknown parameters of (6.6) are $\gamma_r = \dfrac{(\alpha - P_{Fnr})}{p(\mathbf{u}_s|H_0)}$ and $\lambda_r = \Lambda(\mathbf{u}_s)$.

(vi) additionally, Table 6.1 summarizes the list of tests, the categories of the GDFP, the corresponding optimal LR-based decision equations and their solution complexities.

Table 6.1: Categorization of GDFP tests and their LR-based Optimal solution complexities

Test	**GDFP property**	**LRT**	**Complexity**‡	**DP Algo.**
randomized	non-monotonic	single	$\mathcal{O}(M\log(M))$	-
	monotonic	single	$\mathcal{O}(M)$	-
non-randomized	non-monotonic†	multi	$\mathcal{O}(2^M)$	$\mathcal{O}(\alpha CM)$
	semi-monotonic†	multi	$\mathcal{O}(2^M)$	$\mathcal{O}(\alpha CM')$
	monotonic †	multi	$\mathcal{O}(2^M)$	$\mathcal{O}(\alpha CM)$
	monotonic (case-A)	single	$\mathcal{O}(M)$	-

† These problems are known to be NP-hard.
‡ The original complexity.

Focusing on the optimal solution for non-randomized test of GDFP, it is shown to be a classical $0-1$ Knapsack problem (in Chapter 2) and NP-hard in the most general case [31]. The DP based algorithm proposed in Chapter 2 is an integer programming approach and requires the conditional probability $p(\mathbf{u}|H_0)$ (a function of $P_{f_i}, \forall i$) to be scaled to integers. As a result DP requires large scaling factor C for high-precision computations (i.e., when $p(\mathbf{u}|H_0) \ll 10^5$). Its computational complexity (time and space) given by $\mathcal{O}(\alpha CM)$ increases with C, and C increases with N, thereby making DP impractical for such scenarios.

To alleviate this, we now propose to use the simple *branch and bound* (BB) method [31,32] used for $0-1$ Knapsack to obtain the optimal solution for the GDFP. Further improvising the BB, we use a novel termination mechanism (to handle exceptions[1]) that assists in obtaining the solution in $\mathcal{O}(2M^2)$ *quadratic time* complexity.

6.3 Branch and Bound Algorithm

We now focus on the BB method to efficiently search the complete solution space of cardinality 2^M to obtain the M-dimensional optimum fusion vector $\mathbf{x}^*$.

We assume that the observation vectors are sequenced in descending order of their LR-value. Slightly different from the Chapter 2, define a parameterized GDFP $\mathbf{G}(a,b)$, as:

$$\mathbf{G}(a,b) \triangleq \begin{cases} \underset{\mathbf{x^a}}{\text{Max}} & \sum_{m=a}^{M-1} x_m \, p(\mathbf{u}_m|H_1), \\ \text{Sub to:} & \sum_{m=a}^{M-1} x_m \, p(\mathbf{u}_m|H_0) \leq b, \end{cases} \tag{6.8}$$

where $\mathbf{x^a}$ is the initial part of vector $\mathbf{x}$ given by $\mathbf{x^a} = [x_{M-1} \cdots x_a]$, $a \in \{0, \cdots, M-1\}$ and b is a constraint variable, $b \in \mathbb{R}$, $0 < b \leq \alpha$. Further, GDFP (6.8) can be rewritten in the form of a recursive equation as,

$$\mathbf{G}(a,b) = \begin{cases} \max\Big(p(\mathbf{u}_a|H_1) + \mathbf{G}(a+1, b-p(\mathbf{u}_a|H_0)), \\ \qquad \mathbf{G}(a+1,b)\Big), \quad \text{for } p(\mathbf{u}_a|H_0) \leq b, & \text{(6.9a)} \\ \mathbf{G}(a+1,b), \qquad \text{for } p(\mathbf{u}_a|H_0) > b, & \text{(6.9b)} \end{cases}$$

and with final condition as

$$\mathbf{G}(M-1,b) = \begin{cases} p(\mathbf{u}_{M-1}|H_1), & \text{for } p(\mathbf{u}_{M-1}|H_0) \leq b, \quad \text{(6.10a)} \\ 0, & \text{for } p(\mathbf{u}_{M-1}|H_0) > b. \quad \text{(6.10b)} \end{cases}$$

Note that the optimum P_D^* for GDFP of (6.3) can be obtained by computing $\mathbf{G}(0,\alpha)$

[1] Unsuccessful searches

using the recursive equations in (6.9) and (6.10). Simultaneously, the optimum fusion vector $\mathbf{x}^*$ can be obtained by setting each boolean variable of $\mathbf{x}$ corresponding to the parameter index a as $x_a = 1$ when $p(\mathbf{u}_a|H_1)$ contributes to the optimum solution (i.e., first term of 'max()' in (6.9a) and (6.10a)) and $x_a = 0$ otherwise $\forall a$.

Note that in the worst-case each function call of $\mathbf{G}(a, \cdot)$ results in two recursive function calls (namely *branches*) of $\mathbf{G}(a+1, \cdot)$ as in (6.9a), thereby resulting in exponential number of branching operations (BO) ($= 2^M$) for obtaining the optimum solution. Typically some of the branches are pruned (not traversed) as the condition on constraining variable b in (6.9a) is not satisfied, and alternatively the single-branch in (6.9b) is traversed.

We now focus on further reducing the computation complexity by identifying and preempting the BOs that are not likely to improve the objective value beyond what is already achieved ($\widehat{P_D}$) by the traversed branches. To facilitate this, the key idea is to use a linear complexity *upper-bound* operation $ub\big(\cdot\big)$ such that $ub(a,b) \geq \mathbf{G}(a,b)$, $\forall a$ and $\forall b$. Note that a tight upper-bound function is desirable to identify and prune as many non-contributing branches as possible preemptively.

The bound functions typically used are:

UB-1

As a simple option, the optimal objective value obtained by applying *rand. LRT* (6.7) to the sub-problem $\mathbf{G}(a,b)$ can be used as an upper bound,

$$ub(a,b) \triangleq P_{D_r} \quad . \tag{6.11}$$

UB-2

Alternatively $ub(\cdot)$ function which results in a tighter bound is defined as [31]

$$ub(a,b) \triangleq \max\Bigg(P_{D_{nr}} + \Big(b - P_{F_{nr}}\Big)\frac{p(\mathbf{u}_{s+1}|H_1)}{p(\mathbf{u}_{s+1}|H_0)},$$

$$P_{D_{nr}} + p(\mathbf{u}_s|H_1) + \Big(b - P_{F_{nr}} - p(\mathbf{u}_s|H_0)\Big)\frac{p(\mathbf{u}_{s-1}|H_1)}{p(\mathbf{u}_{s-1}|H_0)}\Bigg), \quad (6.12)$$

where $\{s, P_{D_r}, P_{F_r}\}$ are the *non-rand-st* LRT values computed using (6.5) for the sub-problem $\mathbf{G}(a,b)$. Note that the upper-bound from (6.12) is the objective value obtained from a type of *rand. LRT* where $\{0 \leq x_{s+1} \leq 1\}$ or $\{x_s = 1, x_{s-1} \in \mathbb{R}\}$ is used. For $s \in \{a, M-1\}$, $ub(\cdot)$ in (6.12) is not defined and alternatively UB-1 is used in such case.

Algorithm 2 provides the complete implementation of the recursive *branching* equations of the GDFP in (6.9) along with the *bound* mechanism of (6.12). The recursive equation of $\mathbf{G}(a,b)$ is implemented by the function $bb(a,b,\mathbf{x})$ (line 3-15). The execution is initiated with a call to the function $bb(\cdot)$ with the seed parameters on line 2.

The lines 4 and 6 terminate the function when the parameters $\{b,a\}$ cross their valid range. The branches corresponding to $x_a = 1$ and $x_a = 0$ are implemented in lines 7-10 and 11-14 respectively. Execution of a branch is continued only if the corresponding *upper-bound* value of the complete branch is greater than the already achieved objective value $\widehat{P_D}$ (lines 7 and 11). The variables $\widehat{P_D}$, $\widehat{P_F}$ and $\widehat{\mathbf{x}}$ are continously updated (line 5) with the best solution obtained as the algorithm recurs. These variables are updated with the incrementally improved values found and hold the optimal solution $(P_D^*, P_F^*, \mathbf{x}^*)$ by the end of all recursions. Note that the algorithm traverses depth-first into the tree with $x_a = 1$ branches as the best objective values are found in this path (due to the LR-value based ordering), thereby obtaining a high

Algorithm 2 *Branch and Bound* solution for GDFP

Initialize $\widehat{P_D} \leftarrow 0$; $\widehat{P_F} \leftarrow 0$; $\widehat{\mathbf{x}} \leftarrow [0 \cdots 0]$; $fails \leftarrow 0$
call $bb(0, \alpha, \widehat{\mathbf{x}})$

function $bb(a, b, \mathbf{x})$
    if $b < 0$ **then** return **end if**
    call $update(\mathbf{x})$
    if $a > M - 1$ **then** return **end if**
    if $P_D(\mathbf{x}) + \mathrm{ub}(a, b) > \widehat{P_D}$ **then**
        $\mathbf{x}_{copy} \leftarrow \mathbf{x}$; $\mathbf{x}_{copy}(a) \leftarrow 1$
        call $bb(a + 1, b - p(\mathbf{u}_a|H_0), \mathbf{x}_{copy})$
    end if
    if $P_D(\mathbf{x}) + \mathrm{ub}(a + 1, b) > \widehat{P_D}$ **then**
        $\mathbf{x}_{copy} \leftarrow \mathbf{x}$; $\mathbf{x}_{copy}(a) \leftarrow 0$
        call $bb(a + 1, b, \mathbf{x}_{copy})$
    end if
end function

function $update(\mathbf{x})$
    $fails \leftarrow fails + 1$
    if $P_D(\mathbf{x}) > \widehat{P_D}$ **then**
        $\widehat{P_D} \leftarrow P_D(\mathbf{x})$; $\widehat{P_F} \leftarrow P_F(\mathbf{x})$; $\widehat{\mathbf{x}} \leftarrow \mathbf{x}$; $fails \leftarrow 0$
    end if
    if $fails >$ maxFAILS **then**
        Exit
    end if
end function

$\widehat{P_D}$ value in the initial few BOs itself and as a result preempting many BOs later.

It is known that the BB algorithm generally terminates with linear number of BOs due to violation of conditions in lines 4, 6, 7 and 11. However in the exception scenarios the number of BOs could be exponential. To handle this scenario, we propose to add an additional condition based on the number of contiguous unsuccessful[2] calls to the *update*$(\cdot)$ function.

Intuitively as the $ub(\cdot)$ is not tight enough, under the worst-case scenario the recursions continue even after the optimal objective value is obtained (i.e., $\widehat{P_D} = P_D^*$). We propose to identify this scenario by keeping track of contiguous unsuccessful calls ($fails$) to the *update*$(\cdot)$ function and exit the algorithm when a reasonable count (maxFAILS) is reached (line 23). This mechanism improves the average number of BOs (ABOs) at the cost of potentially a slight sub-optimal value for the worst-case scenario.

6.4 Numerical solution and discussion

In Figure 6.1 we plot the average system performance (P_D vs α) obtained for

(i) the randomized test for the GDFP using randomized LRT (labeled "*rand LRT*"),

(ii) the non-randomized test for the GDFP obtained by

- the proposed BB Algorithm 2 using the worst-case termination count maxFAILS = 100 (labeled "*BB*")
- and the conventional non-randomized *single-threshold* LRT (labeled "*non-rand-st LRT*").

We consider a system with $N = \{3, 5, 7, 9, 11\}$, the SU characteristics as $P_{f_i} \sim \mathbf{U}(0, 1)$ and $P_{d_i} = P_{f_i} + \mathbf{U}(P_{f_i}, 1), \forall i$ where $\mathbf{U}(s_1, s_2)$ denotes uniform probability distribution

[2] We count a call to *update*$(\cdot)$ function as unsuccessful when there is no improvement to the achieved objective value.

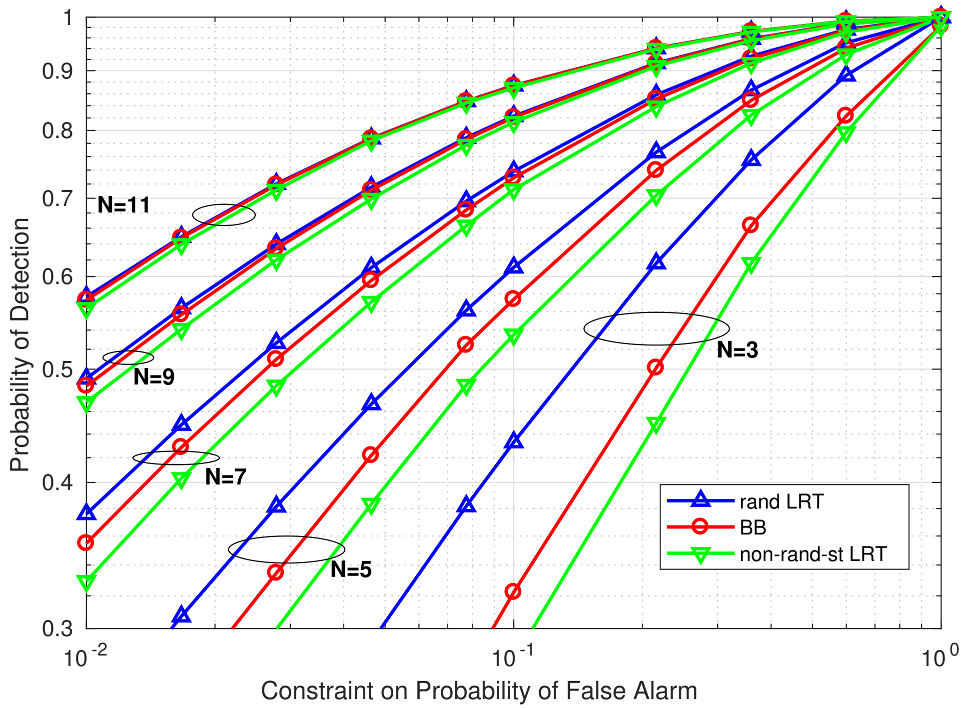

Figure 6.1: P_D vs α plots under NP criterion for different number of SUs N for the most general case.

with supports as s_1 and s_2. The performance curves are obtained under NP criterion (α is varied from 0.01 to 1) using 10^3 realizations of $(\mathbb{P}_f, \mathbb{P}_d)$ (note that this scenario can result in $p(\mathbf{u}|H_0) \ll 10^5$ and thereby making DP impractical).

In the non-randomized test category the ROC "*BB*" is near-optimal and out-performs the sub-optimal ROC "*non-rand-st LRT*" for all N. Note that the non-randomized test ROCs approach the randomized test ROC for larger values of N (i.e., > 11) reaffirming that a non-randomized *single-threshold* LRT is close to optimal for large N.

Table 6.2 presents the computational complexity of the proposed BB algorithm in terms of the ABOs executed by the BB to obtain the optimal solution for $\alpha = 0.1$ and different N when run for 10^3 realizations of $(\mathbb{P}_f, \mathbb{P}_d)$ with different monotonic properties. Note that the BB algorithm has used $\mathcal{O}(M)$ linear number of ABO for all the GDFP types, with each BO consuming $\mathcal{O}(M)$ for computing $ub(\cdot)$ value. Also

Table 6.2: Average number of BOs used by the Branch and Bound algorithm for different N for non-randomized tests

GDFP Type $\downarrow$ $N \rightarrow$	3	5	7	9	11
non-monotonic	10	91	242	349	878
semi-monotonic	9	47	212	497	1647
monotonic	15	98	171	280	714
monotonic (case-A)	11	89	159	397	1371
Exhaustive†	2^8	2^{32}	2^{128}	2^{512}	2^{2048}

† indicates the number of BOs required for the *Exhaustive Search* (i.e., $2^M = 2^{2^N}$).

note that the proposed algorithm obtains the solution for the GDFP with different monotonic properties in similar time complexity, thereby preempting the need to categorize the GDFP apriori based on monotonic properties.

In Figure 6.2 we plot the average system performance (P_D vs α) obtained for the non-randomized test for the GDFP obtained by *(i)* the proposed BB Algorithm (marked in red 'x') and *(ii)* the DP algorithm (marked in blue 'o'). To make it conducive for applying the DP algorithm (i.e., causing $p(\mathbf{u}_m|H_0) \geq 10^5$, $\forall m$), we consider a system with $N = \{3, 5, 7, 9, 11\}$, the SU characteristics as $P_{f_i} \sim \mathbf{U}(0.3, 0.7)$ and $P_{d_i} = P_{f_i} + \mathbf{U}(P_{f_i}, 1), \forall i$. The performance curves are obtained under NP criterion (α is varied from 0.01 to 1) using 10^3 realizations of $(\mathbb{P}_f, \mathbb{P}_d)$.

Table 6.3 lists the average P_D obtained by DP and BB algorithms respectively for different number of SUs N and the DP scaling factor as $C = 10^5$.

From the Figure 6.2 and Table 6.3, we can conclude that

(i) The ROC plots from DP and BB almost match each other.

(ii) There is slight (insignificant) performance drop from BB due to search termination for the exception cases.

(iii) Unlike the DP, the BB algorithm is immune to the precision of the system

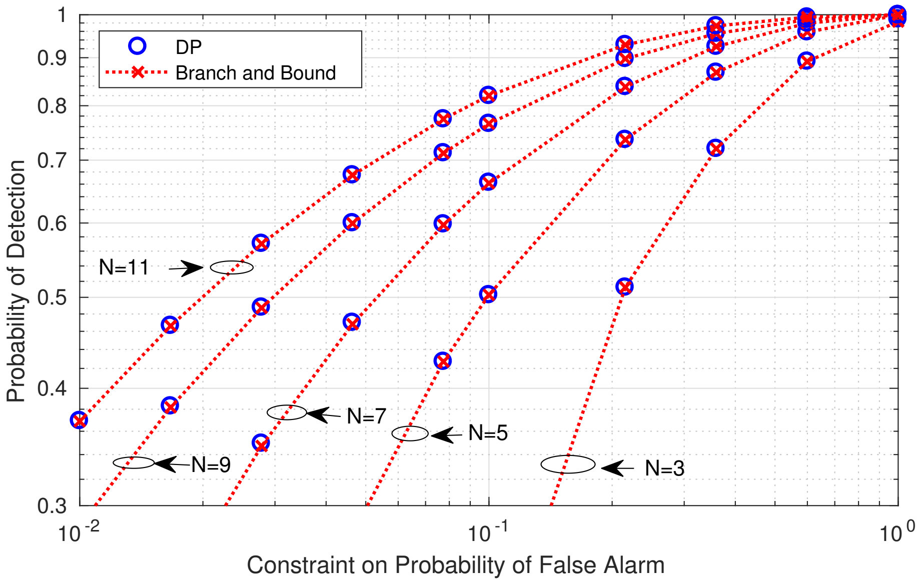

Figure 6.2: P_D vs α plots for different number of SUs N using *DP* and *Branch and Bound* algorithms.

Table 6.3: Average P_D obtained by DP and BB algorithms for $\alpha = 0.1$ for different N values.

N	DP	BB
3	0.1916	0.1916
5	0.5030	0.5030
7	0.6627	0.6615
9	0.7657	0.7654
11	0.8199	0.8199

characteristics. It can be applied to a GDFP with any precision.

(iv) The computational complexity of the BB is conjectured to be *quadratic* in M and is independent of the precision.

6.5 Conclusion

The simple and efficient BB computational algorithm is presented and applied to a wide range of GDFPs to obtain the non-randomized optimal fusion vector in $\mathcal{O}(2M^2)$

quadratic time which was originally an $\mathcal{O}(2^M)$ exponential complex problem. A novel termination mechanism for the BB is proposed to handle the exception scenario. Additionally, the BB has the potential to be used for other problems in the area of distributed detection like joint optimization of decision / fusion rule as in [26, 39–41] etc.

Chapter 7

Conclusions and Future Work

7.1 Conclusions

In this thesis, we have formulated the non-randomized hard decision fusion problem under Neyman-Pearson criterion as the GDFP and related it to the classical $0-1$ Knapsack problem. We have applied dynamic programming concepts and obtained an optimal solution with pseudo-polynomial complexity (i.e., $\mathcal{O}(\alpha CM)$) for the non-monotonic case which originally was $\mathcal{O}(2^M)$ in computational complexity.

We then defined a desirable *semi-monotonic* property that the GDFP exhibits in most practical cases. This property was exploited to reduce the dimension of the feasible solution space and the optimal solution using DP was obtained with $\mathcal{O}(\alpha CM')$ complexity.

For a larger network with participating sensors $N \geq 13$, we showed that the performance of the single-threshold *non-rand-st* LRT (which has a simple solution in $\mathcal{O}(M\log(M))$ and is known to be sub-optimal) approaches the upper-bound obtained by the *rand* LRT.

Using the low complexity solutions presented, we proposed novel (semi-)blind hard decision fusion rules (that are variants of the GDFP) and showed that these rules with slight (or no) additional system knowledge achieve better ROC than the existing alternatives.

As the dynamic programming based solution was constrained by the precision for the problem, we further presented the *branch and bound* based algorithm (with $\mathcal{O}(2M^2)$ complexity) to obtain the near-optimal solution especially for the range $3 \leq N \leq 11$ for wide range of problems with {high, low} precision, {monotonic, semi, non-monotonic} properties. Table 7.1 summarizes all the proposed algorithms, their applicability and the solution characteristics.

Table 7.1: Summary of proposed solutions.

Proposed algorithms	*optimal* solution	*near-optimal* solution
Dynamic programming	$\mathcal{O}(\alpha CM)$ for low-precision GDFPs	
Variable reduction	$\mathcal{O}(\alpha CM')$ for low-precision and semi-monotonic GDFPs	
Single-threshold LRT		$\mathcal{O}(M\log(M))$ for all GDFPs with $N \geq 13$
Branch and bound		Conjectured to be $\mathcal{O}(2M^2)$ for all GDFPs

7.2 Future research avenues

In this thesis, we showed that the hard decision fusion problem is a $0-1$ Knapsack problem and proposed low complexity algorithms to obtain optimal fusion rules. Further, this approach has the potential to be applied to broader categories of problems such as the following:

(i) the fusion problems with continuous observation space using softened hard approach in [21, 24, 36];

(ii) jointly optimizing the decision rules at the SUs and the fusion rule at the FC as in [26, 39–41];

(iii) generalization of conditionally dependent decisions as in [42];

(iv) censoring some of the SUs for resource (like energy, reporting channel bandwidth, system throughput etc.,) optimization as in [43–46].

Appendix A

Background

A.1 Fusion rule performance criteria

A.1.1 Bayesian criterion

The Cost function $\bar{C}$ is defined as

$$\begin{aligned}
\bar{C} &= \sum_{i,j} C_{i,j}\, Pr\{\text{ say } H_i \text{ when } H_j \text{ true }\} = \sum_{i,j} C_{i,j}\, \pi_j\, Pr\{\text{ say } H_i \mid H_j \text{ true }\} \\
&= \sum_{i,j} C_{i,j}\, \pi_j\, Pr\{\mathbf{u} \in \mathfrak{R}_\mathrm{i} \mid H_j \text{ true }\} = \sum_{i,j} C_{i,j}\, \pi_j \sum_{\mathbf{u} \in \mathfrak{R}_\mathrm{i}} p\{\mathbf{u} \mid H_j\} \\
&= \sum_{\mathbf{u} \in \mathfrak{R}_\mathrm{o}} \Big[C_{0,0}\, \pi_0\, p\{\mathbf{u} \mid H_0\} + C_{0,1}\, \pi_1\, p\{\mathbf{u} \mid H_1\} \Big] + \\
&\quad \sum_{\mathbf{u} \in \mathfrak{R}_1} \Big[C_{1,0}\, \pi_0\, p\{\mathbf{u} \mid H_0\} + C_{1,1}\, \pi_1\, p\{\mathbf{u} \mid H_1\} \Big]
\end{aligned}$$

where $C_{i,j}$ is the cost associated with the decision that H_i is declared when H_j is true and π_0, π_1 are the apriori probabilities of the hypothesis H_0 and H_1.

LR-based Test minimizes the cost function $\bar{C}$ and is given as [1]

$$\left(\Lambda(\mathbf{u}) \triangleq \frac{p\{\mathbf{u}|H_1\}}{p\{\mathbf{u}|H_0\}}\right) \underset{\mathbf{u}\in\Re_0}{\overset{\mathbf{u}\in\Re_1}{\gtrless}} \frac{\pi_0\Big[C_{1,0} - C_{0,0}\Big]}{\pi_1\Big[C_{0,1} - C_{1,1}\Big]},$$

and can be simplified to

$$\sum_{i=0}^{N-1} u_i \log\left(\frac{\bar{P_{f_i}}}{P_{f_i}} \frac{P_{d_i}}{\bar{P_{d_i}}}\right) \underset{\mathbf{u}\in\Re_0}{\overset{\mathbf{u}\in\Re_1}{\gtrless}} \lambda,$$

which is also widely known as the *Chair-Varshney* rule. In this case the threshold λ is computed in constant time using the values of the cost function and the apriori probabilities.

A.1.2 Neyman-Pearson criterion

The Neyman-Pearson criterion does not require the knowledge of the cost functions and the apriori probabilities of the hypothesis. It can be defined as,

$$\underset{\Re_1}{\text{Maximize}} \quad P_D, \quad \text{Sub to: } P_F \leq \alpha \,.$$

The optimum decision equation is again given by the LRT,

$$\sum_{i=0}^{N-1} u_i \log\left(\frac{\bar{P_{f_i}}}{P_{f_i}} \frac{P_{d_i}}{\bar{P_{d_i}}}\right) \underset{\mathbf{u}\in\Re_0}{\overset{\mathbf{u}\in\Re_1}{\gtrless}} \lambda,$$

however the threshold(s) λ now need to be computed to satisfy the constraint value α.

A.2 Types of decision equations

Non-randomized decision equations [22, 24–26]

$$
\begin{array}{llcl}
\text{LR Test:} & \Lambda(\mathbf{u}) & \underset{u_{fc}=0}{\overset{u_{fc}=1}{\gtrless}} & \lambda_{lrt} \\
\text{Linear weighted sum:} & \sum_{i=0}^{N-1} W_i u_i & \underset{u_{fc}=0}{\overset{u_{fc}=1}{\gtrless}} & \lambda_{lws} \\
\text{Counting Rule:} & \sum_{i=0}^{N-1} u_i & \underset{u_{fc}=0}{\overset{u_{fc}=1}{\gtrless}} & K
\end{array}
$$

Randomized decision equation [21]

$$
\text{If } \Lambda(\mathbf{u}) \begin{cases} > \lambda_{rnd} & u_{fc} = 1, \\ = \lambda_{rnd} & u_{fc} = 1 \text{ with probability } {\gamma_{rnd}}^{1}, \\ < \lambda_{rnd} & u_{fc} = 0, \end{cases}
$$

A.3 Relevant work

Ref	Criterion	Secondary Users	Local Decisions	Reporting Ch.	Fusion Center
[13]	Bayesian	P_{d_i}, P_{f_i}	Hard (ind.), OOK	Rayleigh Flat-fading MAC	LRT using received energy
[14]	Bayesian	P_d, P_f	Hard (ind.), OOK	Rayleigh, Racian flat-fading MAC	LRT using received energy
[15, 16]	Bayesian	P_d, P_f	Hard (ind.)	Ideal	K-out-of-N (LRT using received decisions)
[17]	Bayesian	P_{d_i}, P_{f_i}	Hard (ind.)	Ideal	LRT using received decisions
[18]	Bayesian	$P_{d,i}$, $P_{f,i}$	Hard (dep.)	Ideal	LRT using received decisions

Table A.1: Summary of relevant work available in the literature.

Ref	**Criterion**	**Secondary Users**	**Local Decisions**	**Reporting Ch.**	**Fusion Center**
[19, 20]	Neyman-Pearson (throughput and P_D under constraint on P_F)	P_d,P_f	Hard (ind.)	Ideal	K-out-of-N, k^*, local threshold λ^*
[21]	Neyman-Pearson	P_{d_i},P_{f_i}	Soft and Hard (ind.)	BSC	rand. LRT

Table A.1: Summary of relevant work available in the literature.

where *OOK* is On-Off Keying, *MAC* is multiaccess channel, *ind.* is independent, *dep.* is dependent, *BSC* is binary symmetric channel.

Appendix B

Examples

B.1 Monotonic case-A

A numerical example for which the GDFP exhibits the *monotonic case-A* property is given in Table B.1.

Table B.1: Numerical values of the SU characteristics for $N = 4$.

i	P_{d_i}	P_{f_i}
3	0.6838	0.3053
2	0.5852	0.3820
1	0.5567	0.4225
0	0.5617	0.4204

We obtain the conditional probabilities $\{p(\mathbf{u}|H_1), p(\mathbf{u}|H_0)\}$ for each of the possible observation vectors $\mathbf{u}$ using (2.8) and list them in Table B.2. Further the function $T(\mathbf{u})$ on which the LR function $\Lambda(\mathbf{u})$ is monotonic is,

$$T(\mathbf{u}) = 7.55u_3 + 3.55u_2 + 1.55u_1 + 2.55u_0 \quad . \tag{B.1}$$

Note in Table B.2 that for this special case, the conditional probability $p(\mathbf{u}|H_1)$ is non-decreasing on $T(\mathbf{u})$ of (B.1) and $p(\mathbf{u}|H_0)$ is non-increasing.

Table B.2: Numerical conditional probabilities of the observation vectors for $N = 4$.

$\mathbf{u}$	$T(\mathbf{u})$	$p(\mathbf{u}\|H_1)$	$p(\mathbf{u}\|H_0)$	$\Lambda(\mathbf{u})$	m
$[0000]^T$	0	0.0255	0.1437	0.1773	0
$[0010]^T$	1.55	0.0320	0.1051	0.3044	1
$[0001]^T$	2.55	0.0327	0.1042	0.3133	2
$[0100]^T$	3.55	0.0359	0.0888	0.4048	3
$[0011]^T$	4.10	0.0410	0.0763	0.5379	4
$[0110]^T$	5.10	0.0452	0.0650	0.6949	5
$[0101]^T$	6.10	0.0461	0.0644	0.7152	6
$[1000]^T$	7.55	0.0551	0.0632	0.8725	7
$[0111]^T$	7.65	0.0579	0.0471	1.2278	8
$[1010]^T$	9.10	0.0692	0.0462	1.4978	9
$[1001]^T$	10.10	0.0706	0.0458	1.5415	10
$[1100]^T$	11.10	0.0777	0.0390	1.9914	11
$[1011]^T$	11.65	0.0887	0.0335	2.6464	12
$[1110]^T$	12.65	0.0976	0.0286	3.4188	13
$[1101]^T$	13.65	0.0996	0.0283	3.5186	14
$[1111]^T$	15.20	0.1251	0.0207	6.0406	15

B.2 Monotonic case-B

A numerical example for which the GDFP exhibits the *monotonic case-B* property is given in Table B.3.

Table B.3: Numerical values of the SU characteristics for $N = 4$.

i	P_{d_i}	P_{f_i}
3	0.6752	0.5924
2	0.6192	0.5700
1	0.5389	0.5115
0	0.6576	0.5829

We obtain the conditional probabilities $\{p(\mathbf{u}|H_1), p(\mathbf{u}|H_0)\}$ for each of the possible observation vectors $\mathbf{u}$ using (2.8) and list them in Table B.4. Further the function $T(\mathbf{u})$ on which the LR function ($\Lambda(\mathbf{u})$) is monotonic is,

$$T(\mathbf{u}) = 6.2u_3 + 2.7u_2 + 1.2u_1 + 5.2u_0 \tag{B.2}$$

Note in Table B.4 that for this special case, both the conditional probabilities $p(\mathbf{u}|H_1)$ and $p(\mathbf{u}|H_0)$ are non-decreasing on $T(\mathbf{u})$ of (B.2).

Table B.4: Numerical conditional probabilities of the observation vectors for $N = 4$.

$\mathbf{u}$	$T(\mathbf{u})$	$p(\mathbf{u}\|H_1)$	$p(\mathbf{u}\|H_0)$	$\Lambda(\mathbf{u})$	m
$[0000]^T$	0	0.0195	0.0357	0.5468	0
$[0010]^T$	1.2	0.0228	0.0374	0.6103	1
$[0100]^T$	2.7	0.0318	0.0473	0.6708	2
$[0110]^T$	3.9	0.0371	0.0496	0.7487	3
$[0001]^T$	5.2	0.0375	0.0499	0.7515	4
$[1000]^T$	6.2	0.0406	0.0519	0.7821	5
$[0011]^T$	6.4	0.0438	0.0523	0.8388	6
$[1010]^T$	7.4	0.0474	0.0543	0.8730	7
$[0101]^T$	7.9	0.0610	0.0662	0.9218	8
$[1100]^T$	8.9	0.0660	0.0688	0.9594	9
$[0111]^T$	9.1	0.0713	0.0693	1.0289	10
$[1110]^T$	10.1	0.0771	0.0720	1.0709	11
$[1001]^T$	11.4	0.0780	0.0725	1.0748	12
$[1011]^T$	12.6	0.0911	0.0759	1.1997	13
$[1101]^T$	14.1	0.1268	0.0961	1.3185	14
$[1111]^T$	15.3	0.1482	0.1007	1.4716	15

B.3 non-monotonic

A numerical example for which the GDFP exhibits the *non-monotonic* property is given in Table B.5.

Table B.5: Numerical values of the SU characteristics for $N = 4$.

i	P_{d_i}	P_{f_i}
3	0.8290	0.5036
2	0.6082	0.5273
1	0.8598	0.5229
0	0.4362	0.4177

We obtain the conditional probabilities $\{p(\mathbf{u}|H_1), p(\mathbf{u}|H_0)\}$ for each of the possible observation vectors $\mathbf{u}$ using (2.8) and list them in Table B.6. Further the function $T(\mathbf{u})$ on which the LR function $\Lambda(\mathbf{u})$ is monotonic is,

$$T(\mathbf{u}) = 4.8u_3 + 2.8u_2 + 6.8u_1 + 0.8u_0 \tag{B.3}$$

Note in Table B.6 that for this special case, both the conditional probabilities $p(\mathbf{u}|H_1)$ and $p(\mathbf{u}|H_0)$ are non-monotonic on $T(\mathbf{u})$ of (B.3).

Table B.6: Numerical conditional probabilities of the observation vectors for $N = 4$.

$\mathbf{u}$	$T(\mathbf{u})$	$p(\mathbf{u}\|H_1)$	$p(\mathbf{u}\|H_0)$	$\Lambda(\mathbf{u})$	m
$[0000]^T$	0	0.0053	0.0652	0.0813	0
$[0001]^T$	0.8	0.0041	0.0468	0.0877	1
$[0100]^T$	2.8	0.0082	0.0727	0.1131	2
$[0101]^T$	3.6	0.0064	0.0522	0.1220	3
$[1000]^T$	4.8	0.0257	0.0661	0.3883	4
$[1001]^T$	5.6	0.0199	0.0474	0.4188	5
$[0010]^T$	6.8	0.0325	0.0714	0.4545	6
$[0011]^T$	7.6	0.0251	0.0512	0.4903	7
$[1100]^T$	7.6	0.0399	0.0738	0.5403	8
$[1101]^T$	8.4	0.0308	0.0529	0.5829	9
$[0110]^T$	9.6	0.0504	0.0797	0.6325	10
$[0111]^T$	10.4	0.0390	0.0572	0.6823	11
$[1010]^T$	11.6	0.1574	0.0725	2.1716	12
$[1011]^T$	12.4	0.1218	0.0520	2.3426	13
$[1110]^T$	14.4	0.2444	0.0809	3.0222	14
$[1111]^T$	15.2	0.1891	0.0580	3.2601	15

B.4 semi-monotonic

A numerical example for which the GDFP exhibits the *semi-monotonic* property is given in Table B.7.

Table B.7: Numerical values of the SU characteristics for $N = 4$.

i	P_{d_i}	P_{f_i}
3	0.6589	0.3588
2	0.7261	0.4490
1	0.8761	0.4576
0	0.5549	0.4367

We obtain the conditional probabilities $\{p(\mathbf{u}|H_1), p(\mathbf{u}|H_0)\}$ for each of the possible observation vectors $\mathbf{u}$ using (2.8) and list them in Table B.8. Further the function $T(\mathbf{u})$ on which the LR function $\Lambda(\mathbf{u})$ is monotonic is,

$$T(\mathbf{u}) = 3.95u_3 + 2.95u_2 + 6.95u_1 + 1.45u_0 \tag{B.4}$$

Note in Table B.8 that for this special case, both the conditional probabilities $p(\mathbf{u}|H_1)$ and $p(\mathbf{u}|H_0)$ are non-monotonic on $T(\mathbf{u})$ of (B.4). However, semi-monotonic property is apparent when the observation vectors and the corresponding values are organized in a graph as depicted in Figure B.1.

Each realization of the observation vector $\mathbf{u}$ is represented by a node (blue box). Each node is connected by an arrow (going out) to another node with higher $T(\mathbf{u})$ and $\Lambda(\mathbf{u})$ value. Note that in every possible path traversed along the arrows from node $\mathbf{u}_0$ to $\mathbf{u}_{15}$, the $\Lambda(\mathbf{u})$ is non-decreasing, $\{p(\mathbf{u}|H_1)$ is non-decreasing and $p(\mathbf{u}|H_0)\}$ is non-increasing. Thereby exhibiting the monotonic case-A property on subset of observation vectors, namely the semi-monotonic property.

Table B.8: Numerical conditional probabilities of the observation vectors for $N = 4$.

$\mathbf{u}$	$T(\mathbf{u})$	$p(\mathbf{u}\|H_1)$	$p(\mathbf{u}\|H_0)$	$\Lambda(\mathbf{u})$	m'
$[0000]^T$	0	0.0052	0.1079	0.0477	0
$[0001]^T$	1.45	0.0064	0.0837	0.0767	1
$[0100]^T$	2.95	0.0137	0.0880	0.1553	4
$[1000]^T$	3.95	0.0100	0.0604	0.1647	8
$[0101]^T$	4.4	0.0170	0.0682	0.2497	5
$[1001]^T$	5.4	0.0124	0.0468	0.2650	9
$[1100]^T$	6.9	0.0264	0.0492	0.5360	12
$[0010]^T$	6.95	0.0364	0.0911	0.4000	2
$[1101]^T$	8.35	0.0329	0.0382	0.8620	13
$[0011]^T$	8.4	0.0454	0.0706	0.6433	3
$[0110]^T$	9.9	0.0966	0.0742	1.3013	6
$[1010]^T$	10.9	0.0704	0.0510	1.3808	10
$[0111]^T$	11.35	0.1204	0.0575	2.0928	7
$[1011]^T$	12.35	0.0877	0.0395	2.2207	11
$[1110]^T$	13.85	0.1866	0.0415	4.4923	14
$[1111]^T$	15.3	0.2326	0.0322	7.2247	15

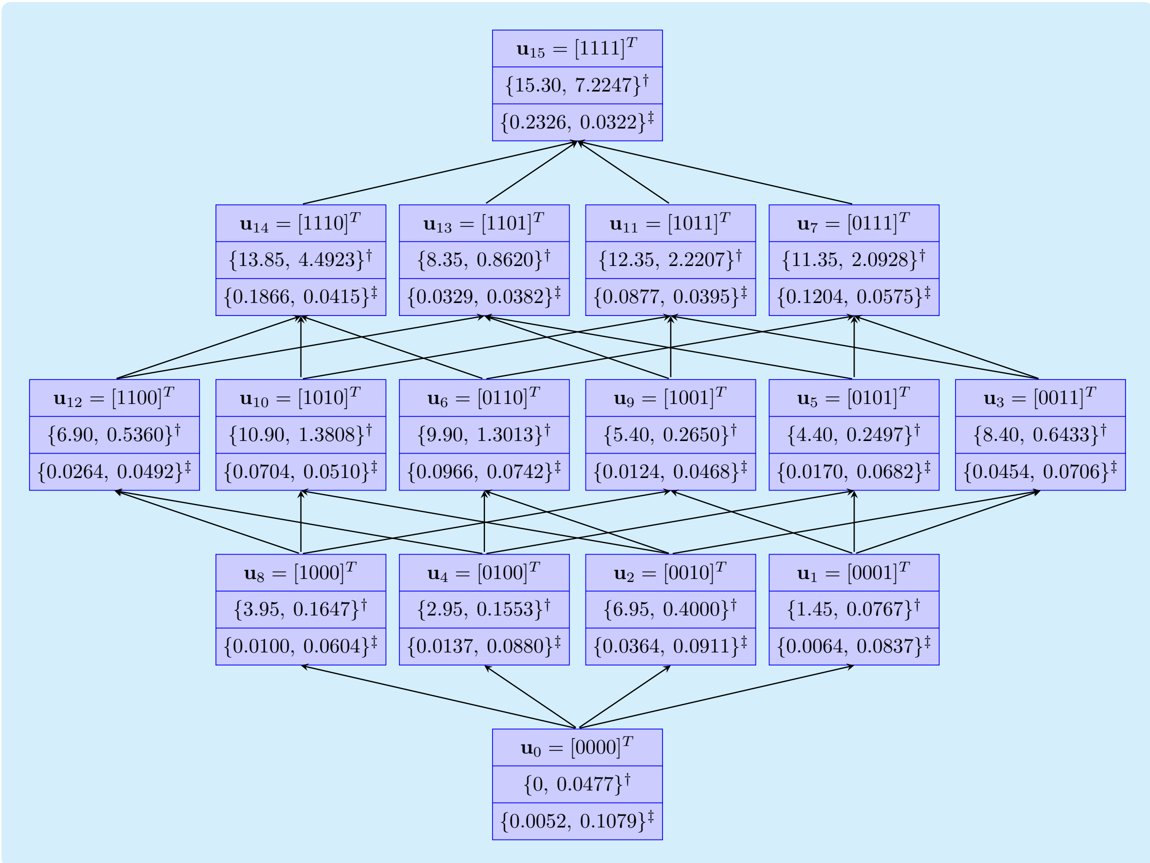

Figure B.1: Depiction of semi-monotonic property where † represents values- $\{T(\mathbf{u}), \Lambda(\mathbf{u})\}$ and ‡ represents values- $\{p(\mathbf{u}|H_1), p(\mathbf{u}|H_0)\}$ corresponding to each observation vector.

Bibliography

[1] P. K. Varshney, *Distributed Detection and Data Fusion.* Springer Science & Business Media, 1997.

[2] R. Viswanathan and P. K. Varshney, "Distributed Detection with Multiple Sensors: Part I-Fundamentals," *Proceedings of the IEEE*, vol. 85, no. 1, pp. 54–63, Jan. 1997.

[3] J. Mitola and G. Q. Maguire, "Cognitive Radio: Making Software Radios More Personal," *IEEE Personal Communications*, vol. 6, no. 4, pp. 13–18, Aug. 1999.

[4] S. Haykin, "Cognitive Radio: Brain-Empowered Wireless Communications," *IEEE Journal on Selected Areas in Communications*, vol. 23, no. 2, pp. 201–220, Feb. 2005.

[5] J. Lunden, V. Koivunen, and H. V. Poor, "Spectrum Exploration and Exploitation for Cognitive Radio: Recent Advances," *IEEE Signal Processing Magazine*, vol. 32, no. 3, pp. 123–140, May 2015.

[6] E. Axell, G. Leus, E. G. Larsson, and H. V. Poor, "Spectrum Sensing for Cognitive Radio : State-of-the-Art and Recent Advances," *IEEE Signal Processing Magazine*, vol. 29, no. 3, pp. 101–116, May 2012.

[7] K. B. Letaief and W. Zhang, "Cooperative Communications for Cognitive Radio Networks," *Proceedings of the IEEE*, vol. 97, no. 5, pp. 878–893, May 2009.

[8] Z. Quan, S. Cui, H. V. Poor, and A. H. Sayed, “Collaborative Wideband Sensing for Cognitive Radios,” *IEEE Signal Processing Magazine*, vol. 25, no. 6, pp. 60–73, Nov. 2008.

[9] S. M. Mishra, A. Sahai, and R. W. Brodersen, “Cooperative Sensing among Cognitive Radios,” in *2006 IEEE International Conference on Communications*, vol. 4, Jun. 2006, pp. 1658–1663.

[10] D. Johnson. (2017) Statistical Signal Processing. Course Text. Rice University. Houston, Tx. [Online]. Available: http://elec531.rice.edu

[11] H. V. Poor, *An Introduction to Signal Detection and Estimation.* Springer Science & Business Media, 1998.

[12] E. Lehmann and J. P. Romano, *Testing Statistical Hypotheses.* Springer-Verlag New York, 2005.

[13] D. Ciuonzo, G. Romano, and P. S. Rossi, “Optimality of Received Energy in Decision Fusion Over Rayleigh Fading Diversity MAC With Non-Identical Sensors,” *IEEE Transactions on Signal Processing*, vol. 61, no. 1, pp. 22–27, Jan. 2013.

[14] F. Li, J. S. Evans, and S. Dey, “Decision Fusion Over Noncoherent Fading Multiaccess Channels,” *IEEE Transactions on Signal Processing*, vol. 59, no. 9, pp. 4367–4380, Sep. 2011.

[15] W. Zhang, R. K. Mallik, and K. B. Letaief, “Optimization of Cooperative Spectrum Sensing with Energy Detection in Cognitive Radio Networks,” *IEEE Transactions on Wireless Communications*, vol. 8, no. 12, pp. 5761–5766, Dec. 2009.

[16] S. C. Thomopoulos, R. Viswanathan, and D. C. Bougoulias, "Optimal Decision Fusion in Multiple Sensor Systems," *IEEE Transactions on Aerospace and Electronic Systems*, no. 5, pp. 644–653, 1987.

[17] Z. Chair and P. K. Varshney, "Optimal Data Fusion in Multiple Sensor Detection Systems," *IEEE Transactions on Aerospace and Electronic Systems*, vol. AES-22, no. 1, pp. 98–101, Jan. 1986.

[18] M. Kam, Q. Zhu, and W. S. Gray, "Optimal Data Fusion of Correlated Local Decisions in Multiple Sensor Detection Systems," *IEEE Transactions on Aerospace and Electronic Systems*, vol. 28, no. 3, pp. 916–920, Jul. 1992.

[19] S. Maleki, S. P. Chepuri, and G. Leus, "Optimal Hard Fusion Strategies for Cognitive Radio Networks," in *2011 IEEE Wireless Communications and Networking Conference*, Mar. 2011, pp. 1926–1931.

[20] E. C. Y. Peh, Y. C. Liang, Y. L. Guan, and Y. Zeng, "Optimization of Cooperative Sensing in Cognitive Radio Networks: A Sensing-Throughput Tradeoff View," *IEEE Transactions on Vehicular Technology*, vol. 58, no. 9, pp. 5294–5299, Nov. 2009.

[21] S. Chaudhari, J. Lunden, V. Koivunen, and H. V. Poor, "Cooperative Sensing With Imperfect Reporting Channels: Hard Decisions or Soft Decisions?" *IEEE Transactions on Signal Processing*, vol. 60, no. 1, pp. 18–28, Jan. 2012.

[22] G. Taricco, "Optimization of Linear Cooperative Spectrum Sensing for Cognitive Radio Networks," *IEEE Journal of Selected Topics in Signal Processing*, vol. 5, no. 1, pp. 77–86, Feb. 2011.

[23] Z. Quan, W. K. Ma, S. Cui, and A. H. Sayed, "Optimal Linear Fusion for Distributed Detection Via Semidefinite Programming," *IEEE Transactions on Signal Processing*, vol. 58, no. 4, pp. 2431–2436, Apr. 2010.

[24] J. Ma, G. Zhao, and Y. Li, "Soft Combination and Detection for Cooperative Spectrum Sensing in Cognitive Radio Networks," *IEEE Transactions on Wireless Communications*, vol. 7, no. 11, pp. 4502–4507, Nov. 2008.

[25] Z. Quan, S. Cui, and A. H. Sayed, "Optimal Linear Cooperation for Spectrum Sensing in Cognitive Radio Networks," *IEEE Journal of Selected Topics in Signal Processing*, vol. 2, no. 1, pp. 28–40, Feb. 2008.

[26] E. C. Y. Peh, Y. C. Liang, Y. L. Guan, and Y. Zeng, "Cooperative Spectrum Sensing in Cognitive Radio Networks with Weighted Decision Fusion Schemes," *IEEE Transactions on Wireless Communications*, vol. 9, no. 12, pp. 3838–3847, Dec. 2010.

[27] E. Drakopoulos and C. C. Lee, "Optimum Multisensor Fusion of Correlated Local Decisions," *IEEE Transactions on Aerospace and Electronic Systems*, vol. 27, no. 4, pp. 593–606, Jul. 1991.

[28] I. Y. Hoballah and P. K. Varshney, "Neyman-Pearson Detection with Distributed Sensors," in *1986 25th IEEE Conference on Decision and Control*, Dec. 1986, pp. 237–241.

[29] G. Casella and R. L. Berger, *Statistical inference.* Duxbury Pacific Grove, CA, 2002, vol. 2.

[30] Z. Kohavi and N. K. Jha, *Switching and Finite Automata Theory.* Cambridge University Press, Oct. 2009.

[31] H. Kellerer, U. Pferschy, and D. Pisinger, *Knapsack Problems.* Springer, Berlin, 2004.

[32] S. Martello, D. Pisinger, and P. Toth, "New Trends in Exact Algorithms for the 01 Knapsack Problem," *European Journal of Operational Research*, vol. 123, no. 2, pp. 325–332, 2000.

[33] E. Demaine and S. Devadas. (2011, Fall) 6.006 Introduction to Algorithms. Video Lectures, MIT OpenCourseWare, License: Creative Commons BY-NC-SA. Massachusetts Institute of Technology. [Online]. Available: https://ocw.mit.edu

[34] R. E. Bellman, *Dynamic Programming.* Princeton university press, 1972.

[35] R. Umar, A. U. H. Sheikh, and M. Deriche, "Unveiling the Hidden Assumptions of Energy Detector Based Spectrum Sensing for Cognitive Radios," *IEEE Communications Surveys Tutorials*, vol. 16, no. 2, pp. 713–728, 2014.

[36] S. J. Zahabi, A. A. Tadaion, and S. Aissa, "Neyman-Pearson Cooperative Spectrum Sensing for Cognitive Radio Networks with Fine Quantization at Local Sensors," *IEEE Transactions on Communications*, vol. 60, no. 6, pp. 1511–1522, Jun. 2012.

[37] D. Ciuonzo, A. D. Maio, and P. S. Rossi, "A Systematic Framework for Composite Hypothesis Testing of Independent Bernoulli Trials," *IEEE Signal Processing Letters*, vol. 22, no. 9, pp. 1249–1253, Sep. 2015.

[38] D. Ciuonzo and P. S. Rossi, "Decision Fusion With Unknown Sensor Detection Probability," *IEEE Signal Processing Letters*, vol. 21, no. 2, pp. 208–212, Feb. 2014.

[39] X. Shen, Y. Zhu, L. He, and Z. You, "A Near-Optimal Iterative Algorithm via Alternately Optimizing Sensor and Fusion Rules in Distributed Decision Systems," *IEEE Transactions on Aerospace and Electronic Systems*, vol. 47, no. 4, pp. 2514–2529, Oct. 2011.

[40] K. Veeramachaneni, W. Yan, K. Goebel, and L. Osadciw, "Improving Classifier Fusion Using Particle Swarm Optimization," in *IEEE Symposium on Computational Intelligence in Multicriteria Decision Making*, Apr. 2007, pp. 128–135.

[41] Y. Zhu, R. S. Blum, Z.-Q. Luo, and K. M. Wong, "Unexpected Properties and Optimum-Distributed Sensor Detectors for Dependent Observation Cases," *IEEE Transactions on Automatic Control*, vol. 45, no. 1, pp. 62–72, Jan. 2000.

[42] H. Chen, B. Chen, and P. K. Varshney, "A New Framework for Distributed Detection With Conditionally Dependent Observations," *IEEE Transactions on Signal Processing*, vol. 60, no. 3, pp. 1409–1419, Mar. 2012.

[43] H. He and P. K. Varshney, "Distributed Detection with Censoring Sensors Under Dependent Observations," in *2014 IEEE International Conference on Acoustics, Speech and Signal Processing (ICASSP)*, May 2014, pp. 5055–5059.

[44] S. Appadwedula, V. V. Veeravalli, and D. L. Jones, "Decentralized Detection With Censoring Sensors," *IEEE Transactions on Signal Processing*, vol. 56, no. 4, pp. 1362–1373, Apr. 2008.

[45] ——, "Energy-Efficient Detection in Sensor Networks," *IEEE Journal on Selected Areas in Communications*, vol. 23, no. 4, pp. 693–702, Apr. 2005.

[46] C. Rago, P. Willett, and Y. Bar-Shalom, "Censoring Sensors: A Low-Communication-Rate Scheme for Distributed Detection," *IEEE Transactions on Aerospace and Electronic Systems*, vol. 32, no. 2, pp. 554–568, Apr. 1996.

[47] B. Chen, L. Tong, and P. K. Varshney, "Channel-Aware Distributed Detection in Wireless Sensor Networks," *IEEE Signal Processing Magazine*, vol. 23, no. 4, pp. 16–26, Jul. 2006.

[48] S. M. Kay, *Fundamentals of Statistical Signal Processing: Detection Theory, vol. 2.* Prentice Hall Upper Saddle River, NJ, USA, 1998.

[49] J. Y. Wu, C. W. Wu, T. Y. Wang, and T. S. Lee, "Channel-Aware Decision Fusion With Unknown Local Sensor Detection Probability," *IEEE Trans. Signal Process.*, vol. 58, no. 3, pp. 1457–1463, Mar. 2010.

[50] R. Niu, B. Chen, and P. K. Varshney, "Fusion of Decisions Transmitted Over Rayleigh Fading Channels in Wireless Sensor Networks," *IEEE Trans. Signal Process.*, vol. 54, no. 3, pp. 1018–1027, Mar. 2006.

[51] M. F. Rahaman and M. Z. A. Khan, "Low-Complexity Optimal Hard Decision Fusion Under the Neyman-Pearson Criterion," *IEEE Signal Process. Lett.*, vol. 25, no. 3, pp. 353–357, Mar. 2018.

[52] P. Salvo Rossi, D. Ciuonzo, and G. Romano, "Orthogonality and Cooperation in Collaborative Spectrum Sensing through MIMO Decision Fusion," *IEEE Trans. Wireless Commun.*, vol. 12, no. 11, pp. 5826–5836, November 2013.

List of Publications

Journals

[J.1] **M. F. Rahaman** and M. Z. A. Khan, "Low-Complexity Optimal Hard Decision Fusion Under the Neyman-Pearson Criterion," IEEE Signal Process. Lett., vol. 25, no. 3, pp. 353-357, Mar. 2018.

[J.2] **M. F. Rahaman**, D. Ciuonzo and M. Z. A. Khan, "Mean-based Hard Decision Fusion Rules," IEEE Signal Process. Lett., vol. 25, no. 5, pp. 630-634, May 2018.

[J.3] **M. F. Rahaman** and M. Z. A. Khan, "Fast Computation of Optimal Hard Decision Fusion under Neyman-Pearson Criterion," (In preparation for *IEEE Signal Process Lett.,*).

Conferences

[C.1] D. Nikhil, **M. F. Rahaman** and M. Z. A. Khan, "Reduced Complexity Optimal Hard Decision Fusion under Neyman-Pearson Criterion," 26^{th} IEEE SIU 2018 conference, pp. 1-4, May 2018, Turkey.

[C.2] **M. F. Rahaman** and M. Z. A. Khan, "On non-Randomized Hard Decision Fusion under Neyman Pearson Criterion using LRT," 88^{th} IEEE Vehicular Technology Conference, Chicago, *(In Press, Aug 2018).*

[C.3] **M. F. Rahaman** and M. Z. A. Khan, "A Novel Approach to Improve the Performance of Truncated SED for Cognitive Radio," in 2015 IEEE International Conference on Communication Workshop (ICCW), London, Jun. 2015, pp. 1629-1634.

IITH Doctoral Committee

1. **Guide:** Prof. Mohammed Zafar Ali Khan, Dept. of Electrical Engineering, IIT Hyderabad

2. **Members:**

   - Prof. Kuchi Kiran Kumar, Dept. of Electrical Engineering, IIT Hyderabad
   - Dr. G.V.V. Sharma, Dept. of Electrical Engineering, IIT Hyderabad
   - Dr. Sumohana S. Channappayya, Dept. of Electrical Engineering, IIT Hyderabad

3. **Chairperson:** Dr. Bheemarjuna Reddy Tamma, Dept. of Computer Science and Engineering, IIT Hyderabad